

IVANO DI MEO

Matr. N°. 725276

**Altered Sulfide Metabolism in
Ethylmalonic Encephalopathy**

Coordinator: Prof. Andrea Biondi

Tutor: Dr. Valeria Tiranti

TABLE OF CONTENTS

Chapter 1: General Introduction

Mitochondria and Mitochondrial medicine	
<i>Mitochondria</i>	page 3
<i>Mitochondrial genetics</i>	page 5
<i>Oxidative Phosphorylation</i>	page 8
<i>Mitochondrial medicine</i>	page 12
<i>Mitochondrial disorders</i>	page 12
- <i>MtDNA mutations</i>	page 16
- <i>Nuclear gene mutations</i>	page 18
<i>Treatment of the mitochondrial diseases</i>	page 24
Hydrogen sulfide in health and diseases	
<i>Physico-chemical properties</i>	page 27
<i>H₂S metabolism in mammals</i>	page 27
<i>Physiological role of H₂S</i>	page 30
<i>Toxic effects of H₂S</i>	page 30
<i>H₂S in human pathology</i>	page 32
- <i>Cardiovascular and neurodegenerative disorders</i>	page 32
- <i>Inborn errors of sulfur metabolism</i>	page 33
Ethylmalonic Encephalopathy	
<i>Clinical features</i>	page 37
<i>Biochemical markers</i>	page 38
<i>Ethylmalonic Encephalopathy 1 (ETHE1) gene and protein</i>	page 39
<i>Ethylmalonic Encephalopathy mouse model</i>	page 42
<i>Treatment</i>	page 43
Scope of the thesis	page 47
References	page 49

Chapter 2: Chronic Exposure to Sulfide Causes Accelerated Degradation of Cytochrome c Oxidase in Ethylmalonic Encephalopathy

page 61

Chapter 3: Ethylmalonic encephalopathy: application of improved biochemical and molecular diagnostic approaches

page 95

Chapter 4: Morphologic evidence of diffuse vascular damage in human and in the experimental model of ethylmalonic encephalopathy.

page 111

Chapter 5: Summary, discussion and future perspective

Summary	page 137
Discussion	page 140
Future perspectives	page 146
References	page 149

Chapter 1

General Introduction

MITOCHONDRIA AND MITOCHONDRIAL MEDICINE

Mitochondria

Mitochondria are subcellular organelles, ubiquitously found in eukaryotes, originated from a bacteria-like organism that colonized primitive eukaryotic cells and created an endosymbiotic relationship with them (Margulis, 1976). The bacteria evolved into mitochondria, thus endowing the host cells with aerobic metabolism, a much more efficient way to produce energy than anaerobic glycolysis. During evolution, they lost their genetic independence and most of their original bacterial proteome, relying on the import of cytosolic protein for several functions (Lister, 2005). Therefore, thanks to their capacity to support aerobic respiration and to generate adenosine triphosphate (ATP), mitochondria became the principal intracellular source of energy. In addition to their primary function, that is the production of ATP by oxidative phosphorylation (OXPHOS), mitochondria have a primary role in different metabolic pathways: the tricarboxylic acid cycle (TCA) and β -oxidation, the metabolism of carbohydrates and fats, the porphyrin, lipid and steroid hormone synthesis. Moreover, mitochondria have been shown to be involved in cell signaling, in particular they play an important role in the apoptosis, and in calcium homeostasis.

The first observations of mitochondria by electron microscope noted a basic morphology of a matrix enclosed by the inner mitochondrial membrane and the inner membrane space between the inner and outer

mitochondrial membrane. The term cristae was coined for the folds of inner mitochondrial membrane, which add to the total membrane area of the mitochondrion (Scheffler, 2001). Nevertheless they can be divided into 4 compartments: the outer membrane (OM), the inter-membrane space (IMS), the inner membrane (IM) and the mitochondrial matrix. The OM is a porous membrane that allows passage of small substances between the cytosol and the IMS. The IM contains the complexes of the mitochondrial respiratory chain (MRC) and functions also as a barrier to ionic diffusion, allowing the creation of the proton gradient necessary to produce ATP. The matrix hosts several enzymes involved in different pathways (i.e. TCA cycle and β -oxidation) and the mitochondrial deoxyribonucleic acid (mtDNA).

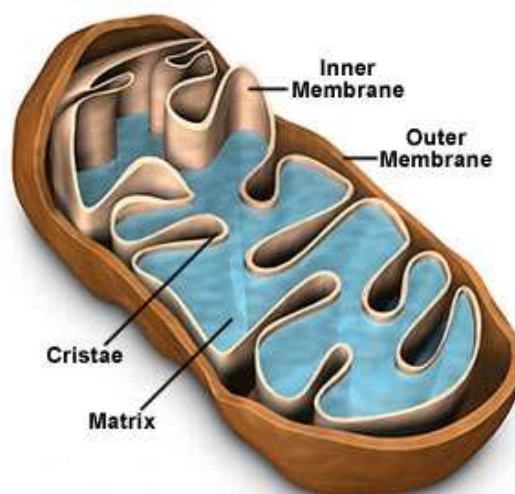


Figure 1. Mitochondrial structure

Schematic representation of the double membrane structure of mitochondria.

They are present in hundreds/thousands copies in every cell, the amount depending on the cell type. Although traditionally considered as isolated organelles, the maintenance of a sufficient pool of mitochondria during cell division and proliferation is assured by the process of fusion and fission (Bereiter-Hahn and Voth, 1994). Cellular distribution and function of mitochondria is based on protein interactions located on the outer mitochondrial surface as well as on mitochondrial membrane interactions with the cytoskeletal elements such as actin filaments, intermediate filaments, and microtubules (Scheffler, 2001).

Mitochondrial genetics

Mitochondria contain a circular double-strand DNA of 16568 base pairs. MtDNA contains no introns and small non-coding regions; it codes for 13 protein of the OXPHOS system and for 2 ribosomal and 22 transfer RNAs, necessary for the mitochondrial protein synthesis (Fig.2). However mitochondria depend upon the nucleus for supplying of all the other OXPHOS proteins and the enzymes necessary for replication, repair, transcription, translation, maintenance and many structural proteins. Each human cell has thousands of mitochondria and every mitochondrion typically has at least one copy of the mitochondrial genome, and a single mitochondrion can carry as many as ten copies.

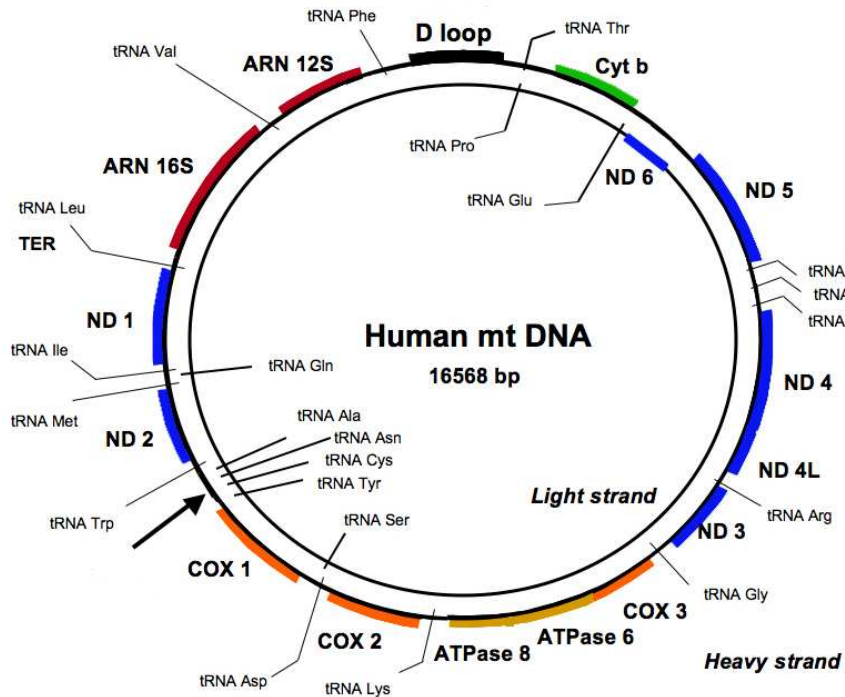


Figure 2. Map of the human mtDNA.

Genes coding for OXPHOS proteins: complex I genes = blue; complex III cytb (cytochrome b) gene = green; complex IV genes = orange; complex V genes = yellow. Genes coding for RNAs: rran genes = red.

Cells with higher demands of ATP typically have more mtDNA copies (St John, 2005). MtDNA is transmitted through the maternal line. This means that only the mother transmits her oocyte mtDNA to all of her offspring, and her daughters transmit their mtDNA to the next generation. A single case of paternal inheritance has been published (Schwartz, 2002) but, despite several studies, further cases of paternal transmission have never been described. The replication of

mtDNA is a continuous process, independent from nuclear DNA replication, and requires several nuclear encoded factors such as DNA polymerase gamma (POLG), mitochondrial transcription factor A (mtTFA), mt single-strand binding protein (mtSSB) and enzymes important for the supply of deoxynucleotides, such as thymidine kinase 2 (TK2) and deoxy-guanosine kinase (dGUOK). MtDNA is transcribed polycistronically and translated by mitochondrial ribosomes. Usually all the mtDNA copies are identical, a status known as homoplasmy. However it is possible that errors occur during replication or repair of mtDNA, leading to the formation of a mutant mtDNA molecule. The rate of mutations in mtDNA is greater than those of genomic DNA probably because of the lack of histones and the presence of high level of free oxygen radicals. Mutant mtDNA could coexist with wt mtDNA in the same cell. This coexistence is called heteroplasmy. This is a dynamic phenomenon and the proportion of mutated vs. wt mtDNA (level of heteroplasmy) can change among cells and tissues, because at every cell division mitochondria are randomly segregated. A bottleneck effect is active in primordial female germinal cells (primary oogonia) that drastically reduces the number of segregating units responsible for the transmission of mtDNA characters to the subsequent generation. Clinical presentations are usually associated with heteroplasmic mutations. Only when mutated gene copies accumulate over a certain “threshold”, the deleterious effects of the mutation will not be counterbalanced by the co-existing wild-type mtDNA, and will be expressed phenotypically as a cellular dysfunction and disease. This threshold is tissue-specific, different for different mutations and in

different individuals. Nevertheless there are diseases caused by homoplasmic mutation, such as Leber's hereditary optic neuropathy (LHON), the first disorder associated to mitochondrial DNA mutation (Wallace et al. 1988). Recent findings have shown that various mtDNA maintenance proteins specifically co-localize with mtDNA in intra-mitochondrial foci designated nucleoids. Mammalian nucleoids are now considered as specialized mtDNA-containing structures within the mitochondrial network, organized as complexes with a variety of proteins that protect mtDNA from insults and provide the appropriate microenvironment for mtDNA maintenance and gene expression.

Oxidative Phosphorylation

The oxidative phosphorylation is the most important activity of mitochondria. (Zeviani and DiDonato, 2004). This process, that provides the most important source of the cell energy, is carried out by a series of multi-heteromeric complexes, located in the mitochondrial inner membrane through sequential reactions of reduction and oxidation, which form the so called "cellular respiration" and constitute the mitochondrial respiratory chain (MRC). Following the dehydrogenation of the redox equivalents nicotinamide adenine dinucleotide (NADH) and flavin adenine dinucleotide (FADH₂), they generate a flow of electrons that results in the extrusion of hydrogen ions from the matrix to the IMS (exploited by proton translocating complexes I, III and IV and generating a membrane potential of about 180 mV) and in the production of water from molecular oxygen (by

complex IV). The energy generated during these reactions, corresponding to the proton gradient across the IM, can be utilized by Complex V, or ATP synthetase, to condensate inorganic phosphate Pi and adenosine diphosphate (ADP) to ATP, the “currency” energy of the cell (Fig. 3).

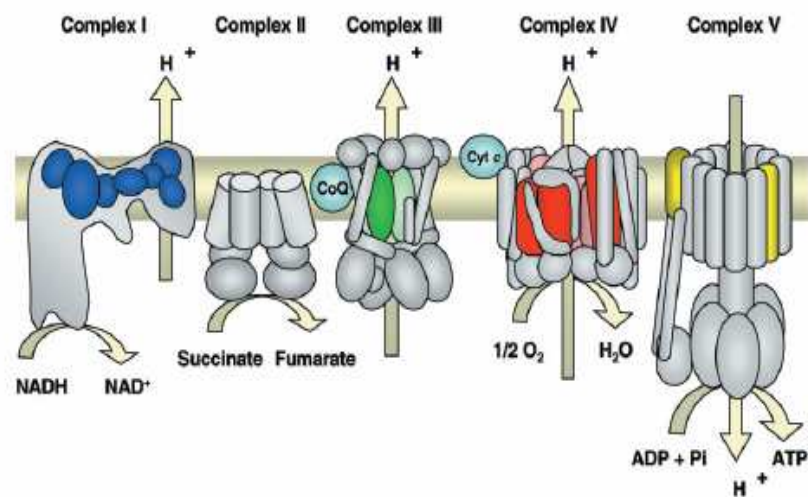


Figure 3. Mitochondrial OXPHOS system

Subunits encoded by mtDNA are shown in different colors in each complex

In addition to the above- mentioned complexes, two electron carriers (ubiquinone or CoQ, and cytochrome *c*) and a set of accessory complexes that can supply electrons take part in this process, including complex II (succinate-ubiquinone reductase), the electron-transfer flavoprotein-ubiquinone reductase (ETF-QR) and dihydroorotate dehydrogenase (DHODH).

In mammalian mitochondria Complex I (NADH-ubiquinone oxidoreductase) catalyzes the oxidation of NADH, derived from the oxidation of pyruvate, fatty acids, and amino acids, by ubiquinone. It is a macromolecular structure composed of ≈ 45 subunits with a total molecular mass of 1000kDa (Carroll, 2006). Seven subunits are encoded by mtDNA, the others by nuclear genes. Complex II (Succinate-ubiquinone reductase) is composed of four subunits all encoded by nuclear genome. It catalyzes the oxidation of succinate to fumarate and transfers electrons to ubiquinone moieties. Complex III (ubiquinol-cytochrome c reductase) is made up of 11 subunits, of which all but one (cytochrome b) are encoded by nuclear DNA. Human cytochrome c oxidase (COX, complex IV) is composed of thirteen subunits: the three largest ones are encoded by mtDNA genes, while the remaining subunits are encoded by nuclear genes. ATP synthase (complex V) comprises an integral membrane component F₀ and a peripheral moiety F₁. All five subunits of F₁ (a, b, c, d, e) and most F₀ subunits of the ATP synthase are nuclear encoded. Only two F₀ proteins (ATP6 and 8) are encoded by mitochondrial DNA (Boyer, 1993). Metabolic fuels feed reducing equivalents to the respiratory chain via glycolysis, fatty acid or amino acid oxidation. Pyruvate, which stands at the crossroads of glycolysis, gluconeogenesis and OXPHOS, is a key point in carbohydrate oxidation and feeds into the TCA cycle via the pyruvate dehydrogenase complex (PDHC) to generate acetyl-CoA. Fatty acids are oxidized within the mitochondrial matrix by β -oxidation, which again generates acetyl-CoA for the TCA cycle (Fig.4). Reducing equivalents generated during the oxidation of the primary substrate or from the TCA cycle

are transferred to OXPHOS as NADH (cI), or reduced flavins (entering at cII or cIII). Mitochondria account for more than ninety percent of the energy utilized by our organism. When a failure in energy supply occurs, due to a defect in mitochondrial OXPHOS, the survival of the cell, and as a consequence, the life of our entire organism, is seriously at risk. Tissues and organs with the highest energy demand, including brain, skeletal muscles, and heart, are usually the most affected ones.

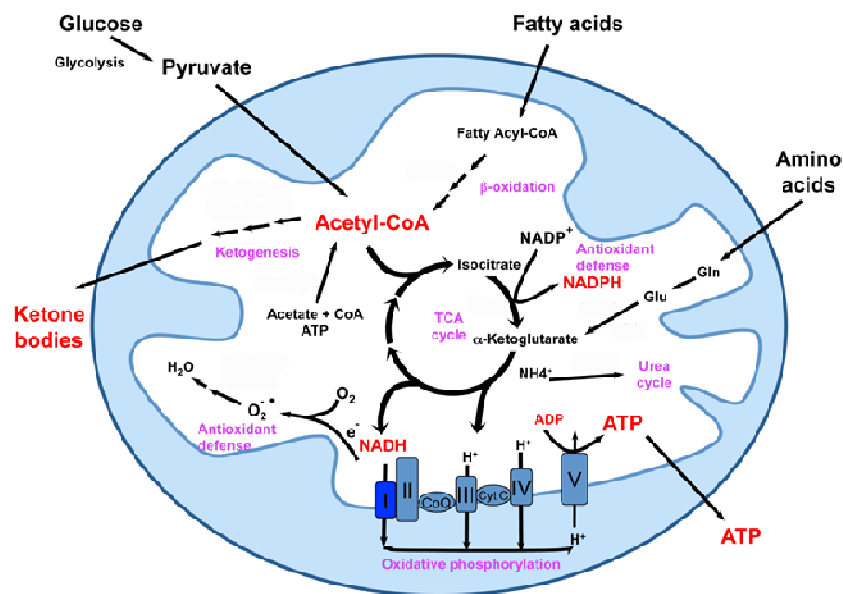


Figure 4. Mitochondrial energy metabolism

Schematic representation of mitochondrial energy metabolism and related pathways.

Mitochondrial medicine

Mitochondria are the organelles responsible for the supply of energy to the cell through the OXPHOS system. For this reason any defect or alteration in this process lead to pathological consequences, mainly in tissues and organs that have a highly energetic request. The consequences of an impairment of the OXPHOS system are decrease of ATP production and increase of reactive oxygen species (ROS), plus their associated up- and downstream effects. More than twenty years ago, the first evidences of direct link between mitochondria and disease arose; in 1988 Wallace et al. found a mtDNA mutation causing Leber's hereditary optic neuropathy (Wallace et al. 1988) and Holt et al. identified deletions in mtDNA causing myopathy (Holt, 1988). After these papers, there has been a series of reports about the clinical, biochemical and genetic characterizations of mitochondrial diseases; moreover an involvement of mitochondria has become evident in many other clinical conditions including neurodegenerative disorders (Swerdlow, 2009), cancer (Carew and Huang, 2002) and ageing (Reddy, 2008). All these considerations lead to the use of the term "mitochondrial medicine" to underline the central role of the mitochondrion not only in the classical mitochondrial diseases but also in a wide and increasing range of illness.

Mitochondrial disorders

Whereas in the past the term "mitochondrial disorders" was used to any alterations affecting mitochondria, it is currently referred to

genetic defects of OXPHOS (Zeviani and Lamantea, 2006). Because OXPHOS is necessary for nearly all cells, any organ can be affected in mitochondrial disease. In addition, given the complexity of mitochondrial genetics and biochemistry, mitochondrial inherited diseases may present with a vast range of symptoms, severity, age of onset and outcome (DiMauro and Davidzon 2005). The maxim “any tissue, any symptom, any age” well resume all these concepts (Munich, 1996). Genetic defects of OXPHOS have an incidence at approximately 1:5000 (Schaefer, 2004) and are therefore not to be considered “so rare” diseases. The clinical manifestations of mitochondrial disorders are extremely heterogeneous. They range from lesions in single tissues, such as the optic nerve in Leber’s hereditary optic neuropathy (LHON), to more diffuse lesions including myopathies, encephalomyopathies, cardiopathies and hepatopathies, to complex multisystem syndromes with onset ranging from neonatal to adult life. Tissue specificity, due to variable metabolic thresholds for the different OXPHOS complexes in each tissue, may limit the systemic effect of metabolic changes. Moreover there are to be considered many contributing factors including tissue-specific expression of OXPHOS genes, different metabolic needs, and tissue dependent segregation of heteroplasmy. Nevertheless mitochondrial disease commonly presents with a combination of muscle and brain involvement; tissues that are post-mitotic and have high metabolic requests. The spectrum of mitochondrial diseases in children is wide, usually different from that found in adults, and new clinical features are continuously reported (Debray, 2008). Some presentations alone are strong indications of a mitochondrial

involvement, but there are often additional albeit not specific symptoms to be taken into account. Common neurological manifestations of mitochondrial disease include seizures, migraine, stroke-like episodes, neuropathy and dystonia. Often, mitochondrial disease is only considered when such features occur in conjunction with other symptoms, such as deafness, visual impairment and/or diabetes. However multi-organ involvement, a hallmark of mitochondrial disease, may not be evident, above all at initial presentations. In general, childhood presentations of mitochondrial disease tend to be more severe than those with adult onset and frequently involve many different organ systems. Adult patients can be affected by isolated myopathy resulting only in fatigue, muscle weakness and/or exercise intolerance, but muscle symptoms can also be associated with involvement of the central and peripheral nervous systems, manifesting symptoms, which may include ataxia (i.e. motor incoordination), sensory-neural hearing loss, seizures, polyneuropathy, retinopathy, and, more rarely, movement disorders and cognitive deterioration. A hallmark of mitochondrial dysfunction is lactic acidosis; acidosis is derived from the reduction to lactate of pyruvate, which accumulates for the block of respiration. Hyperlactatemia however may be absent in clear mitochondrial disease or present only during stress. Liquoral or cerebrospinal fluid (CSF) lactate level is a more reliable diagnostic marker than blood, above all in patients with brain involvement (Brown, 1988). Several morphological and biochemical features characterize many of these syndromes albeit there isn't an always valid rule. Histological and histochemical analysis of muscle biopsy remains a very important step

for the detection of mitochondrial disease, especially in adult patients. One of the best-known morphological alterations is the transformation of scattered muscle fibres into “ragged red fibres” (RRF). RRFs are characterized by the accumulation of abnormal mitochondria under the sarcolemmal membrane. The same aggregations can also be observed using succinate dehydrogenase (SDH) assay, that can be even more useful because complex II (subunits of which are encoded only by nuclear genome) is completely unaffected by abnormalities of mtDNA. This assay can be combined with the cytochrome c oxidase (COX, respiratory complex IV) reaction; in mitochondrial disorders a common finding is the presence of muscle fibres that stain negative to this histochemical reaction. Moreover a mosaic pattern of COX activity is indicative of a heteroplasmic mtDNA mutation, the intensity of the stain depending on the mutation load between different fibres. However, these typical “mitochondrial” alterations may be absent in otherwise demonstrated mitochondrial disorders. The molecular diagnosis of the mitochondrial disease is complex. Because of its dual genetic control, OXPHOS disorders can be due to mutations in mtDNA or nuclear DNA genes (Zeviani and DiDonato 2004). Nuclear genetic defects are easily investigated in freshly extracted DNA from peripheral white blood cells. Blood could be less useful for detecting mtDNA mutations, because the level of heteroplasmy could be too low to be detected. Skeletal muscle is the tissue of choice for molecular genetic analysis of mtDNA. This is because skeletal muscle is often an affected tissue, samples may be already available for enzymatic assays, and for some mutations the

levels of heteroplasmy in skeletal muscle reflect those in other affected post-mitotic tissues such as the brain (Oldfors, 1995).

mtDNA mutations

Even if the proteins encoded by mtDNA are essential, they comprise only a small fraction of the total number of protein involved in a functional OXPHOS system. About 10-25% of mitochondrial diseases are caused by mutations in mtDNA (Mancuso, 2007). When the mtDNA should be analyzed, it is important to take into consideration the following differences from nuclear DNA: 1) The mitochondrial genome is maternally inherited; 2) Mitochondria are polyploidy and the mtDNA genotype can be composed of a single mtDNA species (homoplasmy) or two different genotypes can co-exist in variable proportion (heteroplasmy); 3) A threshold effect modulates the phenotypic expression of a mtDNA-associated symptoms. Mutations of mtDNA can be classified into large-scale rearrangements (deletions or duplications) and point mutations. Both groups have been associated with well-defined clinical syndromes. While large-scale rearrangements are usually sporadic, point mutations are usually maternally inherited.

Large-scale rearrangements of mtDNA

Single, large-scale rearrangements of mtDNA comprise single partial deletions, or partial duplications. The size of deletions can vary from few bases to several kilobases and be located in any part of the molecule. The most common deletion is 5Kb long, and affects a

region containing tRNAs and protein-coding genes. Usually deletions encompass several genes and are invariably heteroplasmic.

Rearranged molecules, lacking a portion of the mitochondrial genome, can be detected as an independent mtDNA species (single mtDNA deletion) or joined to a wild-type molecule or a mixture of the two rearrangements co-exists in the same cell (Zeviani, 1988).

Three main clinical phenotypes are associated with these mutations: **Kearns–Sayre syndrome (KSS, OMIM#530000), sporadic progressive external ophthalmoplegia (PEO) and Pearson’s syndrome (OMIM#557000).**

mtDNA point mutations

These mutations can be substitutions of single bases or micro-insertions/micro-deletions in the mtDNA molecule. They can be localized into transfer RNAs (tRNA), ribosomal RNAs, (rRNA), or genes encoding OXPHOS subunits. Unlike mtDNA rearrangements, mtDNA point mutations are transmitted maternally. They may be heteroplasmic or homoplasmic (DiMauro and Schon, 2003). Nowadays sequencing of the entire mitochondrial genome is feasible and useful in excluding mtDNA involvement prior to investigating candidate nuclear genes. However, in consideration of the highly polymorphic status of mtDNA, it is often difficult to decide which variants are polymorphisms and which are pathogenic mutations. Some criteria to assess the pathogenic role of mtDNA mutations were suggested (DiMauro and Schon, 2001): the mutation must not be a known neutral polymorphism; the base change must affect an

evolutionarily conserved and functionally important site; deleterious mutations are usually heteroplasmic; the degree of heteroplasmy in different family members has to be concordant with the severity of symptoms. The clinical expression associated to mtDNA mutations is wide; the phenotypes more frequent are the following: **Leber's Hereditary Optic Neuropathy (LHON, OMIM#535000)**, **Neurogenic muscle weakness, ataxia, retinitis pigmentosa (NARP, OMIM#551500)**, **Leigh syndrome (MILS, maternally inherited Leigh syndrome OMIM#256000)**, **Mitochondrial Encephalomyopathy, Lactic Acidosis, and Stroke-like episodes (MELAS, OMIM#540000)**, **Myoclonus Epilepsy with Ragged-Red Fibers (MERRF, OMIM#545000)**,

Nuclear gene mutations

In addition to mtDNA, nuclear genes can also be responsible for a wide spectrum of mitochondrial disorders. Nuclear genes are responsible for the greater number of components of OXPHOS system and are also required for the import of proteins into the mitochondrion, for the assembly and many other functions necessary to maintain a functional OXPHOS system. In addition, mtDNA replication, transcription and translation are absolutely dependent on nuclear encoded proteins.

Accordingly, a classification can be proposed for these defects, including:

- 1. Disorders due to defects in nuclear gene encoding structural components of the OXPHOS complexes**
- 2. Disorders due to defects in nuclear gene encoding assembly factors of the OXPHOS complexes**
- 3. Disorders due to gene defects affecting mtDNA maintenance**
- 4. Defects of genes encoding factors involved in the biosynthesis of lipids**
- 5. Defects of proteins involved in mitochondrial biogenesis or factors indirectly related to OXPHOS**

(1) Deficiencies of respiratory chain components

Although 72 of the 85 subunits of the OXPHOS system are encoded by nuclear DNA, mutations of these genes have only rarely been described. This could imply that such mutations are highly deleterious and probably embryolethal. Mutations that have been described in fact are usually associated to a neonatal or early-onset, although occasional patients with a late onset of disease have been reported. On the other hand the screening of the nuclear-encoded subunits of respiratory chain has not always been done in a systematic manner, especially for complex I, and only recently the number of reports regarding mutations in structural OXPHOS component is grown up. The mutations in nuclear encoded subunits identified so far, are mainly abnormalities of complex I found in patients with- infancy or childhood-onset, even if also mutations in structural subunits of complex II and IV were described.

(2) Respiratory chain complex assembly deficiencies

Mutations in assembly factors are a frequent cause of isolated complex I deficiency (Ogilvie, 2005). Mutations in cI assembly cause a wide range of clinical disorders, ranging from lethal neonatal disease to adult-onset neurodegenerative disorders. Phenotypes include macrocephaly with progressive leukodystrophy, nonspecific encephalopathy, cardiomyopathy, myopathy, liver disease, Leigh syndrome, Leber's hereditary optic neuropathy (Loeffen, 2000) Complex III deficiencies are reported, associated to mutations in the BCS1L gene. These mutations have been shown in infantile cases of complex III deficiency associated with neonatal proximal tubulopathy, hepatic involvement and encephalopathy (Zeviani, 2003) and in GRACILE syndrome comprising growth retardation, aminoaciduria, cholestasis, iron overload, lactic acidosis and early death (Visapaa, 2002). Defects of genes encoding assembly factors are also the main cause of complex IV deficiency. Almost all the nuclear-gene defects of COX identified are due to mutations in assembly factors of the enzyme, including SURF1 (Tiranti, 1998), SCO1 (Valnot, 2000a), SCO2 (Papadopoulou, 1999), COX10 (Valnot, 2000b), COX15 (Antonicka, 2003) and possibly LRPPRC (Mootha, 2003), and it is estimated that complex IV alone requires over 20 factors (Fontanesi, 2006). These autosomal recessive COX deficiencies usually present in early life with Leigh syndrome, myopathy, encephalopathy, lactic acidosis and a rapidly progressive course with early death. FASTKD2 mutations, reported in only one kindred, cause encephalomyopathy and convulsions and play a role in the regulation of mitochondrial apoptosis. Only two complex V nuclear mutations have been reported.

The ATP12 gene encodes for an assembly factor for the alpha and beta subunits, and is associated with one case of methylglutaconicaciduria with neurological involvement and dysmorphic features (De Meirleir, 2004). Recently, a large kindred of Gipsy origin with isolated Complex V deficiency and neonatal encephalocardiomyopathy were reported to present mutations in TMEM70, a gene encoding a transmembrane protein involved in the assembly of Complex V (Cizkova, 2008).

(3) Disorders due to gene defects altering the mtDNA maintenance

MtDNA remains dependent upon nuclear genome for the production of factors involved in its integrity and replication. Mutations in these factors affect mtDNA directly, either quantitatively or qualitatively, and cause diseases that are inherited as mendelian traits. A quantitative alteration is exemplified by abnormal reductions in the number of mtDNA molecules (both per cell and per organelle) called mtDNA-depletion syndromes. A qualitative alteration is exemplified by multiple deletions. Both quantitative and qualitative defects may result from impairment of the integrity of the mitochondrial genome. Such impairment can be direct (e.g., affecting proteins required for the replication and maintenance of mtDNA) or indirect (e.g., affecting proteins required to maintain nucleotide pools in mitochondria). For example, some families with autosomal dominant progressive external ophthalmoplegia have mutations in Twinkle (PEO1), a mitochondrial protein similar to bacteriophage T7 primase/helicase, whereas other

families have mutations in the mitochondrial adenine nucleotide translocator 1 (ANT1) (Nishino, 2000; Kaukonen J, 2000). Mutations in mitochondrial-specific DNA polymerase γ (POLG1), the key enzyme for mtDNA replication and repair, have been associated with both dominant and recessive multiple deletion disorders (Van Goethem G, 2001). Mitochondrial neurogastrointestinal encephalomyopathy is clearly due to the loss of function of thymidine phosphorylase (TYMP), resulting in markedly increased concentrations of thymidine in the blood (Nishino I, 2000). Thymidine phosphorylase is not a mitochondrial protein, yet it appears to have a selective effect on mitochondrial nucleotide pools required for maintaining the integrity and abundance of mtDNA.

(4) Defects of genes encoding factors involved in the biosynthesis of lipids

Except for cytochrome *c*, which is located in the intermembrane space, all components of the respiratory chain are embedded in the lipid milieu of the inner mitochondrial membrane, which is composed predominantly of cardiolipin. Cardiolipin is not merely a scaffold but is essential for proper functioning of several mitochondrial OXPHOS complexes and several mitochondrial carrier proteins (Gohil, 2004). This is the reason why defects in cardiolipin could cause OXPHOS dysfunction and hence mitochondrial disease. In fact there is an example on this regard, the Barth syndrome (mitochondrial myopathy, cardiomyopathy, growth retardation, and leukopenia) (Barth, 1999). The mutated gene in this syndrome, *TAZ* (or *G4.5*), encodes an acyl-coenzyme A synthetase (tafazzin) that must have an

important role in cardiolipin synthesis, because cardiolipin concentrations are markedly decreased in skeletal and cardiac muscle and in platelets from affected patients (Schlame, 2000).

(5) Defects of proteins involved in mitochondrial biogenesis or factors indirectly related to OXPHOS

Fission and fusion defects

Mitochondria are not static and isolated organelles but form a complex network. Mitochondrial fusion and fission require conserved protein machineries at the outer and inner membranes that mediate membrane mixing and division events. The proteins that regulate mitochondrial dynamics are now associated with a broad range of cellular functions: they play roles in maintaining the (1) integrity of mitochondria, (2) electrical and biochemical connectivity, (3) turnover of mitochondria, and (4) segregation and protection of mitochondrial DNA (Okamoto, 2005).

Defects of mitochondrial protein import

Two known mitochondrial diseases are clearly attributable to abnormal protein import.

X-linked Mohr–Tranebjaerg syndrome is characterized by deafness, followed by progressive neurological troubles, including dystonia and optic atrophy (Roesch, 2002); this disorder is due to mutations in *TIMM8A*, encoding DDP1 (deafness–dystonia protein1), a component of the import machinery for mitochondrial carrier proteins.

Mutation of *DNAJC19*, encoding a putative mitochondrial import protein, causes autosomal recessive dilated cardiomyopathy with ataxia (Davey, 2006).

Treatment of the mitochondrial diseases

There are many strategies to treat mitochondrial disease albeit an effective therapy is missing, to date. They are based on genetic or metabolic interventions, involving either correction of the affected gene or attenuation of the negative up- or downstream effects caused by the defective enzyme complex/complexes. These include (i) preventing transmission of mtDNA and mitochondrial nDNA gene defects, (ii) gene therapy (replacement or repair), (iii) altering the balance between wild-type and mutated mtDNA (i.e. exercise training), (iv) controlled regulation of specific transcriptional regulators and (v) metabolic manipulation (radical oxygen scavenging, mitochondrial calcium homeostasis, and uncoupling proteins). A recent and comprehensive review on this topic, was written by Koene et al. (2009), with the last new approaches, some of which have yet to be explored in humans.

An intervention used in patients with mitochondrial disease is the metabolic therapy.

Metabolic acidosis resulting from increased lactate production, a common feature in mitochondrial defects, can be treated, at least in the short-term, buffering with antacids such as sodium bicarbonate. Some drugs, which stimulates pyruvate oxidation (i.e.

dichloroacetate), has also been used to lower lactate concentration, but adverse effects preclude its widespread clinical use (Barshop, 2004).

In the rare mitochondrial disorder, MNGIE, due to mutations in *TP* gene (Hirano, 2005), the problem is the accumulation of dangerous nucleoside precursors, thymidine. A therapeutical symptomatic approach is to try to decrease the blood level of these substances through transfusions or by binding them to a water-soluble compound facilitating urinary excretion. Dietary supplementation of cofactors and vitamins is also widely used in the treatment of OXPHOS disease, but there is little evidence, apart from anecdotal reports, to support their use.

Creatine is the substrate for the synthesis of phosphocreatine, the most abundant energy storage compound in muscle, heart and brain. Different trials in patients with neuromuscular disorders gave opposite results regarding the efficacy of this substance. However considering the absence of adverse effects, creatinine supplementation may be warranted in patients with muscle weakness even before the confirmation of its efficacy.

Ubiquinone (CoQ) and its shorter chain analogue idebenone, could theoretically be effective for improving OXPHOS or, alternatively, as antioxidants or ROS scavengers. Although CoQ has shown some preliminary promising results in Parkinson's disease and Friedreich's ataxia (Rustin 1999), there have been no large-scale studies to determine the effectiveness of CoQ in these disorders. This treatment is most clearly effective in the small number of patients who have a specific CoQ deficiency (Salviati 2005).

Since defects of OXPHOS result in the increased production of free radicals, the use of antioxidants has some sound basis. This is the reason of the supplementation with vitamins like tocopherols (Kir, 2005). The above reported CoQ and N-acetylcysteine reduce free radical production in cybrids (Mattiuzzi, 2004). More recently, antioxidant compounds, which are directly targeted to mitochondria have been shown to be effective in cultured cell models of OXPHOS disease, but has yet to be tested in a clinical trial (James, 2005).

HYDROGEN SULFIDE IN HEALTH AND DISEASES

Physico-chemical properties

Sulfur, one of the essential elements for life, occurs in different oxidation states, from -2 (as in sulfide, S^{2-}) to +6 (as in sulfate, SO_4^{2-}). It is present in living organisms as a constituent of proteins (mainly in sulfurated aminoacids such as cysteine and methionine), in coenzymes (namely CoA, biotine and thiamine), and as a component of iron-sulfur clusters in metalloproteins. From a physico-chemical standpoint, H_2S is the sulfur analog of water, but, since its intermolecular bounds are weaker than H_2O , at room temperature and atmospheric pressure is a gas. In mammals, at a physiological pH of 7.4, approximately one-third of H_2S exists as the un-dissociated form and two-thirds as the hydrosulfide anion (HS^-) (Wang R, 2002). In the un-dissociated form, H_2S can easily penetrate the plasma membranes of cells because of its high solubility in lipids.

H_2S metabolism in mammals

H_2S is endogenously produced in mammals by two pyridoxal-5'-phosphate-dependent enzymes, cystathionine β -synthase (CBS) and cystathionine γ -lyase (CSE) that both utilize L-cysteine as a substrate (Abe K, 1996). The latter is either taken up with the diet, extracted from endogenous proteins, or synthesized endogenously via trans-

sulfuration of serine by L-methionine. In humans, the end products of cysteine sulfur catabolism are sulfate, which accounts for 77-92% of the total sulfur excreted in the urine, sulfate esters (7-9%), and taurine (2-6%) (Stipanuk MH, 2004). In some tissues, both CBS and CSE can generate H₂S, whereas in others only one enzyme is present. For instance, CBS is predominantly expressed in the nervous system but is also active in liver and kidney. CSE is mainly expressed in liver, as well as vascular and non-vascular smooth muscle, e.g. small intestine and stomach.

An important, additional source of H₂S is the enterobacterial anaerobic flora. The intestinal epithelium expresses specialized enzyme systems that efficiently convert H₂S into thiosulfate and sulfate, to both prevent the local increase of H₂S to toxic levels, and its entry through the portal vein system in the liver and other organs.

A third, however marginal, source of H₂S is the non-enzymatic reduction of elemental sulfur, which is present in traces in human and mouse blood, into H₂S by electrons provided through glycolysis.

The main catabolic pathway of H₂S takes place in mitochondria, and consists of a series of oxidative reactions ultimately yielding thiosulfate (S₂O₃²⁻), sulfite (SO₃²⁻) and sulfate (SO₄²⁻) (Szabó C, 2007). The existence of such a pathway is known since more than 20 years, although the enzymatic actors and detailed steps have been elucidated only recently (Hildebrandt TM, 2008). The pathway consists of (i) a mitochondrial inner membrane-bound sulfide-quinone reductase (SQR), that fixes H₂S to an -SH containing substrate, to form a persulfide (R-S-SH) species; (ii) a mitochondrial matrix sulfur

dioxygenase (SDO), that oxidizes the sulfur atom extracted from persulfide, converting it into sulfite (SO_3^{2-}); and (iii) either sulfite oxidase, that further oxidizes sulfite into sulfate (SO_4^{2-}), or rhodanese, a sulfur transferase that can combine two sulfite molecules to form thiosulfate (SSO_3^{2-}). Thiosulfate can eventually be converted into two molecules of sulfate by the combined action of a thiosulfate reductase and sulfite oxidase. Additional mechanisms of detoxification rely on the fixation of H_2S to methemoglobin, which is formed from hemoglobin by oxidation of the Fe center, for instance by sodium nitrate, to produce sulfmethemoglobin, or on the administration of oxidised glutathione (GSSG), that is able to fixate H_2S to produce glutathione persulfide (GSSH), thus preventing the interaction of H_2S with critical enzymatic activities.

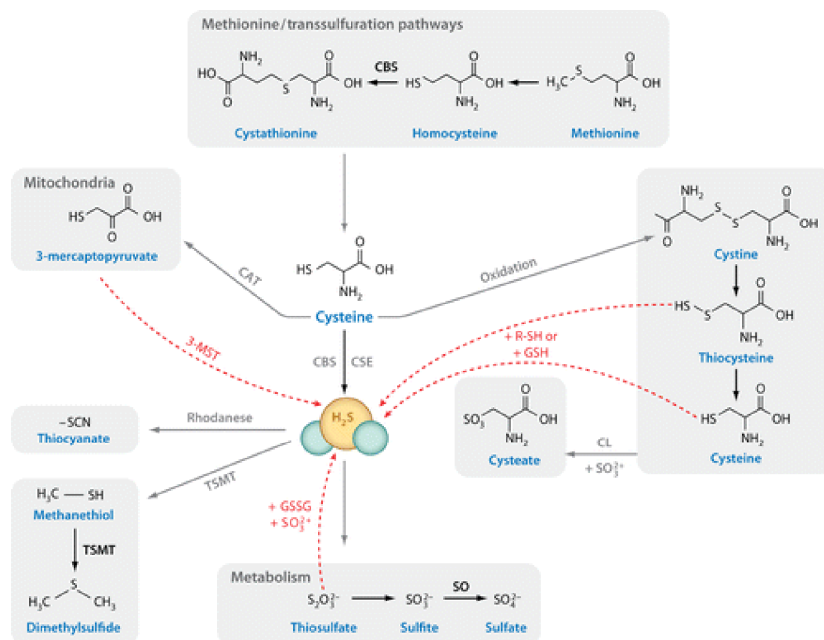


Figure 5. Hydrogen sulfide metabolism in mammals

Physiological role of H₂S

H₂S possess a multiplicity of physiological functions, including up-regulation of antioxidant systems; up-regulation of anti-inflammatory and cytoprotective genes including heme oxygenase (HO1) in pulmonary smooth muscle cells, and macrophages. In the central nervous system (CNS), low concentrations of H₂S increase the production of cAMP, enhance N-methyl-d-aspartate (NMDA)-receptor mediated responses, and facilitate the induction of long-term potentiation in hippocampal neurons (Kimura Y, 2004). H₂S acts also on myocardial cells and vascular smooth muscle. By activating K_{ATP} channels, H₂S increases the membrane potential of vascular smooth muscle cells that become hyperpolarized, causing vasorelaxation (Eley DJ, 2010). H₂S plays a role as a smooth muscle relaxant, and suggesting that it may physiologically regulate blood pressure. Another effect is the induction of smooth muscle cells proliferation by activating the PI3 Kinase/Akt pathway, thus stimulating angiogenesis, and apoptosis by activating the mitogen activated protein kinase (MAPK) pathway (Yang G, 2004). Finally, H₂S can directly modulate the function of the heart, with negative inotropic and chronotropic effects, that are mediated by activation of K_{ATP} channels (Ferdinandy P, 2007).

Toxic effects of H₂S

Whilst H₂S acts as a cytoprotective agent at physiological (nanomolar) concentrations, at micromolar concentrations it can interfere with a

variety of cellular functions, including mitochondrial respiration, via inhibition of cytochrome c oxidase, (Hill B. C., 1984). COX activity is inhibited by the formation of a covalent bond between H₂S and the Fe atom coordinated by heme a, which is exquisitely sensitive to the toxic action of H₂S (and cyanide as well). H₂S is also an inhibitor of carbonic anhydrase (Coleman J. E., 1967), an effect that could explain the alterations of ventilatory dynamics in response to inhaled H₂S, due to changes in the reactivity and distribution of intrapulmonary CO₂ receptors. A further effect of H₂S is inhibition of enzymatic activity of short-chain acyl-CoA dehydrogenase (SCAD), which can cause dicarboxylic aciduria (Pedersen CB, 2003). Acute exposure to gaseous H₂S causes anoxic brain injury, pulmonary edema, and death. Neurological impairment is consistent with prolonged brain hypoxia while respiratory insufficiency and pulmonary edema are consistent with acute respiratory syndrome. These two injuries are the most likely cause of death after acute exposure to H₂S, while chronic exposure to low levels determines irritant effects including upper airway inflammation, conjunctivitis, and wheezing. A direct effect of H₂S on the respiratory center in the brainstem, resulting in apnea, is likely to be caused by inhibition of cytochrome c oxidase activity (Yalamanchili C, 2008).

H₂S in human pathology

Cardiovascular and neurodegenerative disorders

H₂S has recently been shown to play an important role in the pathogenesis of atherosclerosis, a complex degenerative process of large- and medium-size arteries. As a major by-product of sulfate-reducing bacteria, H₂S has been implicated in the pathogenesis of ulcerative colitis (Roediger WE, 1993), by, for instance, toxicity on colonocytes due to the block of butyrate oxidation via SCAD inhibition.

Overproduction of H₂S has been documented in Down-syndrome patients since the CBS gene is localized on chromosome 21. CBS transcript is in fact over-expressed in fibroblasts and myeloblasts of individuals affected by Down syndrome. The abnormally high concentration of thiosulfate, the main catabolite of H₂S detected in Down syndrome patients can account for symptoms such as muscle hypotonia and mental retardation (Kamoun P, 2003).

Low levels of H₂S have been found in the substantia nigra (SN) of a pharmacologically-induced rat model of Parkinson's disease (PD) (Hu LF, 2010). A role of H₂S in the cognitive decline of Alzheimer's disease (AD) patients has also been proposed. AD brains show severe reduction of both CBS activity and H₂S amount, compared to age-matched control individuals. Accordingly, S-adenosyl-L-methionine, a CBS activator, is reduced in AD brains and homocysteine, a CBS substrate, accumulates in the serum of AD patients (Clarke R, 1998).

Inborn errors of sulfur metabolism

Sulfite Oxidase Deficiency (SUOX)

Sulfite oxidase (SUOX) deficiency (OMIM #606887) is a severe, autosomal recessive inborn error of metabolism impairing the catabolism of sulfur-containing amino acids. The disease affects newborn individuals that show intractable seizures, characteristic dysmorphic features, lens dislocation, and profound mental retardation (Irreverre F, 1967). Genetic defects of SUOX are associated with the accumulation of sulphite and thiosulfate. SUOX is a mitochondrial enzyme located in the intermembrane space and works as a homodimer with a molecular mass of around 110kDa. SUOX is a metalloenzyme containing a molybdenum cofactor (Moco) that catalyzes the oxidation of sulfite to sulfate, in the last step of the metabolism of sulfur-containing compounds. The treatment of SUOX deficiency is based on a low-protein diet, supplemented with non-sulfurated aminoacids (Shih VE, 1977). This regimen determined a decrease of urinary thiosulfate and S-sulfocysteine, and of plasma methionine and cystine in two patients, which grew normally with no signs of neurologic deterioration, and with progresses in psychomotor development.

Molybdenum cofactor deficiency

Molybdenum cofactor deficiency (OMIM #252150) is a rare autosomal recessive disorder that results in pleiotropic loss of all molybdoenzyme activities, resulting in neonatal seizures and severe neurologic damage leading to early death. Moco biosynthesis involves

the formation of precursor Z by proteins encoded by MOCS1 genes, the subsequent conversion of precursor Z to molybdopterin (MPT) is carried out by the two subunits of MPT synthase, which are coded by a bicistronic MOCS2 gene (Reiss J, 1999). In the final step, molybdenum is attached to the dithiolene moiety of MPT by gephyrin (GPHN). Patients with molybdenum cofactor deficiency can be classified as having complementation group A or B deficiency, both of which have identical phenotypes. Patients with group A deficiency have mutations in MOCS1 and are defective in the formation of precursor Z from GTP. Patients with group B deficiency are defective in MPT synthase. A third complementation group, group C, is due to defects in the gephyrin gene. In the majority of the cases, the main clinical manifestations include brain abnormalities, mental retardation and intractable seizures. In comparison with sulfite oxidase deficiency due to SUOX gene mutations, molybdenum cofactor deficiency responds better to dietary interventions (Shih VE, 1977). In a 5-month-old girl with molybdenum cofactor deficiency the dietary restriction of methionine accompanied by supplementation of cysteine led to rapid clearance of urinary sulfites, and improvement of neurological development.

Homocystinuria due to CBS (cystathionine Beta-Synthase) deficiency

Cystathionine beta-synthase (CBS) condensates homocysteine and serine to form cystathionine, which is subsequently converted into cysteine and alpha-ketobutyrate. The active enzyme is a homotetramer composed of four 63-kD subunits and requires pyridoxal phosphate and heme (Meier M, 2001). Each subunit binds three ligands;

pyridoxal 5'-phosphate (PLP), AdoMet, an allosteric activator, and heme, the function of which is unknown. The onset of CBS deficiency (OMIM #236200) is usually in the first or second decade of life. Clinical features include myopia, ectopia lentis, mental retardation, skeletal anomalies resembling Marfan syndrome (Pyeritz RE, 1979), and thromboembolic episodes. Light skin and hair can also be present, possibly because of an inhibitory effect of homocysteine on tyrosinase. Biochemical features include increased urinary levels of homocysteine and methionine. Two main presentations have been reported: a milder pyridoxine (vitamin B6)-responsive form, and a more severe pyridoxine-non responsive form (Testai FD, 2010). Additional therapeutic treatments include a low methionine diet with cysteine supplementation and betaine.

Cystathionase deficiency

Cystathionase deficiency (OMIM #219500) is an autosomal recessive, relatively benign condition with no striking pathological features except for the accumulation in plasma and increased urinary excretion, of cystathionine. Nonsense and missense mutations have been identified in the CTH gene in 4 unrelated patients with cystathioninuria (Wang J, 2003).

ETHYLMALONIC ENCEPHALOPATHY

Clinical features

Ethylmalonic encephalopathy (EE) (OMIM #602473) is a rare, autosomal recessive, invariably fatal disorder mainly found in families of Mediterranean or Arabic decent. Only 70 cases worldwide have been documented since the disease was first described by Burlina and collaborators in 1991, demonstrating the rarity of this disorder (Burlina, 1991). Common symptoms found in EE patients include chronic hemorrhagic diarrhea, a delay in neural development, symmetric brain lesions, recurrent petechiae, muscle hypotonia, and severe orthostatic acrocyanosis, which ultimately lead to death within the first decade of life. The onset and degree of severity of these symptoms vary from patient to patient; however, the majority of these symptoms occur early in development. All patients with EE display some level of muscle weakness and spasms as well as abnormal cranial MRI scans with varying levels of brain atrophy depending on disease progression. The main neuroimaging features of the disease are patchy, bilateral necrotic lesions in the basal ganglia and brainstem, thinning of the brain cortical ribbon and corpus callosum, and leukodystrophic changes in the centrum semiovale. The majority of these patients showed severe delays in both cognitive and psychomotor functions (Burlina et al, 1991; Garcia-Silva, 1994; Garavaglia et al, 1994).

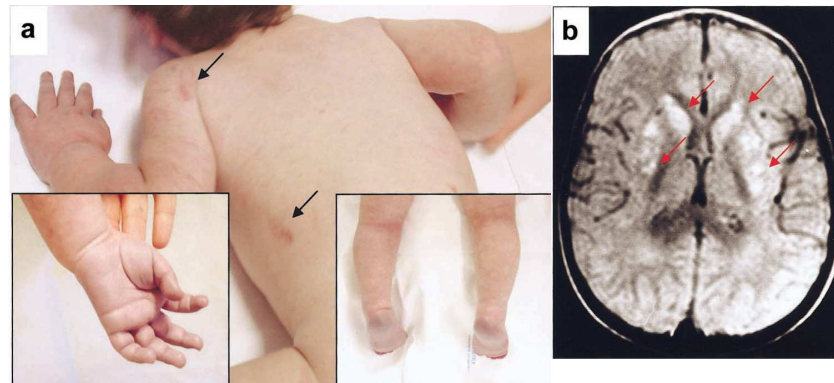


Figure 6. Clinical features of EE.

(a), Skin areas with petechiae are indicated by arrows. The boxed pictures show acrocyanosis of hands and feet. (b), On MRI images of a transverse section of the brain, symmetrical, patchy, high-intensity signals are present in the head of nucleus caudatus and in the putamen (*arrows*).

Biochemical Markers

In addition to the common symptoms associated with EE, patients also exhibit several biochemical traits including lactic acidemia, deficiency of Cytochrome C Oxidase (COX), the last component (complex IV, cIV) of the mitochondrial respiratory chain (RC), in the skeletal muscle and brain, increase in C₄₋₅ acylcarnitines in blood, elevated levels of methylsuccinic and ethylmalonic acid (EMA) and thiosulfate in urine, and accumulation of sulfide (H₂S), the most recently discovered gasotransmitter, in tissues and plasma (Tiranti, 2009). The production of EMA is elevated when there are high levels of butyryl-CoA that can be carboxylated through propionyl-CoA carboxylase to ethylmalonyl-CoA allowing for the hydrolysis of ethylmalonyl-CoA to free EMA (Burlina, 1994). The abnormal accumulation of butyryl-CoA can occur through at least two possible pathways: disorders of the short-chain fatty acid cycle resulting in a

build-up of butyryl-CoA or the R-isoleucine catabolism pathway from 2-ethylmalonic- semialdehyde. Evidence for the production of EMA as a result of defects in β -oxidation is seen in disorders involving mutations in the short-chain acyl-CoA dehydrogenase (SCAD), as well as glutaric academia type 2, and Jamaican vomiting sickness, although none of these disorders can account for all the symptoms associated with EE, including diarrhea and the recurrent petechiae seen in EE patients. Lactic acidemia is a very common hallmark in a number of metabolic disorders and can result from a cascade of events in cellular respiration that depletes the cellular central energy pathways. Lactic acid build up results from a blockage in glycolysis, which in turn, limits acetyl-CoA thereby inactivating the citric acid cycle (CAC). This inactivation of the CAC further leads to the depletion of NADH and reduces the activity of the electron transport system. Additionally, the excretion of acylcarnitines suggests a buildup of acyl-CoAs found typically when there is a block in fatty acid oxidation, further leading to a depletion of energy metabolism.

Ethylmalonic Encephalopathy 1 (ETHE1) gene and protein

In 2004, homozygosity mapping revealed the molecular defect associated with EE. In this technique, mapped restriction length polymorphisms (RFLPs) in the DNA of affected EE children from inbred marriages were analyzed, and the disease locus detected using the assumption that the adjacent region of the locus was homozygous by descent in inbred children (Tiranti V, 2004). Using this technique, it was shown that mutations in the gene Ethylmalonic Encephalopathy

protein 1 (ETHE1) are directly associated with the disease EE. Preliminary characterization of ETHE1 revealed that it contains orthologs in a wide range of organisms, including archaeobacteria, fungi, plants, and animals, suggesting that ETHE1 serves a fundamental biochemical role. A pairwise alignment of ETHE1-like proteins from a variety of organisms identified a number of highly-conserved residues including the amino acids Y38, T136, C161, R163, and L185, of which mutations were found in EE patients (Tiranti V, 2004; Tiranti V, 2006). Therefore, these residues are likely critical for ETHE1 function.

The ETHE1 protein, a 30 kDa polypeptide located in the mitochondrial matrix, is a homodimeric, β -lactamase Fe-binding enzyme. ETHE1 is actively translocated across the inner mitochondrial membrane and is processed to a mature form by the cleaving off of a small N-terminal mitochondrial targeting sequence. The mature protein starts from Val8, and that the mitochondrial targeting sequence is cut off at the Arg7-Val8 (Tiranti V, 2009).

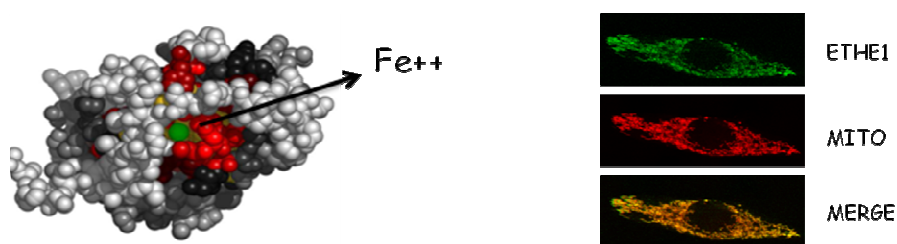


Figure 7. ETHE1 protein structure and localization

Left: three-dimensional representation of ETHE1 protein structure; *Right:* ETHE1 mitochondrial localization showed by co-immunofluorescence assay with MitoTracker® Red in HeLa cells.

ETHE1 protein possess a sulfur dioxygenase (SDO) activity (Tiranti V, 2009), being part of a mitochondrial oxidative pathway for inorganic sulfur that ultimately converts sulfide into harmless compounds, such as thiosulfate and sulfate. This pathway is composed of four enzymes. First, a membrane-bound mitochondrial Sulfide Quinone Reductase (SQR) is involved in the initial oxidation of H_2S and the fixation of its sulfur atom to a sulfur acceptor, with the formation of a persulfide (-SSH). SQR conveys the hydrogen atoms extracted from H_2S to feed respiratory complex III. Next, the persulfide compound is further oxidized to sulfite by molecular oxygen through the action of ETHE1-SDO. The enzyme Rhodanese, which displays a sulfur transferase activity, acts in the third step, allowing sulfite to be trans-sulfurated in the mitochondrial matrix and converted into a metabolic end product, thiosulfate (Hildebrandt TM and Grieshaber MK, 2008). Alternatively, sulfite can also be directly oxidized to sulfate by another mitochondrial matrix enzyme, Sulfite Oxidase (SUOX).

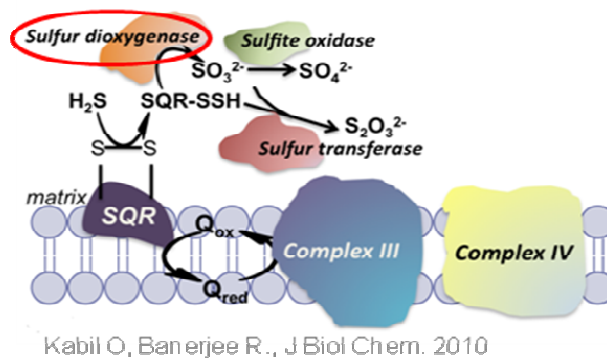


Figure 8. Mitochondrial oxidative pathway for inorganic sulfur
 SQR: sulfide-quinone reductase; H_2S : hydrogen sulfide; SO_3^{2-} : sulfite; SO_4^{2-} : sulfate; $S_2O_3^{2-}$: thiosulfate; Q_{ox} : oxidized ubiquinone; Q_{red} : reduced ubiquinone.

Ethylmalonic Encephalopathy mouse model

To further explore the pathophysiological role of the ETHE1 protein, in 2009 Tiranti and collaborators generated a constitutive knockout mouse model for ETHE1 gene. This animal model recapitulates all the main phenotypical and biochemical features of the human EE. *Ethe1*^{-/-} mice show growth arrest from postnatal day 15 and reduced motor activity with wide-based gait, and they die between the fifth and sixth week after birth. Histochemical and biochemical analysis revealed that COX activity was normal in liver, moderately decreased in jejunum, and markedly low in muscle and brain. It was also virtually absent in luminal colonocytes but present in cryptal colonocytes.; activities of other mitochondrial respiratory chain (MRC) enzymes, including complex I and complex II, were normal. Analysis of body fluids showed increased amounts of lactate and C₄₋₅ acylcarnitines in blood and increased concentrations of ethylmalonic acid in *Ethe1*^{-/-} mice urines, similarly to individuals with ethylmalonic encephalopathy. Urinary thiosulfate abundance was several-fold higher, and sulfate abundance was lower than in controls, whereas sulfite was undetectable. In addition, thiosulfate was markedly increased in *Ethe1*^{-/-} kidney and liver, and a similar trend was present in muscle and brain, suggesting increased endogenous production of thiosulfate. The concentration of H₂S in liver, muscle and brain of *Ethe1*^{-/-} mice was indeed much higher than in wild-type littermate tissues (Tiranti V, 2009). H₂S is a colorless gas with a characteristic smell of rotten eggs. In mammalian tissues, H₂S is a gasotransmitter acting as a signaling molecule, but at supraphysiological concentrations it is a powerful inhibitor of COX (Leschelle X, 2005) and of the short-chain

acyl-CoA dehydrogenase (SCAD) (Tiranti V, 2009). H₂S is released in large amounts by bacteria residing in the lumen of the large intestine (Furne J, 2001). The marked reduction of COX activity in *Ethe1*^{-/-} luminal colonocytes, whereas COX activity was normal in cryptal colonocytes that are relatively secluded from the luminal surface, reflects different degrees of exposure of the two cell populations to the inhibitory action of exogenous H₂S. Notably, a decrease in H₂S detoxification could have a major role in colonic mucosal damage that is characteristic of conditions associated with severe chronic diarrhea, for instance ulcerative colitis (Roediger WE, 2008). H₂S is vasoactive and, at high concentrations, is toxic to endothelial cells (Szabo C, 2007), which explain the acrocyanosis and the vascular damage that is characteristic of EE. The study of the ETHE1 mouse model indicate that EE is a disease associated with impaired catabolism of inorganic sulfur leading to accumulation of H₂S in key tissues. The toxic effects of H₂S can account for several features of EE, including ethylmalonic aciduria, COX deficiency, microangiopathy, acrocyanosis and chronic diarrhea.

Treatments

H₂S is mainly released by bacterial anaerobes of the large intestine, but endogenous production in trace amounts occurs in virtually all organs. Viscomi and collaborators used the *Ethe1*^{-/-} mouse model to test a therapeutic strategy aiming at decreasing bacterial production of H₂S and neutralizing toxic H₂S (Viscomi C, 2010). Metronidazole (Mancardi D, 2009) is a bactericidal nitroimidazole effective against

anaerobic bacteria. *N*-acetylcysteine, a cell-permeable precursor of GSH (Atkuri KR, 2007) that can accept the sulfur atom of H₂S through the action of sulfide-CoQ reductase (Hildebrandt TM, 2008), forming nontoxic GSSH persulfide (which can, in turn, become a substrate of ETHE1). Combined treatment led the median survival of *Ethe1*^{-/-} mice to shift from 24 to 71.5 d, indicating an additive effect. Although the serum concentration of thiosulfate, a stable and readily measurable index of H₂S, was still much higher than normal, it significantly decreased in treated *Ethe1*^{-/-} mice compared to untreated *Ethe1*^{-/-} mice, suggesting that the combined therapy acted specifically against accumulation of H₂S and H₂S-related compounds. In sharp contrast with untreated *Ethe1*^{-/-} mice, treated *Ethe1*^{-/-} mice had an increase in body weight similar to, albeit less than, control littermates. Although the histochemical reaction to COX was equally low in muscle and brain of treated and untreated *Ethe1*^{-/-} mice and remained low in a treated *Ethe1*^{-/-} mouse, the severe COX depletion in colonocytes of untreated *Ethe1*^{-/-} mice disappeared completely and persistently in the treated *Ethe1*^{-/-} mice.

Given the results in the mouse model, an Italian patient, carrying a homozygous mutation in ETHE1 (Mineri R, 2008) encoding an L55P substitution, was treated. He had manifested the clinical and biochemical signs typical of ethylmalonic encephalopathy since 6 months of age. Despite dietary manipulations consisting of reducing intake of monosaccharides, which have a stronger osmotic effect, in favor of polysaccharides and consuming only hydrolyzed proteins, as well as coenzyme Q10 supplementation (50 mg per day), progression of his main clinical features occurred in the following months. A

magnetic resonance imaging (MRI) scan at 28 months showed brain atrophy, leukodystrophy and patchy lesions of the basal nuclei. Diffuse petechiae of the trunk and limbs and acrocyanosis were worsened, as observed by the patient's physician. At 29 months of age, the patient was treated with a daily therapy consisting of oral metronidazole and *N*-acetylcysteine. During the next 8 months, patient shows an increase in body weight, a marked reduction and then virtual disappearance of diarrhea, petechial showers and acrocyanosis and marked neurological improvement, with a lower frequency of seizure attacks from several per day to less than one a week. The EEG showed the disappearance of slow-voltage waves. Truncal hypotonia became less severe, and spontaneous motor activity ensued at the lower limbs. A brain MRI at 36 months of age showed a reversion of brain atrophy and a reduction in leukodystrophy, although the lesions in the neostriatum had become more evident. Ethylmalonic acid (EMA) in urine and plasma dropped significantly and persistently, and so did the concentrations of C4 acylcarnitines. The noteworthy prolongation of lifespan in *Ethel*^{-/-} mice and the evidence-based clinical improvement in patients make the combined treatment with metronidazole and *N*-acetylcysteine at the moment the most effective therapy available for ethylmalonic encephalopathy (Viscomi C, 2010).

SCOPE OF THE THESIS

My researches during the DIMET project have been focused on the investigation of the molecular pathogenesis of the Ethylmalonic Encephalopathy and on the implementation of the diagnostic applications.

Ethylmalonic Encephalopathy, EE, is an autosomal recessive, invariably fatal disorder characterized by early-onset brain failure, microangiopathy, chronic diarrhoea, defective cytochrome c oxidase (COX) in muscle and brain, and high excretion of ethylmalonic acid (EMA) in urine. ETHE1, a gene encoding a mitochondrial beta-lactamase-like, iron-coordinating metalloprotein, is mutated in EE. We generated an *Ethe1*-null mouse that manifested the EE cardinal features. We found that thiosulfate was excreted in massive amount in urines of both *Ethe1*^{-/-} mice and EE patients. High thiosulfate (H₂SSO₃) and sulfide (H₂S) levels were present in *Ethe1*^{-/-} mouse tissues. Sulfide is a powerful inhibitor of COX and terminal beta-oxidation, with vasoactive and vasotoxic effects that could explain the microangiopathy in EE patients. Sulfide is detoxified by a mitochondrial pathway that includes a sulfur dioxygenase (SDO). SDO activity was absent in *Ethe1*^{-/-} mice, whereas ETHE1 overexpression in HeLa cells and *E. coli* markedly increased it. Therefore, ETHE1 is a mitochondrial SDO involved in catabolism of sulfide, which accumulates to toxic levels in EE.

An important question that warranted the PhD experimental work concerns the source of H₂S in ETHE1 mutant patients, and how accumulated sulfide can act on the cytochrome c oxidase complex at molecular level. The presence of elevated levels of thiosulfate in several tissues of the *Ethe1*^{-/-} mouse suggests endogenous production of H₂S from catabolism of cysteine and other sulfur-containing organic compounds. H₂S is also a major product of the intestinal bacterial flora, especially anaerobic species residing in the colon. The presence of a gradient of COX deficiency in luminal vs. cryptal colonocytes in *Ethe1*^{-/-} colon mucosa suggests that a defect of ETHE1-SDO activity results in faulty detoxification of exogenously produced H₂S. In order to achieve effective reduction of H₂S production, it is crucial to clarify which are the sources of this compound in the body that can then constitute specific targets for therapy. Another important issue is to understand the organ-specific mechanisms, which lead to failure of some organs, such as the brain and the skeletal muscle, but not of others, such as the liver. These aims can be implemented through the creation and characterization of conditional tissue-specific KO animals.

A further research line concerns the improvement of biochemical and molecular approaches for the diagnosis of EE.

References:

Abe K, Kimura H (1996). The possible role of hydrogen sulfide as an endogenous neuromodulator. *J Neurosci.* 16: 1066-711996.

Antonicka H, Mattman A, Carlson CG, Glerum DM., Hoffbuhr KC, Leary SC, Kennaway NG, and Shoubridge EA (2003). Mutations in COX15 produce a defect in the mitochondrial heme biosynthetic pathway, causing early-onset fatal hypertrophic cardiomyopathy. *Am J Hum Genet* 72, 101-114.

Atkuri KR, Mantovani JJ, Herzenberg LA, Herzenberg LA (2007). N-Acetylcysteine-a safe antidote for cysteine/glutathione deficiency. *Curr Opin Pharmacol.*7: 355-359.

Barshop BA, Naviaux RK, McGowan KA, Levine F, Nyhan WL, Loupis-Geller A, Haas RH. (2004) Chronic treatment of mitochondrial disease patients with dichloroacetate. *Mol Genet Metab.* 83(1-2):138-49.

Barth PG, Wanders RJ, Vreken P, Janssen EA, Lam J, Baas F. (1999) X-linked cardioskeletal myopathy and neutropenia (Barth syndrome) (MIM 302060). *J Inheret Metab Dis.* 22(4):555-67.

Bereiter-Hahn J, Vöth M. (1994) Dynamics of mitochondria in living cells: shape changes, dislocations, fusion, and fission of mitochondria. *Microsc Res Tech.* 15;27(3):198-219.

Boyer PD (1993). The binding change mechanism for ATP synthase - some probabilities and possibilities. *Biochim Biophys Acta* 1140, 215-250.

Brown RE, Bhuvaneshwaran C, Brewster M. (1988) Effects of peroxidized polyunsaturated fatty acids on mitochondrial function and structure: pathogenetic implications for Reye's syndrome. *Ann Clin Lab Sci.* 18(4):337-43.

Burlina A, Zacchello F, Dionisi-Vici C, Bertini E, Sabetta G, Bennet MJ, Hale DE, Schmidt-Sommerfeld E, Rinaldo P (1991). New clinical phenotype of branched-chain acyl-CoA oxidation defect. *Lancet*. 338: 1522-3.

Burlina AB, Dionisi-Vici C, Bennett MJ, Gibson KM, Servidei S, Bertini E, Hale DE, Schmidt-Sommerfeld E, Sabetta G, Zacchello F, et al. (1994). A new syndrome with ethylmalonic aciduria and normal fatty acid oxidation in fibroblasts. *J Pediatr.*;124(1):79-86.

Carew JS, and Huang P (2002). Mitochondrial defects in cancer. *Mol Cancer* 1, 9.

Carroll J, Fearnley IM, Skehel JM, Shannon RJ, Hirst J, and Walker JE (2006). Bovine Complex I Is a Complex of 45 Different Subunits. *J. Biol. Chem.* 281, 32724-32727.

Cízková A, Stránecký V, Mayr JA, Tesarová M, Havlícková V, Paul J, Ivánek R, Kuss AW, Hansíková H, Kaplanová V, Vrbacký M, Hartmannová H, Nosková L, Honzík T, Drahotka Z, Magner M, Hejzlarová K, Sperl W, Zeman J, Houstek J, Kmoch S. (2008) TMEM70 mutations cause isolated ATP synthase deficiency and neonatal mitochondrial encephalocardiomyopathy. *Nat Genet.* 40(11):1288-90.

Clarke R., Smith D., Jobst K.A., Fefsum H., Sutton L., Ueland P.M. (1998) Folate, vitamin B12, and serum total homocysteine levels in confirmed Alzheimer disease, *Arch. Neurol.* 55: 1449–1455.

Coleman, J. E (1967). Mechanism of action of carbonic anhydrase. Substrate, sulfonamide, and anion binding. *J. Biol. Chem.* 242: 5212–5219.

Davey KM, Parboosingh JS, McLeod DR, Chan A, Casey R, Ferreira P, Snyder FF, Bridge PJ, Bernier FP. (2006) Mutation of DNAJC19, a human homologue of yeast inner mitochondrial membrane co-chaperones, causes DCMA syndrome, a novel autosomal recessive Barth syndrome-like condition. *J Med Genet.* 43(5):385-93.

- Debray FG, Lambert M, Mitchell GA. (2008) Disorders of mitochondrial function. *Curr Opin Pediatr*.20(4):471-82.
- De Meirleir L, Seneca S, Lissens W, De Clercq I, Eyskens F, Gerlo E, Smet J, and Van Coster R (2004). Respiratory chain complex V deficiency due to a mutation in the assembly gene ATP12. *J Med Genet* 41, 120-124.
- Dimauro S, & Davidzon G. (2005) Mitochondrial DNA and disease. *Ann Med* 37: 222–32.
- DiMauro S, & Schon EA. (2001) Mitochondrial DNA mutations in human disease. *Am J Med Genet* 106: 18–26.
- DiMauro S, and Schon EA (2003). Mitochondrial respiratory-chain diseases. *N Engl J Med* 348, 2656-2668.
- Elsley DJ, Fowkes RC, Baxter GF (2010). Regulation of cardiovascular cell function by hydrogen sulfide (H₂S). *Cell Biochem Funct*, 28: 95-106.
- Ferdinandy P, Schulz R, Baxter GF (2007). Interaction of cardiovascular risk factors with myocardial ischemia/reperfusion injury, preconditioning, and postconditioning. *Pharmacol Rev.* 59: 418-58.
- Fontanesi F, Soto IC, Horn D, Barrientos A. (2006) Assembly of mitochondrial cytochrome c-oxidase, a complicated and highly regulated cellular process. *Am J Physiol Cell Physiol.* 291(6):C1129-47.
- Garavaglia B, Colamaria V, Carrara F, Tonin P, Rimoldi M, Uziel G (1994). Muscle cytochrome c oxidase deficiency in two Italian patients with ethylmalonic aciduria and peculiar clinical phenotype. *J Inherit Metab Dis* ;17(3):301-3.
- García-Silva MT, Campos Y, Ribes A, Briones P, Cabello A, Santos Borbujo J, Arenas J, Garavaglia B (1994). Encephalopathy, petechiae,

and acrocyanosis with ethylmalonic aciduria associated with muscle cytochrome c oxidase deficiency. *J Pediatr* ;125(5 Pt 1):843-4.

Gohil VM, Hayes P, Matsuyama S, Schägger H, Schlame M, Greenberg ML. (2004) Cardiolipin biosynthesis and mitochondrial respiratory chain function are interdependent. *J Biol Chem.* 279(41):42612-8.

Hildebrandt TM, Grieshaber MK (2008). Three enzymatic activities catalyze the oxidation of sulfide to thiosulfate in mammalian and invertebrate mitochondria. *FEBS J.* 275: 3352-61.

Hill, B. C. et al (1984). Interactions of sulphide and other ligands with cytochrome c oxidase. An electron-paramagnetic-resonance study. *Biochem. J.* 224: 591–600.

Hirano M, Lagier-Tourenne C, Valentino ML, Martí R, Nishigaki Y. (2005) Thymidine phosphorylase mutations cause instability of mitochondrial DNA. *Gene* 354:152-6.

Holt IJ, Harding AE, and Morgan-Hughes JA (1988) Deletions of muscle mitochondrial DNA in patients with mitochondrial myopathies. *Nature* 331, 717-719.

Hu LF, Lu M, Tiong CX, Dawe GS, Hu G, Bian JS (2010). Neuroprotective effects of hydrogen sulfide on Parkinson's disease rat models. *Aging Cell.* 9: 135-46.

Irreverre, F., Mudd, S. H., Heizer, W. D., Laster, L (1967). Sulfite oxidase deficiency: studies of a patient with mental retardation, dislocated ocular lenses, and abnormal urinary excretion of S-sulfo-L-cysteine, sulfite and thiosulfate. *Biochem. Med.* 1: 187-199.

James AM, Cochemé HM, Smith RA, Murphy MP. (2005) Interactions of mitochondria-targeted and untargeted ubiquinones with the mitochondrial respiratory chain and reactive oxygen species. Implications for the use of exogenous ubiquinones as therapies and experimental tools. *J Biol Chem.* 280(22):21295-312.

Kamoun P, Belardinelli MC, Chabli A, Lallouchi K, Chadefaux-Vekemans B (2003). Endogenous hydrogen sulfide overproduction in Down syndrome. *Am J Med Genet A*. 116A: 310-1.

Kaukonen J, Juselius JK, Tiranti V, Kyttälä A, Zeviani M, Comi GP, Keränen S, Peltonen L, Suomalainen A. (2000) Role of adenine nucleotide translocator 1 in mtDNA maintenance. *Science*. 4;289(5480):782-5.

Kimura, Y. & Kimura, H (2004). Hydrogen sulfide protects neurons from oxidative stress. *FASEB J*. 18: 1165–1167.

Kir HM, Dillioglugil MO, Tugay M, Eraldemir C, Ozdoğan HK. (2005) Effects of vitamins E, A and D on MDA, GSH, NO levels and SOD activities in 5/6 nephrectomized rats. *Am J Nephrol*.25(5):441-6.

Koene S. & Smeitink J. (2009) Mitochondrial medicine: entering the era of treatment. *Journal of Internal Medicine* 265; 193–209.

Lister R, Hulett JM, Lithgow T, Whelan J. (2005) Protein import into mitochondria: origins and functions today. *Mol Membr Biol* 22: 87–100.

Loeffen JL, Smeitink JA, Trijbels JM et al. (2000) Isolated complex I deficiency in children: clinical, biochemical and genetic aspects. *Hum Mutat* 15: 123–34.

Mancardi D, Penna C, Merlino A, Del Soldato P, Wink DA, Pagliaro P (2009). Physiological and pharmacological features of the novel gasotransmitter: hydrogen sulfide. *Biochim Biophys Acta*.;1787(7):864-72.

Mancuso C, Scapagini G, Currò D, Giuffrida Stella AM, De Marco C, Butterfield DA, Calabrese V. (2007) Mitochondrial dysfunction, free radical generation and cellular stress response in neurodegenerative disorders. *Front Biosci*. 12:1107-23.

Margulis L. (1976) Genetic and evolutionary consequences of symbiosis. *Exp Parasitol* 39: 277–349.

Mattiazzi M, Vijayvergiya C, Gajewski CD, DeVivo DC, Lenaz G, Wiedmann M, Manfredi G. (2004) The mtDNA T8993G (NARP) mutation results in an impairment of oxidative phosphorylation that can be improved by antioxidants. *Hum Mol Genet.* 13(8):869-79.

Meier M, Janosik M, Kery V, Kraus JP, Burkhard P (2001). Structure of human cystathionine beta-synthase: a unique pyridoxal 5'-phosphate-dependent heme protein. *EMBO J.* 20: 3910-6.

Mineri R, Rimoldi M, Burlina AB, Koskull S, Perletti C, Heese B, von Döbeln U, Mereghetti P, Di Meo I, Invernizzi F, Zeviani M, Uziel G, Tiranti V (2008). Identification of new mutations in the ETHE1 gene in a cohort of 14 patients presenting with ethylmalonic encephalopathy. *J Med Genet.* 45: 473-8.

Mootha VK, Lepage P, Miller K et al. Identification of a gene causing human cytochrome c oxidase deficiency by integrative genomics. (2003) *Proc Natl Acad Sci USA* 100: 605–10.

Munich A, Rotig A, Chretien D, Saudubray JM, Cormier V, Rustin P (1996) Clinical presentation, and laboratory investigations in respiratory chain deficiency. *Eur J Pediatr* 155:262–264.

Nishino I, Spinazzola A, Papadimitriou A, Hammans S, Steiner I, Hahn CD, Connolly AM, Verloes A, Guimarães J, Maillard I, Hamano H, Donati MA, Semrad CE, Russell JA, Andreu AL, Hadjigeorgiou GM, Vu TH, Tadesse S, Nygaard TG, Nonaka I, Hirano I, Bonilla E, Rowland LP, DiMauro S, Hirano M. (2000) Mitochondrial neurogastrointestinal encephalomyopathy: an autosomal recessive disorder due to thymidine phosphorylase mutations. *Ann Neurol.* 47(6):792-800.

Ogilvie I, Kennaway NG, and Shoubridge EA (2005). A molecular chaperone for mitochondrial complex I assembly is mutated in a progressive encephalopathy. *J. Clin. Invest.* 115, 2784-2792

Okamoto K & Shaw JM. (2005) Mitochondrial morphology and dynamics in yeast and multicellular eukaryotes. *Annual Review of Genetics* 39: 503-536.

Oldfors A, Holme E, Tulinius M, Larsson NG. (1995) Tissue distribution and disease manifestations of the tRNA(Lys) A→G(8344) mitochondrial DNA mutation in a case of myoclonus epilepsy and ragged red fibres. *Acta Neuropathol* 90: 328–33.

Papadopoulou LC, Sue CM, Davidson MM, Tanji K, Nishino I, Sadlock JE, Krishna S, Walker W, Selby J, Glerum DM, et al. (1999). Fatal infantile cardioencephalomyopathy with COX deficiency and mutations in SCO2, a COX assembly gene. *Nat Genet* 23, 333-337.

Pedersen CB, Bross P, Winter VS, Corydon TJ, Bolund L, Bartlett K, Vockley J, Gregersen N (2003). Misfolding, degradation, and aggregation of variant proteins. The molecular pathogenesis of short chain acyl-CoA dehydrogenase (SCAD) deficiency. *J Biol Chem*, 278: 47449-58.

Pyeritz, R. E., McKusick, V. A. (1979). The Marfan syndrome. *New Eng. J. Med.* 300: 772-777.

Reddy PH. (2008) Mitochondrial medicine for aging and neurodegenerative diseases. *Neuromol. Med.* 10: 291–315.

Reiss J, Dorche C, Stallmeyer B, Mendel RR, Cohen N, Zobot MT (1999). Human molybdopterin synthase gene: genomic structure and mutations in molybdenum cofactor deficiency type B. *Am J Hum Genet.* 64: 706-11.

Roediger WE, Duncan A, Kapaniris O, Millard S (1993). Sulphide impairment of substrate oxidation in rat colonocytes: a biochemical basis for ulcerative colitis? *Clin Sci (Lond).* 85: 623-7.

Roediger WE (2008). Review article: nitric oxide from dysbiotic bacterial respiration of nitrate in the pathogenesis and as a target for therapy of ulcerative colitis. *Aliment Pharmacol Ther.* 1;27(7):531-41.

Roesch K, Curran SP, Tranebjaerg L, Koehler CM. (2002) Human deafness dystonia syndrome is caused by a defect in assembly of the DDP1/TIMM8a–TIMM13 complex. *Human Molecular Genetics* 11 (5) 477-486.

Rustin P, von Kleist-Retzow JC, Chantrel-Groussard K, Sidi D, Munnich A, Rotig A. (1999) Effect of idebenone on cardiomyopathy in Friedreich ataxia: a preliminary study. *Lancet* 354: 477–479.

Salviati L, Sacconi S, Murer L, Zacchello G, Franceschini L, Laverda AM, Basso G, Quinzii C, Angelini C, Hirano M, Naini AB, Navas P, DiMauro S, Montini G. (2005) Infantile encephalomyopathy and nephropathy with CoQ10 deficiency: A CoQ10-responsive condition. *NEUROLOGY* 65: 606-608.

Schaefer AM, Taylor RW, Turnbull DM, and Chinnery PF (2004). The epidemiology of mitochondrial disorders--past, present and future. *Biochim Biophys Acta* 1659, 115-120.

Scheffler IE. (2001) A century of mitochondrial research: achievements and perspectives. *Mitochondrion* 1(1):3-31.

Schlame M, Rua D, Greenberg ML. (2000) The biosynthesis and functional role of cardiolipin. *Prog. Lipid. Res.* 39: 257–288.

Schwartz M, Vissing J. (2002) Paternal inheritance of mitochondrial DNA. *N Engl J Med* 347: 576–80.

Shih, V. E., Abrams, I. F., Johnson, J. L., Carney, M., Mandell, R., Robb, R. M., Cloherty, J. P., Rajagopalan, K. V (1977). Sulfite oxidase deficiency: biochemical and clinical investigations of a hereditary metabolic disorder in sulfur metabolism. *New Eng. J. Med.* 297: 1022-1028.

Stipanuk MH (2004). Role of the liver in regulation of body cysteine and taurine levels: a brief review. *Neurochem Res.* 29:105-10.

St John JC, Jokhi RP, Barratt CL. (2005) The impact of mitochondrial genetics on male infertility. *Int J Androl.* 28(2):65-73.

Swerdlow RH, Khan SM (2009) The Alzheimer's disease mitochondrial cascade hypothesis: an update. *Exp Neurol* 218(2):308-15.

Szabó C (2007). Hydrogen sulphide and its therapeutic potential. *Nat Rev Drug Discov.* 6: 917-35.

Testai FD, Gorelick PB (2010). Inherited metabolic disorders and stroke part 2: homocystinuria, organic acidurias, and urea cycle disorders. *Arch Neurol.* 67: 148-53.

Tiranti V, Hoertnagel K, Carozzo R, Galimberti C, Munaro M, Granatiero M, Zelante L, Gasparini P, Marzella R, Rocchi M, et al. (1998). Mutations of SURF-1 in Leigh disease associated with cytochrome c oxidase deficiency. *Am J Hum Genet* 63, 1609-1621.

Tiranti V, D'Adamo P, Briem E, Ferrari G, Mineri R, Lamantea E, Mandel H, Balestri P, Garcia-Silva MT, Vollmer B, Rinaldo P, Hahn SH, Leonard J, Rahman S, Dionisi-Vici C, Garavaglia B, Gasparini P, Zeviani M (2004). Ethylmalonic encephalopathy is caused by mutations in *ETHE1*, a gene encoding a mitochondrial matrix protein. *Am J Hum Genet.*74: 239-52.

Tiranti V, Briem E, Lamantea E, Mineri R, Papaleo E, De Gioia L, Forlani F, Rinaldo P, Dickson P, Abu-Libdeh B, Cindro-Heberle L, Owaidha M, Jack RM, Christensen E, Burlina A, Zeviani M (2006). *ETHE1* mutations are specific to ethylmalonic encephalopathy. *J Med Genet.* 43: 340-6.

Tiranti V, Viscomi C, Hildebrandt T, Di Meo I, Mineri R, Tiveron C, Levitt MD, Prella A, Fagiolari G, Rimoldi M, Zeviani M (2009). Loss of *ETHE1*, a mitochondrial dioxygenase, causes fatal sulfide toxicity in ethylmalonic encephalopathy. *Nat Med.* 15: 200-5.

Valnot I, Osmond S, Gigarel N, Mehaye B, Amiel J, Cormier-Daire V, Munnich A, Bonnefont JP, Rustin P, and Rotig A (2000a). Mutations of the *SCO1* gene in mitochondrial cytochrome c oxidase

deficiency with neonatal-onset hepatic failure and encephalopathy. *Am J Hum Genet* 67, 1104-1109.

Valnot I, von Kleist-Retzow JC, Barrientos A, Gorbatyuk M, Taanman JW, Mehaye B, Rustin P, Tzagoloff A, Munnich A, and Rotig A (2000b). A mutation in the human heme A:farnesyltransferase gene (COX10) causes cytochrome c oxidase deficiency. *Hum Mol Genet* 9, 1245-1249.

Van Goethem G, Dermaut B, Löfgren A, Martin JJ, Van Broeckhoven C. (2001) Mutation of POLG is associated with progressive external ophthalmoplegia characterized by mtDNA deletions. *Nat Genet.* 28(3):211-2.

Visapaa I, Fellman V, Vesa J, Dasvarma A, Hutton JL, Kumar V, Payne GS, Makarow M, Van Coster R, Taylor RW, et al. (2002). GRACILE syndrome, a lethal metabolic disorder with iron overload, is caused by a point mutation in BCS1L. *Am J Hum Genet* 71, 863-876.

Viscomi C, Burlina AB, Dweikat I, Savoiaro M, Lamperti C, Hildebrandt T, Tiranti V, Zeviani M (2010). Combined treatment with oral metronidazole and N-acetylcysteine is effective in ethylmalonic encephalopathy. *Nat Med.* 16: 869-71.

Wallace DC, Singh G, Lott MT, Hodge JA, Schurr TG, Lezza AM, Elsas LJ, and Nikoskelainen EK (1988). Mitochondrial DNA mutation associated with Leber's hereditary optic neuropathy. *Science* 242, 1427-1430.

Wang, R. (2002) Two's company, three's a crowd: can H₂S be the third endogenous gaseous transmitter? *FASEB J.* 16: 1792–1798.

Wang J, Hegele RA (2003). Genomic basis of cystathioninuria (MIM 219500) revealed by multiple mutations in cystathionine gamma-lyase (CTH). *Hum Genet.* 112: 404-8.

- Yalamanchili C, Smith MD (2008). Acute hydrogen sulfide toxicity due to sewer gas exposure. *Am J Emerg Med.* 26: 518.e5-7.
- Yang G, Sun X, Wang R (2004). Hydrogen sulfide-induced apoptosis of human aorta smooth muscle cells via the activation of mitogen-activated protein kinases and caspase-3. *FASEB J.* 18: 1782-4.
- Zeviani M, Moraes CT, DiMauro S, Nakase H, Bonilla E, Schon EA, and Rowland LP (1988). Deletions of mitochondrial DNA in Kearns-Sayre syndrome. *Neurology* 38, 1339-1346.
- Zeviani M, Spinazzola A, Carelli V. (2003) Nuclear genes in mitochondrial disorders. *Curr Opin Genet Dev* 2003; 13: 262–70.
- Zeviani M & DiDonato S. (2004) Mitochondrial disorders. *Brain* 10: 2153–72.
- Zeviani M & Lamantea E. (2006) Genetic Disorders of the Mitochondrial OXPHOS System. *SCIENCE & MEDICINE* vol. 10(3):154-167.

Chapter 2:

Chronic Exposure to Sulfide Causes Accelerated Degradation of Cytochrome *c* Oxidase in Ethylmalonic Encephalopathy

Ivano Di Meo,¹ Gigliola Fagiolari,² Alessandro Prella,³ Carlo Viscomi,¹ Massimo Zeviani,¹ and Valeria Tiranti¹

¹Unit of Molecular Neurogenetics, Pierfranco and Luisa Mariani Center for Research on Children's Mitochondrial Disorders, Institute of Neurology "Carlo Besta" – IRCCS Foundation, Milan, Italy.

²Division of Neurology, Dino Ferrari Center, Ospedale Maggiore Policlinico, Ca` Granda-IRCCS Foundation, Milan, Italy.

³Neuroscience Department, Azienda Ospedaliera Fatebenefratelli e Oftalmico, Milan, Italy.

ANTIOXIDANTS & REDOX SIGNALING 15;15(2):353-62,

July 2011; Epub February 2011

Abstract

Ethylmalonic encephalopathy (EE) is an autosomal recessive, invariably fatal disorder associated with mutations in *ETHE1*, a gene encoding a mitochondrial sulfur dioxygenase (SDO). The main consequence of the absence of Ethe1-SDO is the accumulation of sulfide (H₂S) in critical tissues, including colonic mucosa, liver, muscle and brain.

Aims: In order to make progress in the elucidation of the biochemical mechanisms leading to COX deficiency, we (i) generated tissue-specific conditional *Ethe1* knockout mice to clarify the different contributions of endogenous and exogenous H₂S production, and (ii) studied the development of H₂S-driven COX deficiency in *Ethe1*^{-/-} mouse tissues and human cells.

Results: *Ethe1*^{-/-} conditional animals displayed COX deficiency limited to the specific targeted tissue. The accumulation of H₂S over time causes progressive COX deficiency in animal tissues and human cells, which is associated with reduced amount of COX holoenzyme, and of several COX subunits, including MTCO1, MTCO2, COX4, and COX5A. This reduction is not paralleled by consistent down-regulation in the expression of the corresponding mRNAs.

Conclusions: Tissue-specific ablation of *Ethe1* causes COX deficiency in targeted organs, suggesting that failure in neutralizing endogenous, tissue-specific production of H₂S is sufficient to cause the biochemical defect but neither to determine a clinical impact nor to induce the biomarker profile typical of EE. The mechanism by

which H₂S causes COX deficiency consists of rapid *heme a* inhibition and accelerated long-term degradation of COX subunits. However, the pleiotropic devastating effects of H₂S accumulation in EE cannot be fully explained by the sole defect of COX in critical tissues, but are likely consequent to several toxic actions on a number of enzymatic activities in different tissues, including endothelial lining of the small vessels, leading to multi-organ failure.

Introduction

Ethylmalonic encephalopathy, EE, (OMIM#602473), is an autosomal recessive fatal infantile disease caused by accumulation of sulfide, H₂S, a mitochondrial poison produced exogenously by the anaerobic enterobacterial flora and synthesized endogenously in various mammalian tissues. Failure to detoxify sulfide is due to the absence or malfunctioning of a mitochondrial sulfur dioxygenase, encoded by the *ETHE1* gene, which is mutated in EE (1).

EE has been reported in numerous infants of Mediterranean or Arab origin who are clinically characterized by 1) progressive encephalopathy; 2) chronic diarrhea; 3) petechial purpura and severe orthostatic acrocyanosis. Biochemically, EE presents an unusual combination of severe deficiency of cytochrome c oxidase, COX, the last component (complex IV, cIV) of the mitochondrial respiratory chain (RC), in both muscle and brain, accumulation in blood of C4 and C5 acylcarnitines and urinary excretion of ethylmalonic acid (EMA), the dicarboxylic derivative of butyrate (2). We found that the

ETHE1 gene codes for a sulfur dioxygenase (SDO) of the mitochondrial matrix, being part of a mitochondrial oxidative pathway for inorganic sulfur that ultimately converts sulfide into harmless compounds, such as thiosulfate and sulfate. This pathway is composed of four enzymes. First, a membrane-bound mitochondrial sulfide quinone reductase (SQR) is involved in the initial oxidation of H₂S and the fixation of its sulfur atom to a sulfur acceptor, with the formation of a persulfide (3). Next, the persulfide compound is further oxidized to sulfite by molecular oxygen through the action of ETHE1-SDO. The enzyme rhodanese, which displays a sulfur transferase activity, acts in the third step allowing sulfite to be trans-sulfurated in the mitochondrial matrix and converted into a metabolic end product, thiosulfate (3). Alternatively, sulfite can also be directly oxidized to sulfate by another mitochondrial matrix enzyme, sulfite oxidase. Wilson et al. (4) have proposed that yet another enzyme, sulfide oxidase, is active in the colonic mucosa, where it catalyzes the first and rate-limiting step of local sulfide catabolism, consisting of the oxidation/condensation of two molecules of H₂S to thiosulfate (H₂SO₃). Thiosulfate would then react with cyanide, being ultimately converted into thiocyanate by the trans-sulfurase activity of rhodanese. However, the very existence of sulfide oxidase has not been demonstrated, whereas *in vivo* experiments (5) have clearly shown that hardly any cyanide is produced in the large intestine, either by the mucosal cells or by the bacterial flora. Consequently very little, if any, thiosulfate can be converted into thiocyanate *in vivo*, casting doubt that this pathway exists *in vivo*. In any case, the consequence of impaired ETHE1 activity is the accumulation of sulfide, a harmful,

biologically active compound that at micromolar concentrations acts as a powerful inhibitor of both COX and short-chain acyl-CoA dehydrogenase, SCAD, and possibly other enzymatic activities as well, damages the mucosa of the large intestine and endothelia, and alters the vessel tone, thereby accounting for the main clinical and biochemical features of EE. H₂S, together with NO and CO, belongs to a family of biological mediators termed gasotransmitters. H₂S exerts a host of biological actions on various targets, resulting in responses that range from cytotoxic to cytoprotective effects (6). Taken together, this data suggests that, in *Ethe1*^{-/-} mice as in EE patients, low COX activity in muscle, as well as brain, is due to the toxic accumulation of H₂S. We have previously shown that the biochemical defect of COX activity is paralleled in both tissues by concordant reduction in the steady-state amount of COX holoenzyme, suggesting that persistent inhibition of COX activity can induce its structural destabilization and accelerated degradation.

Besides endogenous production from catabolism of cysteine and other sulfur organic compounds, a substantial amount of H₂S derives from the anaerobic bacterial flora residing in the lumen of the large intestine (7). Similar to the EE intestinal lesions, excessive production and absorption of H₂S, combined with its reduced detoxification by colonocytes are thought to play an important role in the mucosal damage of ulcerative colitis. In order to understand the contribution of exogenous vs. endogenous H₂S production we have characterized the phenotype of conditional *Ethe1*^{-/-} mice in extra-intestinal organs, namely liver, brain and skeletal muscle.

In addition, we investigated the consequences on COX of chronic exposure to H₂S in the *Ethe1*^{-/-} mouse model, and in cultured human cells.

Materials and Methods

Cell Lines, Culture Conditions and Treatments

Human primary fibroblasts and HeLa cells were grown in a Dulbecco's modified Eagle medium (DMEM) supplemented with 10% fetal bovine serum at 37°C in 5% CO₂ atmosphere. The cells were cultured without or with increasing concentrations (0.1 to 0.5 mM) of NaHS (Sigma) freshly dissolved in the culture medium.

Creation and characterization of brain-, muscle- and liver- specific conditional Ethe1^{-/-} mice

Recombinant *Ethe1*^{-/-} mice were obtained as described (1). A neomycin-resistance cassette flanked by frt sites was removed by crossing with a *Flpe* transgenic mouse (8), thus obtaining *Ethe1*^{+/*LoxP*} mice. The *Ethe1*^{+/*LoxP*} animals were mated with three different transgenic strains expressing the *Cre* recombinase under (i) the liver-specific *Albumin* (9), (ii) the muscle-specific *MyoD* (10), and (iii) the brain-specific *Nestin* (11) promoters. *ETHE1*^{+/*LoxP*,*Cre*} were eventually crossed with *Ethe1*^{*LoxP*/*LoxP*} in order to obtain *Ethe1*^{*LoxP*/*LoxP*, *Cre*} individuals. Animals were euthanized at post-partum day 90 (P90) and the absence of the *Ethe1* gene and protein was verified in the tissues of each conditional model by PCR-based diagnosis on genomic DNA, and western-blot analysis with a specific a-ETHE1 antibody. Biochemical evaluation of complex IV activity was measured in

muscle, brain, and liver homogenates. The measurement of thiosulfate in urine was performed as previously described (12).

Immunoblotting

Western-blot analysis was performed with a-ETHE1 (13), a-MTCO1 (1 µg/ml), a-MTCO2 (1 µg/ml), a-COX4 (0,5 µg/ml), a-COX5A (1 µg/ml), a-SDH-A (0,1 µg/ml), a-Rieske iron-sulfur protein (RISP) (0,5µg/ml) and a-NDUFA9 (0,5 µg/ml) (Invitrogen) antibodies, using the ECL chemiluminescence kit (Amersham), as described elsewhere (14). Cells lysates were prepared from cells cultured in T-25 cm² flasks and resuspended in MOPS-sucrose buffer. Digitonin (0,2 mg/ml) was added and incubation was carried out on ice for 5 min. After centrifugation at 5,000x g for 3 min, the pellet was resuspended in 1 mM EDTA, MOPS-sucrose buffer. After a second 5 min incubation on ice, cells were centrifuged at 10,000x g for 3 min. The pellet was resuspended in RIPA buffer (Tris-HCl 50 mM pH 7.5, NaCl 150 mM, EDTA 5 mM, NP40 1%, NaDOC 0,5%) plus protease inhibitors and incubated on ice for 30 min. Soluble proteins were separated from insoluble material by centrifugation at 18,000x g for 20 min. Mouse tissues were homogenized in 10 x (v/w) of 10 mM PK buffer, pH 7.5. Mitochondrial enriched fractions were collected after centrifugation at 800x g for 10 min in the presence of protease inhibitors, and frozen & thawed twice in liquid nitrogen. Approximately 60 µg of proteins was used for each sample in denaturing sodium-dodecyl sulfate polyacrylamide gel electrophoresis (SDS-PAGE).

Real-Time quantitative PCR

Total RNA was extracted from cells using RNeasy Mini Kit (Quiagen) according to the manufacturer's protocol. Tissue-derived RNA was isolated with TRIzol reagent (Invitrogen). Two μg of total RNA was treated with RNase-free DNase and retro-transcribed by using the Cloned AMV First-strand cDNA Synthesis kit and protocol (Invitrogen). Approximately 2-5 ng of cDNA was used for SYBR-GREEN based Real-Time PCR using primers specific for amplification of several COX-subunit encoding genes according to the ABI-Primer Express software; standard transcripts HPRT and GPADH were co-amplified using suitable primers (see Supplementary Table). Real-time quantitative PCR was carried out using an ABI PRISM 7000 Sequence Detection System. The amplification profile was according to a two-step protocol: one cycle at 50°C for 2 min, one cycle at 95°C for 10 min, and then 40 cycles of 95°C for 15 s and 60°C for 1 min. A final dissociation step (95°C for 15 s, 60°C for 20 s, 95° for 15 s) was added to assess for unspecific primer-dimer amplifications.

Morphological and Biochemical analyses

For light microscopy, samples from different tissues were frozen in liquid-nitrogen-cooled isopentane. Standard histological and histochemical techniques for the detection of mitochondrial alterations and muscle fiber distribution were performed on serial cryostat cross sections as previously described. Standard histochemical method for the detection of SDH activity on 8-micron-thick cryostat sections was followed by dissolving 3.2 mM phenazine methosulfate (PMS), 12

mM succinic acid and 1.2 mM nitro blue tetrazolium (NBT) in 10 ml of 0.1M phosphate buffer, pH 7.4. The pH of this incubation solution was adjusted to 7.6 and filtered through a Whatman No. 1 filter paper. Sections were incubated for 30 min at 37°C and then rinsed three times, 5 min each in distilled water at room temperature and then mounted on glass slides with warm glycerin. In some SDH reactions, the following compounds were added: 10 mM Na malonate or 1 mM NaHS. Standard histochemical reaction on cryostat sections for COX was performed as described (15). For COX+SDH double staining, the COX reaction was performed first, followed by the SDH reaction after rinsing the sections three times for 5 min each in distilled water. Biochemical assays of the individual MRC complexes and of citrate synthase (CS) on tissues and cells were carried out as described (16). The specific activities of each complex were normalized to CS, an indicator of the number of mitochondria. COX activity was evaluated in the homogenates incubated with 10mM NaHS after addition of COX reaction mixture. The first measurement was performed within 2 min and then repeated every 10 min for one hour. COX activity was recorded in parallel in untreated homogenates. Residual activity in treated samples was calculated as percentage of the normal activity measured in untreated homogenates.

In Vivo Mitochondrial Translation Assay

Analysis of mitochondrial protein synthesis was performed according to Chomyn (17) with some modifications. For the “pulse” experiment, cells at 70% confluence in T25 flasks, were cultured for 24 h in the presence or absence of 0.5 mM NaHS and then incubated for 2 h with

100 µg/ml of emetine, an irreversible inhibitor of cytosolic protein synthesis, in the presence of 160 µCi/ml of [³⁵S]-Met/Cys (Express Protein Labeling Mix, Perkin Elmer) in methionine and cysteine deficient DMEM. For the “chase” experiment, cells were pre-incubated with 40 µg/ml chloramphenicol for 15 h. Cells were then labeled for 2 h in the presence of 100 µg/ml cycloheximide, and further incubated in complete medium for 24 h, with or without 0.5 mM NaHS. Following washing and harvesting, cells were kept at -80°C until use. An equal amount of total cellular proteins was loaded on a 15 to 20% exponential gradient SDS-PAGE. The gel was then fixed, dried, and autoradiographed using a PhosphorImager apparatus (BioRad).

Results

*Evaluation of brain-, muscle- and liver-specific conditional *Ethel*^{-/-} mice*

Absence of the *Ethel* gene and protein in liver-specific albumin, muscle-specific myoD, and brain-specific nestin conditional animals, was verified by PCR (not shown) and Western-blot analyses (Figure 1A). The muscle homogenate of the myoD-specific, and the brain homogenate of the nestin-specific conditional knockout animals, both showed a 50-60% isolated reduction of the COX activity, whereas neither the brain of the former, nor the muscle of the latter animals showed the defect (Figure 1B). In contrast, COX activity was normal in the liver, muscle and brain of the liver-specific *Ethel*^{-/-} animals (Figure 1B).

None of the three conditional mouse models showed the clinical and biological hallmarks of EE, at least for the period of our observation (90 days). In particular, urinary thiosulfate levels were comparable between conditional and wild-type animals (Figure 1C).

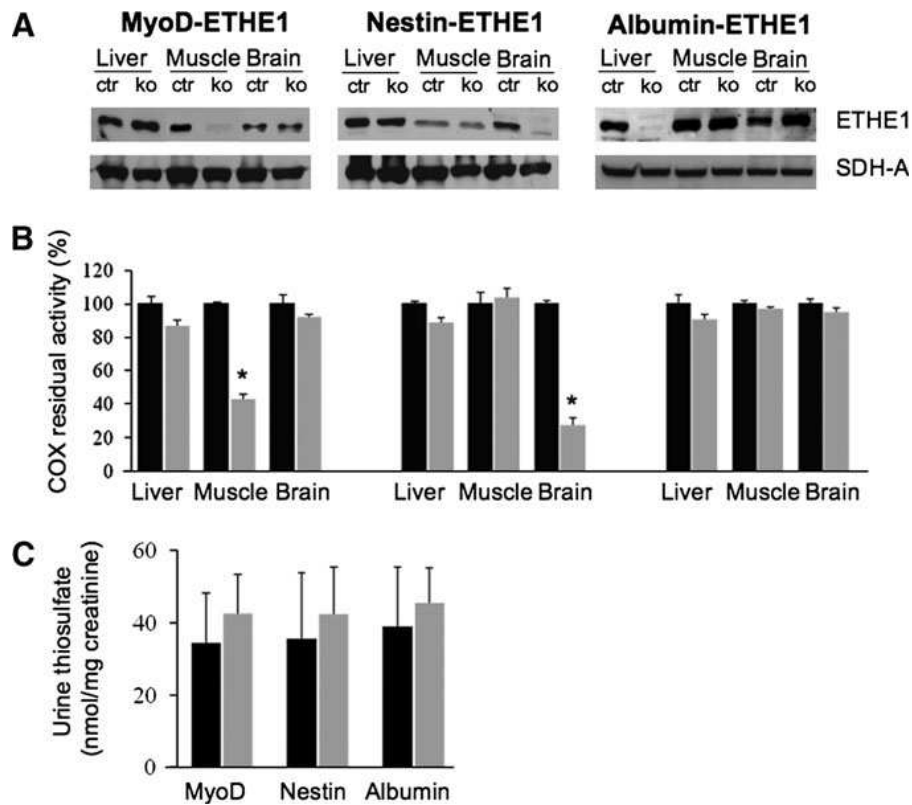


FIG. 1. Analysis of conditional ETHE1^{-/-} animals.

(A) Western blot assay using an a-ETHE1 antibody in different tissues of musclespecific (MyoD), brain-specific (nestin), and liver-specific (albumin) Ethe1^{-/-} mice. An a-SDH-A antibody was used as a protein-loading standard. (B) COX activity in different tissues of MyoD, nestin, and albumin-conditional Ethe1^{-/-} mice. Black bars: control animals; gray bars: Ethe1^{-/-} animals. (C) Thiosulfate concentration in the urine of MyoD, nestin, and albumin conditional Ethe1^{-/-} mice. Blue bars: control animals; red bars: Ethe1^{-/-} animals. COX, cytochrome c oxidase.

*Histochemical staining of *Ethe1*^{-/-} constitutive animals*

Constitutive *Ethe1*^{-/-} mice are characterized by a downhill clinical course which, starting at around P15, i.e. the weaning time, leads the animals invariably to death within 30-35 days after birth. Severe COX deficiency is detected in brain and muscle of P30 *Ethe1*^{-/-} mice by both histochemical and biochemical assays. In order to understand if the onset of the clinical deterioration at P15 coincides with the onset and progression of COX deficiency, we analyzed histochemically the muscle, brain and colon of P15, P21 and P30 *Ethe1*^{-/-} mice. In muscle, COX deficiency progressed from mild reduction at P15, to severe reduction at P21, which further worsened in the terminal stage, at P30 (Figure 2). The same progression was found in brain tissue (Figure 3).

Examination of the intestinal tract showed diffuse, mild reduction of COX activity in the jejunal mucosa (not shown). In colonic mucosa, COX deficiency at P15 was limited to the colonocytes located on the luminal surface. Over time, COX deficiency progressively diffused, from the luminal surface through the internal part of the mucosa to reach the deeper segments of the Lieberkhün crypts (Figure 4). In all three tissues, i.e. muscle, brain and colon, we found a parallel strong increase in the histochemical reaction used to visualize the activity of succinate dehydrogenase, SDH, which is part of complex II (Figures 1- 3). This reaction is based on the capacity of SDH to reduce tetrazolium, a colorless salt, into formazan, a blue dye, in the presence of succinate. A hyper-intense SDH reaction is typical of conditions characterized by proliferation of mitochondria, e.g. ragged-red fibers

in mitochondrial myopathies, and is accompanied by increased biochemical activities of SDH and citrate synthase (CS), another index of mitochondrial mass, in tissue homogenate. However, neither SDH nor CS enzymatic activities were increased in *Ethe1*^{-/-} tissue homogenates, nor was proliferation of mitochondria detected by ultra-structural studies (not shown), suggesting that the strong blue staining obtained histochemically was not due to increased SDH activity and mitochondrial proliferation, but rather to the presence of direct, non-enzymatic conversion of tetrazolium into formazan by H₂S and its persulfide derivatives (18). To test this hypothesis, we first incubated 1mM of NaHS with 0.1 mM NBT in a test-tube and verified that NBT was indeed reduced, by reading absorbance at 412 nm with spectrophotometric analysis. We then exposed wild-type muscle sections to 1 mM NaHS, which dissociates to Na⁺ and HS⁻ in solution. HS⁻ then associates with H⁺ and produces H₂S. At pH=7.4, in which the SDH reaction has been carried out, approximately one third of the H₂S exists as the un-dissociated form (H₂S), the remaining two-thirds being present as HS (19). To avoid evaporation, the reactions were performed in cover-slip tightly capped.

While the standard SDH reaction gave a normal staining in the muscle of *Ethe1*^{+/+} animals (Figure 5, panel A), a strong reaction was present in both NaHS-treated *Ethe1*^{+/+} (panel B) and untreated *Ethe1*^{-/-} muscles (panel C). Next, we treated muscle sections of *Ethe1*^{+/+} and *Ethe1*^{-/-} animals with (a), malonate, a specific inhibitor of complex II (Figure 5: D= *Ethe1*^{+/+} animals; E= *Ethe1*^{-/-} animals) or, (b) without succinate, the specific substrate of SDH (Figure 5: F= *Ethe1*^{+/+} animals; G= *Ethe1*^{-/-} animals). As expected, the *Ethe1*^{+/+}

muscle displayed the normal pattern in standard SDH protocol, but developed hardly any staining in the presence of malonate or in the absence of succinate, indicating that the reaction was indeed specific to SDH. However, the *Ethe1*^{-/-} muscle sections still turned deep blue in the presence of the SDH inhibitor (malonate) or in the absence of the reducing substrate (succinate). A blank reaction performed by omitting NBT failed to stain both *Ethe1*^{+/+} (Figure 5, H) and *Ethe1*^{-/-} muscle specimens (Figure 5, I). Taken together these results indicate that (i) H₂S is capable of directly reducing tetrazolium into formazan and (ii) the deep-blue staining observed in *Ethe1*^{-/-} muscle is, at least partly, independent of SDH activity.

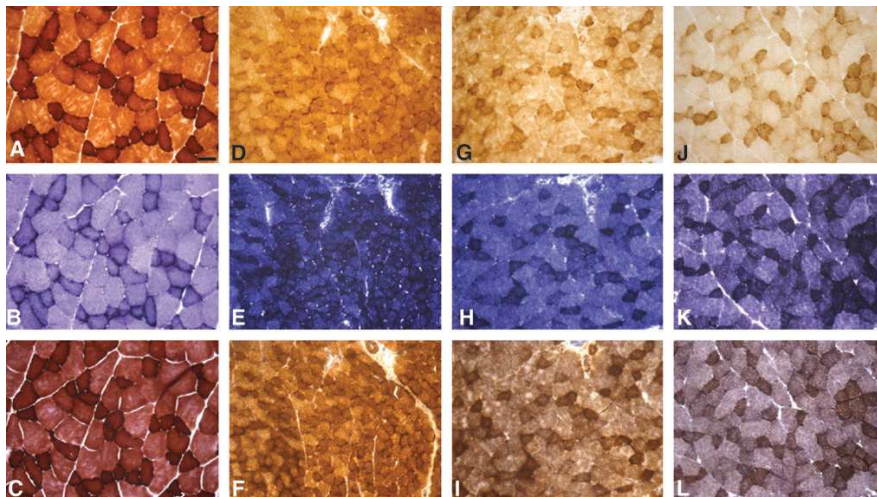


FIG. 2. Muscle histochemistry of constitutive *Ethe1*^{-/-} mice.

Muscle serial sections, scale bars: 20 mm. COX activity in WT animals (A); *Ethe1*^{-/-} animals at P14 (D), P21 (G), and P30 (J). SDH activity in WT animals (B); *Ethe1*^{-/-} animals at P14 (E), P21 (H), and P30 (K). COX-SDH double-stain in WT animals (C); *Ethe1*^{-/-} animals at P14 (F), P21 (I), and P30 (L). SDH, succinate dehydrogenase; WT, wild type.

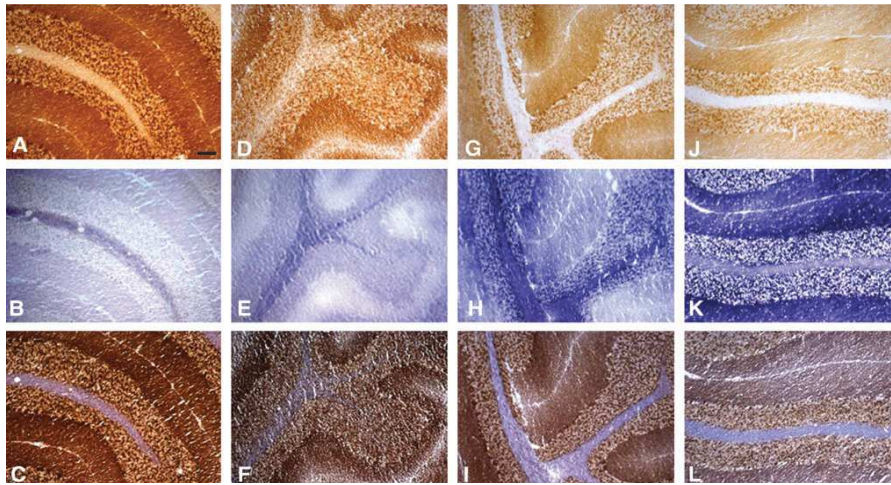


FIG. 3. Brain histochemistry of constitutive Ethe1^{-/-} mice.

Brain serial sections, scale bars: 50 μm. COX activity in WT animals (A); Ethe1^{-/-} animals at P14 (D), P21 (G), and P30 (J). SDH activity in WT animals (B); Ethe1^{-/-} animals at P14 (E), P21 (H), and P30 (K). COX-SDH double-stain in WT animals (C); Ethe1^{-/-} animals at P14 (F), P21 (I), and P30 (L).

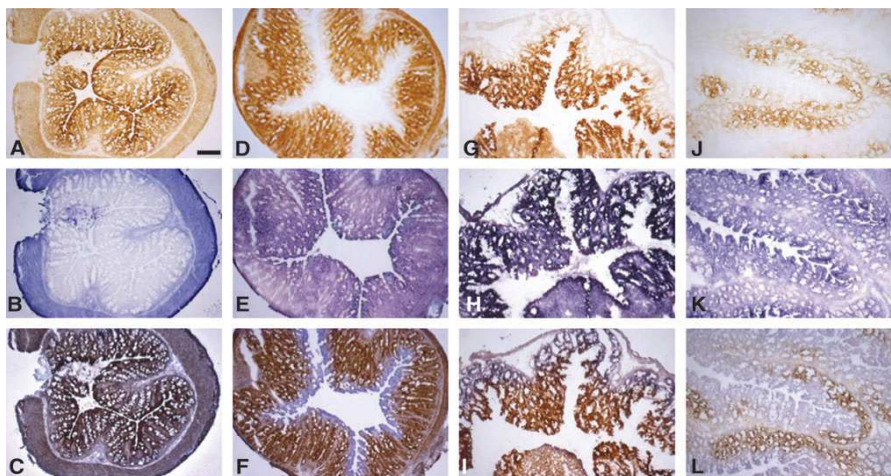


FIG. 4. Colon histochemistry of constitutive Ethe1^{-/-} mice.

Colon serial sections, scale bars: 50 μm. COX activity in WT animals (A); Ethe1^{-/-} animals at P14 (D), P21 (G), and P30 (J). SDH activity in WT animals (B); Ethe1^{-/-} animals at P14 (E), P21 (H), and P30 (K). COX-SDH double-stain in WT animals (C); Ethe1^{-/-} animals at P14 (F), P21 (I), and P30 (L).

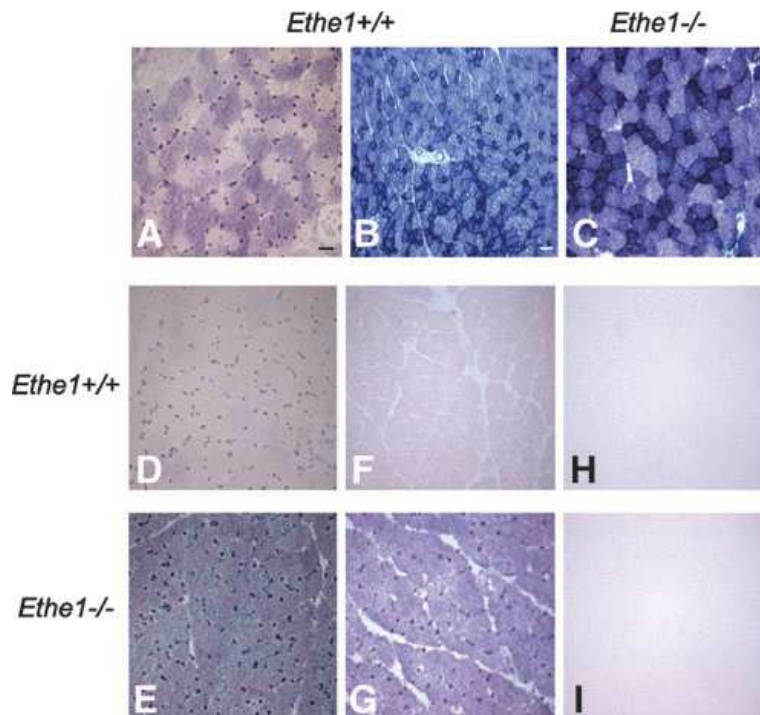


FIG. 5. SDH histochemistry on muscle sections under different conditions.

Standard SDH reaction is shown on muscle sections of *Ethe1*^{+/+} and *Ethe1*^{-/-} animals. Addition or elimination of specific compounds (see the Materials and Methods section) in the standard SDH incubation mixture are indicated. (A) Standard SDH reaction on *Ethe1*^{+/+} muscle. (B) Standard SDH reaction with addition of 1mM NaHS on *Ethe1*^{+/+} muscle. (C) Standard SDH reaction on muscle of *Ethe1*^{-/-} mice. (D) Sodium malonate (10mM), an SDH inhibitor, was added to the incubation medium of standard SDH reaction on *Ethe1*^{+/+} muscle. (E) Sodium malonate (10mM), an SDH inhibitor, was added to the incubation medium of standard SDH reaction on *Ethe1*^{-/-} muscle. (F) SDH reaction was performed without succinate on *Ethe1*^{+/+} muscle. (G) SDH reaction was performed without succinate on *Ethe1*^{-/-} muscle. (H) SDH reaction was performed without nitro blue tetrazolium on *Ethe1*^{+/+} muscle. (I) SDH reaction was performed without nitro blue tetrazolium on *Ethe1*^{-/-} mice muscle. NaHS, sodium hydrosulfide.

Evaluation of COX expression

In order to understand the mechanism of COX deficiency in EE, we performed Western-blot immunovisualization on several COX subunits in liver, muscle and brain homogenates of constitutive *Ethel*^{-/-} mice at different ages. P15, P21 and P30. The amount of the mtDNA-encoded MTCO1 subunit decreased progressively over time in muscle and brain, but not in liver (Figure 6A). The same phenomenon was observed for the nucleus-encoded subunits of COX; for instance, hardly any COX4-specific cross-reacting material was detectable in muscle at P30; subunit 5A was also decreased, in the same tissue, albeit to a lesser extent (Figure 6A). Therefore, the reduction of nuclear and mitochondrial encoded COX subunits seems to be time-dependent, according to a mechanism associated with chronic, progressive accumulation of H₂S in critical tissues, and are in excellent agreement with the progressive reduction of COX activity.

The same reduction of subunits MTCO1 and COX5A was observed in muscle of the Myo-D specific *Ethel*^{-/-} conditional model, and in the brain of the nestin-specific model. No reduction was observed in the liver, muscle and brain of the liver-specific *Ethel*^{-/-} animals (Figure 6B).

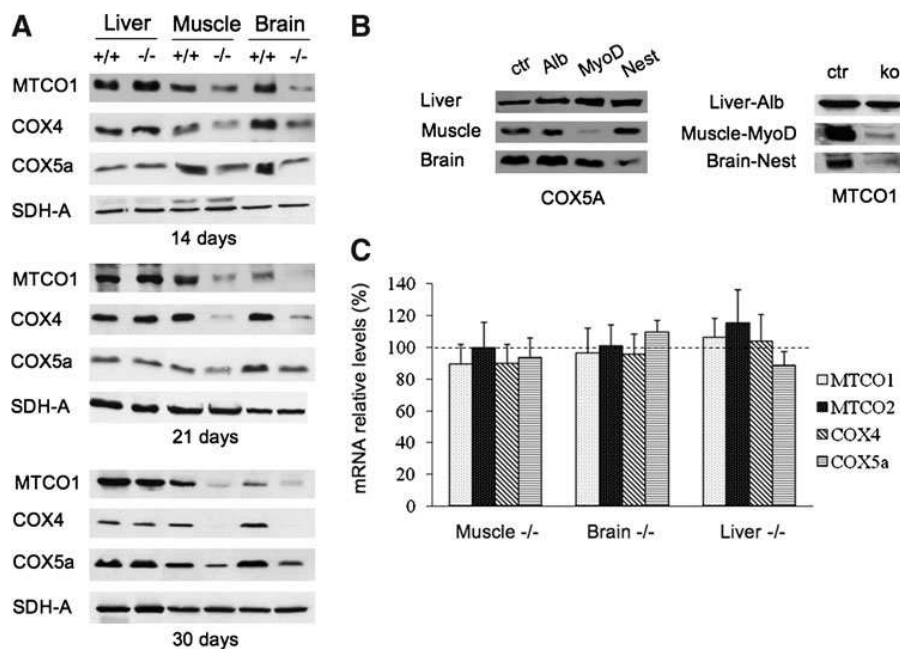


FIG. 6. COX expression in mouse tissues.

(A) Western blot analysis of COX protein subunits in the liver, muscle, and brain of constitutive *Ethe1*^{-/-} mice at different ages (P14, P21, and P30). (B) Western blot analysis using a-COX5A in different tissues of MyoD, nestin, and albumin-conditional *Ethe1*^{-/-} mice; a-MTCO1 was used only in tissues specifically targeted for *Ethe1* gene ablation. ctr: *Ethe1*^{+/+} mouse (WT); ko: conditional *Ethe1*^{-/-} mouse (*Ethe1* knockout in the liver, muscle, and brain). (C) Real-time quantitative PCR analysis of COX transcripts in the liver, muscle, and brain of *Ethe1*^{-/-} mice at P30. Dashed line indicates the expression level of the RNase P control transcript. MTCO, mitochondrially encoded cytochrome c oxidase.

The decrease in the amount of single COX subunits reflects a parallel decrease of steady-state COX holoenzyme. What is the mechanism underpinning this phenomenon? A first possibility is reduced expression of COX-encoding genes. This hypothesis was ruled out by real-time quantitative PCR analysis in different tissues of wild-type and *Ethe1*^{-/-} animals. We found no differences in the transcript level for MTCO1, MTCO2, COX4 and COX5A, indicating that the decrease in the amount of COX subunits and holoenzyme occurs post-

transcriptionally (Figure 6C). A second possibility is impaired translation and assembly, and a third is accelerated degradation of COX.

To test these hypotheses, we performed mitochondrial *in vivo* pulse-chased translation assay in primary human fibroblasts exposed to NaHS. The “pulse” experiment, in which mitochondrial translation is allowed to proceed for two hours, evaluates the capacity of NaHS to affect the *de novo* synthesis of mitochondrial proteins, while the “chase” experiment, which follows the persistence of radiolabeled proteins over a prolonged period of time (24 h), explores the effects of NaHS on protein stability. As shown in Figure 7, the pulse experiment showed no difference in mitochondrial *de novo* protein synthesis in the absence or presence of NaHS. In contrast, the chase experiment showed a strong reduction in the amount of COX specific subunits in cells exposed to NaHS as compared to untreated cells, clearly suggesting accelerated degradation.

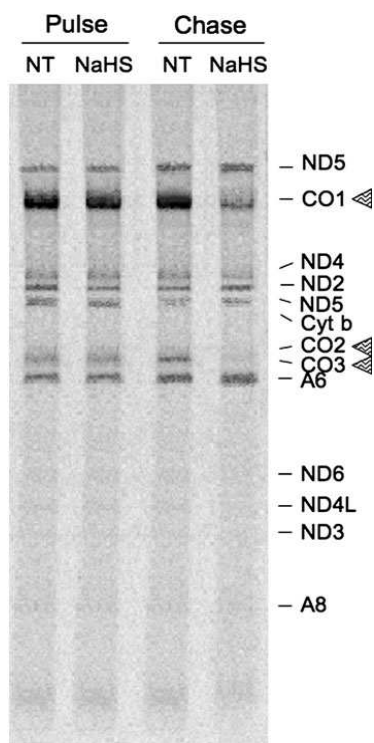


FIG. 7. Mitochondrial in vivo translation.

mtDNA-specific protein synthesis in fibroblasts in the absence (nontreated, NT) or presence of 0.5mM NaHS. Pulse experiment is reported on the left; chase experiment on the right. The autoradiographic bands are labeled according to molecular weight and to standard nomenclature: ND1, ND2, ND3, ND4, ND4L, ND5, and ND6 are subunits of cI; Cyt b is cytochrome b, a subunit of cIII; CO1, CO2, and CO3 are subunits of cIV; and A6 and A8 are subunits of cV (see www.mitomap.org=MITOMAP=MitoPolypeptide). Arrows indicate the absence of MTCO1, MTCO2, and MTCO3.

Likewise, Western-blot analysis performed on HeLa cells showed that the amount of cross-reacting material specific to COX1, 2, 4 and 5A decreased in a dose- and time-dependent manner, and COX4 underwent partial proteolytic degradation (Figure 8A). These effects were specific to COX, since no decrease in the amount of either complex I (i.e. NDUFA9) or complex III (i.e. RISP) subunits was

detected in either experiment, and the corresponding holocomplexes were both normal as demonstrated by measuring their biochemical activity (1). COX activity in NaHS-treated cells after 24 h was decreased, in parallel with the reduction in COX amount (Figure 8B). Again, the transcript levels for COX1, 2, 4 and 5A, were similar to those of untreated cells (Figure 8C).

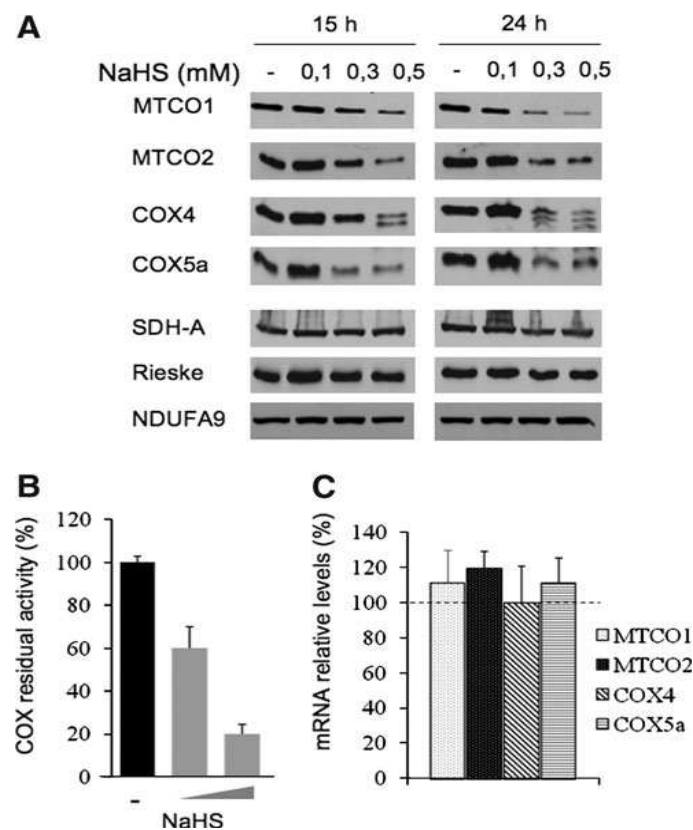


FIG. 8. COX expression in cells.

(A) Western blot analysis of COX protein subunits in HeLa cells treated for 15 or 24 h with different concentration (0.1, 0.3, and 0.5mM) of NaHS. (B) COX residual activity in HeLa cells treated with increasing concentration of NaHS (gray bars) or untreated (black bar).

(C) Real-time quantitative PCR analysis of COX transcripts in HeLa cells treated with 0.5mM NaHS for 24 h. Values are expressed as percentage (%) relative to the mean values of two standard transcripts, HPRT and GAPDH, taken as 100% (dashed line). See Materials and Methods section for details.

Recovery of COX activity in tissue homogenates exposed to NaHS

Biochemical activity of COX was spectrophotometrically measured after incubating liver, muscle and brain homogenates with 10 μ M NaHS and then leaving them exposed to air for as long as 1 hour. As shown in Figure 9, COX activity progressively recovered over time, since after 30 min, COX activity reached 98% of the normal activity in liver, 64% in muscle and 49% in brain, indicating different efficiency of the three tissues in detoxifying H₂S.

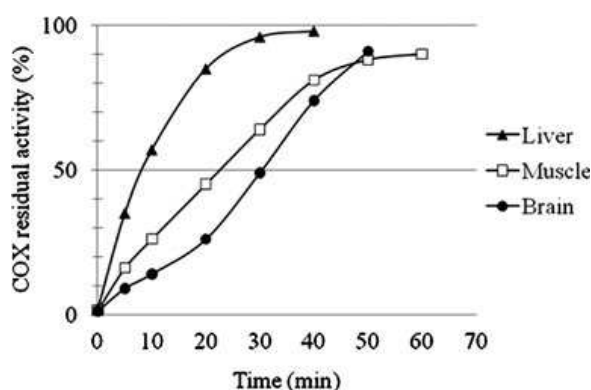


FIG. 9. Biochemical activity of COX in the presence of NaHS.

Recovery of COX activity in the liver, muscle, and brain homogenates assayed at different time points after the addition of 10 mM NaHS.

Discussion

COX is the terminal enzyme of the mitochondrial respiratory chain, catalyzing the electron transfer from reduced cytochrome c to molecular oxygen. According to the bovine enzyme structure, mammalian complex IV is a heteromeric complex composed of 13 different subunits. The catalytic core of the enzyme consists of MTCO1 and MTCO2, two mtDNA-encoded subunits, which contain

the two *heme a* moieties (*a* and *a3*), and the two copper centers (Cu_A and Cu_B) responsible for electron transfer. A third mtDNA-encoded subunit (MTCO3) is part of the structural core and may play a role in proton pumping. The remaining ten subunits (COX4; COX5A,B; COX6A,B C; COX7A,B,C; and COX8) are encoded by nuclear genes and must be imported, processed and assembled together with the mtDNA-encoded subunits. The function of these subunits is currently unknown but they plausibly regulate the activity and stability of the complex. COX deficiency is a frequent cause of disease in humans, being associated with different clinical syndromes and a spectrum of gene defects (20). We demonstrated that a new pathogenic mechanism is at work in EE, based on H₂S-mediated poisoning of COX.

Since COX catalyses the oxidation of ferrocyanochrome c by gaseous molecular oxygen, it is not surprising that other gases, such as NO, CO, and H₂S can also interact with this enzyme. However, whilst at high concentration these gases inhibit COX activity, in trace amounts they play a physiological role as signaling molecules and are in fact produced by normal tissues (19). H₂S, which is endogenously released from L-cysteine by either cystathionine beta-synthase or cystathionine gamma-lyase (21, 22), has been proposed to regulate the vascular tone, myocardial contractility, neurotransmission, and insulin secretion.

We have demonstrated here that the ablation of *Ethel* restricted to muscle or brain is clearly associated with an isolated COX deficiency in the targeted tissue, but not in other, *Ethel*-competent, tissues. This data unequivocally demonstrates that failure to neutralize the

endogenous production of H₂S is sufficient for COX activity to decrease, but not for the animals to become sick, nor for thiosulfate, an EE biomarker of H₂S levels, to increase. This observation suggests that multiorgan accumulation of H₂S and diffusion of exogenously released H₂S from the bacterial flora (23, 24) are both needed to determine the severe metabolic impairment and the fatal clinical course of *Ethel*-less mice and humans. Acute exposure to NaHS for just a few minutes is sufficient to inhibit COX, but this phenomenon is reversible and normal activity can be restored by competitive displacement operated by the oxygen contained in the air. Previous studies have shown that isolated COX is in fact reversibly inhibited by H₂S with a K_i of 0.2 μM, which is independent of oxygen concentration (25). In addition, respiration of isolated mitochondria is 50% reduced at 10 μM H₂S (26), and that of intact cells at about 30 μM (27). H₂S can also interact with the enzyme substrate, cytochrome c, and reduce it (28). However, we showed that, besides direct COX inhibition, chronic exposure to H₂S elicits a time- and dosage-dependent decrease in the amount of the holoenzyme, making the defect permanent and irreversible. Taken together, these findings indicate that in spontaneous and experimental EE the chronic exposure to high levels of H₂S causes a progressive intoxication of tissues, due to a variety of effects, including, among others, COX deficiency.

Since COX-specific transcription was normal in *Ethel*^{-/-} tissues and NaHS-treated cells, the decrease of COX holoenzyme must be due to either defective assembly or accelerated degradation of the enzyme. Whilst the former possibility is unlikely, since assembly

intermediates, which are usually observed in defects of COX assembly, were consistently absent in *Ethel*^{-/-} tissues (1), the concordant decrease of both COX holoenzyme and individual subunits, demonstrated by in vitro translation assay and Western-blot analysis, indicates accelerated degradation of a (crippled) enzyme.

What is the mechanism underlying this phenomenon? COX inhibition by H₂S is exerted on the oxidized states of the binuclear centre of the enzyme; in the fully inhibited state, COX captures two sulfide molecules, one bound to reduced Cu_B, the second to oxidized heme a₃ (29). An excess of sulfide maintains in a reduced state cytochrome a, Cu_A and Cu_B, and determines the formation of cytochrome a₃-SH complex. According to a recently proposed functional COX model under conditions mimicking rate-limiting electron flux (30), at high concentration, H₂S binds to the reduced, FeII, active metal center of heme a₃ (31), thus competing with O₂ for binding to the reduced FeIICuI active site (31). Based on our results, we propose that the binding of H₂S to the metal core causes fully assembled COX to become destabilized and get degraded, possibly starting from the protein backbone that forms its catalytic core. Accordingly, we observed stronger reduction in the amount of MTCO1, MTCO2, COX4 and COX5A, which are the first subunits to be incorporated in the nascent holoenzyme during the assembly process, together with the metal-containing moieties. Interestingly enough, we observed the same accelerated COX degradation in normal human cells chronically treated with H₂S. Similar to that observed in mouse tissues, COX deficiency was associated with reduction in the protein amount of subunits MTCO1, MTCO2, COX4 and COX 5A, but transcription of

the corresponding genes was normal. Importantly, no other respiratory chain complex appeared to be affected, although other enzymatic activities, not directly correlated with the function of the respiratory chain, are also likely to be inhibited by sulfide.

A baffling observation is that, despite the presence of elevated sulfide concentrations, COX is not inhibited in *Ethel*^{-/-} hepatocytes. In agreement with our results, Dorman et al (32) observed significantly elevated, rather than reduced, COX activity in livers of rats exposed to >10 ppm H₂S for 3 h. Along the same line, Huang and co-workers (33) also observed a small, albeit statistically non-significant, increase in liver COX activity of rats exposed to 100 ppm H₂S for 8 h/day, 5 days/week, for 5 weeks. The biological significance of this observation is unclear, but our data on the conditional liver-specific *Ethel*^{-/-} mouse model also suggests that respiration in liver is not inhibited by H₂S, possibly because H₂S neutralization is carried out in this tissue by either additional or more efficient detoxifying systems. In line with this idea, we showed that the most rapid recovery of H₂S-induced COX inhibition was indeed obtained in control liver homogenate, compared to a much slower recovery of muscle and brain.

Acknowledgements

This work was supported by the Pierfranco and Luisa Mariani Foundation Italy, Fondazione Telethon-Italy grant number GGP07019, and grant RF-INN-2007-634163 of the Italian Ministry of Health.

References

1. Tiranti V, Viscomi C, Hildebrandt T, Di Meo I, Mineri R, Tiveron C, Levitt MD, Prella A, Fagiolari G, Rimoldi M, Zeviani M. Loss of ETHE1, a mitochondrial dioxygenase, causes fatal sulfide toxicity in ethylmalonic encephalopathy. *Nat Med* 15: 200-5, 2009.
2. Burlina AB, Dionisi-Vici C, Bennett MJ, Gibson KM, Servidei S, Bertini E, Hale DE, Schmidt-Sommerfeld E, Sabetta G, Zacchello F, et al. A new syndrome with ethylmalonic aciduria and normal fatty acid oxidation in fibroblasts. *J Pediatr* 124: 79-86, 1994.
3. Hildebrandt TM, Grieshaber MK. Three enzymatic activities catalyze the oxidation of sulfide to thiosulfate in mammalian and invertebrate mitochondria. *FEBS J* 275: 3352-61, 2008.
4. Wilson K, Mudra M, Furne J, Levitt M. Differentiation of the roles of sulfide oxidase and rhodanese in the detoxification of sulfide by the colonic mucosa. *Dig Dis Sci* 53(1): 277-83, 2008.
5. Furne J, Springfield J, Koenig T, DeMaster E, Levitt MD. Detoxification of hydrogen sulfide and methanethiol in the cecal mucosa. *J Clin Invest* 104(8): 1107-14, 1999.
6. Szabó C. Hydrogen sulphide and its therapeutic potential. *Nat Rev Drug Discov* 6: 917-35, 2007.

7. Rowan FE, Docherty NG, Coffey JC, O'Connell PR. Sulphate-reducing bacteria and hydrogen sulphide in the aetiology of ulcerative colitis. *Br J Surg* 96(2): 151-8, Review 2009.
8. Kanki H, Suzuki H, Itohara S. High-efficiency CAG-FLPe deleter mice in C57BL/6J background. *Exp Anim* 55(2): 137-41, 2006.
9. Postic C, Shiota M, Niswender KD, Jetton TL, Chen Y, Moates JM, Shelton KD, Lindner J, Cherrington AD, Magnuson MA. Dual roles for glucokinase in glucose homeostasis as determined by liver and pancreatic beta cell-specific gene knock-outs using Cre recombinase. *J Biol Chem* 274(1): 305-15, 1999.
10. Chen JC, Mortimer J, Marley J, Goldhamer DJ. MyoD-cre transgenic mice: a model for conditional mutagenesis and lineage tracing of skeletal muscle. *Genesis* 41(3): 116-21, 2005.
11. Tronche F, Kellendonk C, Kretz O, Gass P, Anlag K, Orban PC, Bock R, Klein R, Schütz G. Disruption of the glucocorticoid receptor gene in the nervous system results in reduced anxiety. *Nat Genet* 23(1): 99-103, 1999.
12. Shih VE, Carney MM, Mandell R. A simple screening test for sulfite oxidase deficiency: detection of urinary thiosulfate by a modification of Sörbo's method. *Clin Chim Acta* 95(1): 143-5, 1979.

13. Tiranti V, D'Adamo P, Briem E, Ferrari G, Mineri R, Lamantea E, Mandel H, Balestri P, Garcia-Silva MT, Vollmer B, Rinaldo P, Hahn SH, Leonard J, Rahman S, Dionisi-Vici C, Garavaglia B, Gasparini P, Zeviani M. Ethylmalonic encephalopathy is caused by mutations in ETHE1, a gene encoding a mitochondrial matrix protein. *Am J Hum Genet* 74: 239-52, 2004.
14. Tiranti V, Galimberti C, Nijtmans L, Bovolenta S, Perini MP, Zeviani M. Characterization of SURF-1 expression and Surf-1p function in normal and disease conditions. *Hum Mol Genet* 8: 2533-2540, 1999.
15. Sciacco M and Bonilla E. Cytochemistry and immunocytochemistry of mitochondria in tissue sections. *Methods Enzymol* 264: 509-21, 1996.
16. Bugiani M, Tiranti V, Farina L, Uziel G, Zeviani M. Novel mutations in COX15 in a long surviving Leigh syndrome patient with cytochrome c oxidase deficiency. *J. Med. Genet* 42(5): e28, 2005.
17. Chomyn A. In vivo labeling and analysis of human mitochondrial translation products. *Methods Enzymol* 264: 197-211, 1996.
18. Kabil O, Banerjee R. The redox biochemistry of hydrogen sulfide. *J Biol Chem* 285(29): 21903-7, 2010.

19. Reiffenstein RJ, Hulbert WC, Roth SH. Toxicology of hydrogen sulfide. *Annu Rev Pharmacol Toxicol* 32: 109-34, 1992
20. DiMauro S, Schon EA. Mitochondrial respiratory-chain diseases. *N Engl J Med* 348(26): 2656-68, 2003.
21. Chiku T, Padovani D, Zhu W, Singh S, Vitvitsky V, and Banerjee R. H₂S biogenesis by human cystathionine gamma-lyase leads to the novel sulfur metabolites lanthionine and homolanthionine and is responsive to the grade of hyperhomocysteinemia. *J Biol Chem* 284: 11601-11612, 2009.
22. Singh S, Padovani D, Leslie RA, Chiku T, and Banerjee R. Relative contributions of cystathionine beta-synthase and gamma-cystathionase to H₂S biogenesis via alternative trans-sulfuration reactions. *J Biol Chem* 284: 22457-22466, 2009.
23. Blachier F, Davila AM, Mimoun S, Benetti PH, Atanasiu C, Andriamihaja M, Benamouzig R, Bouillaud F, Tomé D. Luminal sulfide and large intestine mucosa: friend or foe? *Amino Acids*. 39(2): 335-47, 2010
24. Levitt MD, Springfield J, Furne J, Koenig T, Suarez FL. Physiology of sulfide in the rat colon: use of bismuth to assess colonic sulfide production. *J Appl Physiol* 92: 1655–1660, 2002.

25. Petersen LC. The effect of inhibitors on the oxygen kinetics of cytochrome c oxidase. *Biochim Biophys Acta* 460(2): 299-307, 1977.
26. Yong R, Searcy DG. Sulfide oxidation coupled to ATP synthesis in chicken liver mitochondria. *Comp Biochem Physiol B Biochem Mol Biol* 129(1): 129-37, 2001.
27. Leschelle X, Gubern M, Andriamihaja M, Blottière HM, Couplan E, Gonzalez-Barroso MD, Petit C, Pagniez A, Chaumontet C, Mignotte B, Bouillaud F, Blachier F. Adaptative metabolic response of human colonic epithelial cells to the adverse effects of the luminal compound sulfide. *Biochim Biophys Acta* 1725(2): 201-12, 2005.
28. Nicholls P, Kim JK. Sulphide as an inhibitor and electron donor for the cytochrome c oxidase system. *Can J Biochem* 60(6): 613-23, 1982.
29. Hill BC, Woon TC, Nicholls P, Peterson J, Greenwood C, Thomson AJ. Interactions of sulphide and other ligands with cytochrome c oxidase. An electron-paramagnetic-resonance study. *Biochem J* 224(2): 591-600, 1984.
30. Collman JP, Devaraj NK, Decréau RA, Yang Y, Yan YL, Ebina W, Eberspacher TA, Chidsey CE. A cytochrome C oxidase model catalyzes oxygen to water reduction under rate-limiting electron flux. *Science* 315(5818): 1565-8, 2007.

31. Collman JP, Ghosh S, Dey A, Decréau RA. Using a functional enzyme model to understand the chemistry behind hydrogen sulfide induced hibernation. *Proc Natl Acad Sci U S A* 106(52): 22090-5, 2009.
32. Dorman DC, Moulin FJ, McManus BE, Mahle KC, James RA, Struve MF. Cytochrome oxidase inhibition induced by acute hydrogen sulfide inhalation: correlation with tissue sulfide concentrations in the rat brain, liver, lung, and nasal epithelium. *Toxicol Sci* 65(1): 18-25, 2002.
33. Huang J, Niknahad H, Khan S, O'Brien PJ. Hepatocyte-catalysed detoxification of cyanide by L- and D-cysteine. *Biochem Pharmacol* 55(12): 1983-90, 1998.

Chapter 3:

Ethylmalonic encephalopathy: application of improved biochemical and molecular diagnostic approaches

Drousiotou A¹, DiMeo I², Mineri R², Georgiou Th¹, Stylianidou G³, Tiranti V².

¹Department of Biochemical Genetics, The Cyprus Institute of Neurology and Genetics, Nicosia, Cyprus,

²Unit of Molecular Neurogenetics, Pierfranco and Luisa Mariani Center for Research on Children's Mitochondrial Disorders, Institute of Neurology "Carlo Besta" – IRCCS Foundation, Milan, Italy.

³ Department of Paediatric Neurology, Archbishop Makarios III Hospital, Nicosia, Cyprus

CLINICAL GENETICS. 2011 Apr;79(4):385-90.

Abstract

Ethylmalonic encephalopathy (EE, OMIM # 602473) is an autosomal recessive metabolic disorder of infancy affecting the brain, the gastrointestinal tract and peripheral vessels. It is caused by a defect in the *ETHE1* gene product, which was recently shown to be part of a metabolic pathway devoted to sulphide detoxification. We report the application of improved biochemical and molecular approaches to the diagnosis of three cases of EE from two unrelated Cypriot families. The children presented all the typical biochemical hallmarks of the disease including elevated lactate and butyrylcarnitine in blood and elevated urinary excretion of ethylmalonic acid, 2-methylsuccinate, isobutyrylglycine and isovalerylglycine. We also detected an elevated level of thiosulphate in urine, which we propose as an additional biochemical marker of the disease. The proband of the first family was shown to be a compound heterozygote for a missense mutation in exon 5, L185R, and a deletion of exon 4. The deletion was identified using quantitative real-time polymerase chain reaction (qRT-PCR). Using the same technique, the proband of the second family was found to be homozygous for the exon 4 deletion. A prenatal diagnosis was performed for the second family using qRT-PCR, thus establishing the usefulness of RT-PCR in prenatal diagnosis.

Introduction

Ethylmalonic encephalopathy (EE, OMIM # 602 473) is a devastating metabolic disorder of infancy affecting the brain, the gastrointestinal

tract, and peripheral vessels. It was originally reported in Italian families in 1991 (1) and subsequently in other populations, mostly Mediterranean and Arabic (2–4). The disorder is characterized by neurodevelopmental delay and regression, prominent pyramidal and extrapyramidal signs, recurrent petechiae, orthostatic acrocyanosis and chronic diarrhoea and leads to death in the first decade of life. The magnetic resonance imaging (MRI) shows symmetrical necrotic lesions in the deep grey matter structures. Biochemically, the disorder is characterized by persistent lactic acidemia, elevated concentration of C4 and C5 plasma acylcarnitine species, and in the urine, elevated concentration of ethylmalonic acid (EMA), isobutyrylglycine and 2-methylbutyryl glycine. Recently, elevated urinary thiosulphate was shown to be an additional biomarker of EE (5). Cytochrome *c* oxidase activity is reduced in muscle but not in fibroblasts. Tiranti et al. (2) identified the gene responsible for EE, on chromosome 19q13, using a combination of homozygosity mapping, integration of physical and functional genomic data sets and mutational screening. Twenty-seven different mutations have been so far identified in the *ETHE1* gene (2–4, 6, 7). The product of the *ETHE1* gene (GenBank D83198) is a protein targeted to mitochondria and internalized into the matrix after an energy-dependent cleavage of a short leader peptide (2, 3). A recent study (5) has shown that the human *ETHE1* protein has a homodimeric structure, contains one iron atom per monomer and has sulphur dioxygenase (SDO) activity, being part of a mitochondrial metabolic pathway responsible for sulphide detoxification. In this study, we present three cases of EE from two unrelated Cypriot families. In addition to the usual biochemical markers, these subjects

were also analysed for the presence of urinary thiosulphate, a new metabolic marker of the disease. The molecular characterization of the *ETHE1* gene was performed using direct sequencing and quantitative real-time PCR (qRT-PCR).

Materials and methods

Subjects

The three children studied came from two unrelated Greek Cypriot families. Informed consent was obtained from the parents of the patients.

Patient 1

This was the third child of non-consanguineous parents. Delivery and perinatal period were unremarkable. She presented at the age of 21/2 months with feeding difficulties, failure to thrive, petechiae and ecchymosis. She was found to be floppy with severe head lag and microcephaly but with no dysmorphic features. Her responses to auditory and visual stimuli were poor. Her muscle tone varied from hypotonia to hypertonia, particularly in the lower limbs. Deep tendon reflexes were exaggerated, and there was sustained clonus and bilateral Babinski. She subsequently developed chronic diarrhoea and seizures. Her neurological condition showed regression. MRI of the brain revealed multiple loci of high intensity on the T2-weighted images and low-signal intensity on the Flair and T1W/SE images of the basal ganglia bilaterally. The biochemical findings are

summarized in Table 1. She is currently 51/2 years old and is fed through a gastrostomy. She suffers from frequent aspiration-induced infections.

Patient 2

The second case was the older brother of the first case. He had a history of failure to thrive and chronic diarrhoea. At the age of 6 months, he presented with a chest infection during which he developed seizures and required mechanical ventilation. An ultrasound of the brain showed prominent hyperechogenicity of gyri and sulci. The biochemical findings are summarized in Table 1. He died a few days after admission to hospital without a diagnosis. No tissues were available for confirmation of diagnosis when the diagnosis of his sister was made.

Patient 3

The third case was a girl, the first child of nonconsanguineous parents and unrelated to the first family. She was delivered at 36 weeks of gestation by elective caesarean section due to intrauterine growth retardation. She was transferred to the neonatal intensive care unit where she stayed for 1 week without any complications. She presented at 6 months of age with feeding difficulties, hypotonia and global developmental delay. Later on, she started having diarrhoea and developed petechiae and ecchymosis as well as seizures. MRI of the brain showed evidence of high-signal foci at the basal ganglia and thinning of the corpus calosum. The biochemical findings are

summarized in Table 1. She showed psychomotor regression and died at 8 months of age from cardiopulmonary arrest.

Mutation analysis

DNA extracted from fibroblasts was used as a template for PCR amplification of the seven exons of the *ETHE1* gene, using intronic primers as previously described (2). Sequence analysis was performed on a 3100 ABI Automated Sequencer using the BigDye Terminator Kit and the seqscape software (Applied Biosystems, Foster City, CA). qRT-PCR was performed using a TaqMan (5' nuclease) assay system with signal from exon 4 *ETHE1*-specific probe that is normalized to the signal for a reference gene (*RNase P*). Primer pairs and probe were selected to be unique using primer express 2.0 software (Applied Biosystems). To assay *ETHE1* exon 4 copy number relative to reference gene *RNase P*, duplicate PCRs using 15 ng of genomic DNA, 0.6 mM of each *ETHE1* primer (forward, 5'-CCAGGCTGTGTCACCTTCGT-3'; reverse, 5'-CAACAGGGCATCTCCAGTGAA-3'), 1× final concentration of 20 × *RNase P* Primer-Probe (VIC™ dye) mix, and 0.2 mM of fluorescent product-specific oligonucleotide probe (*ETHE1*, 6FAM-TGAATGACCACAGCATGG-MGB) were prepared in 1× Master Mix (Applied Biosystems). Thermal cycling conditions were as follows: 50°C for 2 min, 95°C for 10 min, followed by 40 cycles at 95°C for 15 s and 60°C for 1 min. PCR was performed in a 96-well optical plate using the ABI PRISM 7000 Sequence Detection System

(Applied Biosystems). Data analysis was conducted by adapting the $\Delta\Delta C_t$ method of relative quantification (8) to estimate copy numbers of the *ETHE1* exon 4. Known negative control samples (carrying no deletion) and positive control samples (carrying deletion on both alleles) were analysed in each reaction as calibrators.

Haplotype analysis

A dense haplotype analysis was performed using four intragenic single-nucleotide polymorphisms as previously reported (4). Western blot analysis on homogenized fibroblasts from the affected children was carried out as previously described (2, 3). A polyclonal antibody, anti-Ethe1pC17, against an oligopeptide encompassing amino acids 190–206 in the C-terminal of the Ethe1p, was used. The same filter was hybridized with the anti-Ethe1p antibody and, after stripping, with a mixture of anti- α and anti- β electron transfer factor subunits.

Thiosulphate determination in urine

Using a modification of the spectrophotometric method of Shih et al. (9), thiosulphate was detected and measured in urine samples of EE patients and controls. Urine (0.2 ml) and water (1.4 ml) were mixed in a test tube and the pH was adjusted to 10 with 0.1 ml of 4 M NH_4OH . This was followed by the addition of 0.2 ml of 100 mM KCN and then of 0.12 ml of 100 mM CuCl_2 . After mixing, 0.2 ml of $\text{Fe}(\text{NO}_3)_3$ reagent was added. The absorbance at 460 nm was determined by reading within 1 h. A standard curve was obtained using different concentrations of thiosulphate. The procedure is based on the

cyanolysis of thiosulphate to thiocyanate, thiocyanate itself, if present in urine, would produce colour. Thiosulphate concentration is reported as nmol/mg creatinine.

Patient /sex	Clinical features	Plasma			Urine			Muscle	Fibroblasts	DNA
		Lactate (mmol/l; NR: 0.3–1.30)	Butyryl-carnitine	Ethylmalonic acid (μmol/mmol creatinine; NR: up to 60)	Methylsuccinate (μmol/mmol creatinine; NR: up to 10)	Butyrylglycine/isobutyrylglycine	Thiosulphate (nmol/mg creatinine; NR: 100–560)			
Patient 1 ^b /F	Presented at 2½ months. Feeding difficulties, FTT, petechiae, hypotonia, seizures, diarrhoea, abnormal MRI. Alive at 5½ years	6.47	↑	331	42	↑	2307	8%	No ETHE1 protein	L185P/deletion of exon 4
Patient 2 ^b /M	Presented at 6 months. FTT, diarrhoea, seizures, abnormal brain U/S. Died at 6 months	16.74	ND	213	18	ND	18175	ND	ND	L185P/deletion of exon 4 (assumed, sibling of patient 1)
Patient 3 ^b /F	Presented at 6 months. Hypotonia, global developmental delay, feeding difficulties, diarrhoea, petechiae, seizures, abnormal MRI. Died at 8 months	3.93	ND	↑↑	↑	↑	2119	ND	No ETHE1 protein	deletion of exon 4/deletion of exon 4

FTT, failure to thrive; MRI, magnetic resonance imaging; U/S, ultrasound; NR, normal range; ND, not determined.
^aDNA mutation numbering is based on cDNA sequence starting from the first ATG.
^bSiblings.

Table 1. Clinical, biochemical and molecular data of Cypriot patients with Ethylmalonic encephalopathy

Results

The clinical, biochemical and molecular data of the three Cypriot patients are summarized in Table 1. The clinical picture of patients 1 and 3 is the typical picture associated with EE and includes diarrhoea, petechiae and orthostatic acrocyanosis. Patient 2, who died soon after presentation with a poorly documented clinical picture, was presumed to be affected by EE, based on the clinical and molecular diagnosis performed in his sister. The biochemical findings include elevations in blood lactate, urine EMA, methylsuccinate, butyryl/isobutyrylglycine and thiosulphate. In patient 1, from whom a muscle biopsy was taken, cytochrome *c* oxidase activity was reduced to 8% of the normal mean. Western blot analysis in patients 1 and 3 showed complete absence of the *ETHE1* protein (Fig. 1). DNA sequencing in the first patient revealed the presence of a missense mutation in exon 5, c.554T>G resulting in the substitution of leucine by arginine (L185R). We consistently failed to identify the second mutation using PCR amplification followed by sequence analysis. However, Western blot analysis on the patient's fibroblasts showed the absence of the *ETHE1* protein (Fig. 1). This observation prompted us to search for the second mutation in the *ETHE1* gene, which we hypothesized to be a deletion.

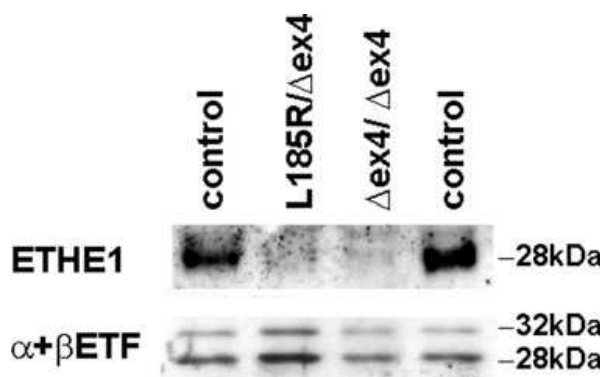


Fig. 1. Western blot analysis for the ETHE1 protein on fibroblasts from patient 1 (lane 2) and patient 3 (lane 3). The membrane was probed with a polyclonal antibody (anti-Eth1pC17) against an oligopeptide encompassing amino acids 190–206 in the C-terminal of the ETHE1 protein. The membrane was reprobbed, after stripping, with antibodies specific to the α (32 kDa) or β (28 kDa) subunit of the electron transfer factor as a control.

Because one of the most frequent mutations affecting this gene is a deletion of exon 4, we analyzed this exon using qRT-PCR. As a control, we also used primers covering exon 3, and this was found to be present in normal amount (data not shown). We performed qRT-PCR on DNA extracted from the patient and her parents (Fig. 2). The patient as well as her father was found to carry the deletion of exon 4 in a heterozygous state, whereas the mother, who had the L185R mutation on one allele, carried both copies of exon 4. No material was available from the first child of this family (patient 2) for DNA or Western blot studies. However, from the clinical and biochemical findings, we can assume that he had the same genotype as his sister. The proband from the second family was found to be homozygous for the deletion in exon 4, and in this case, qRT-PCR showed that the parents were both heterozygous for the deletion (Fig. 2).

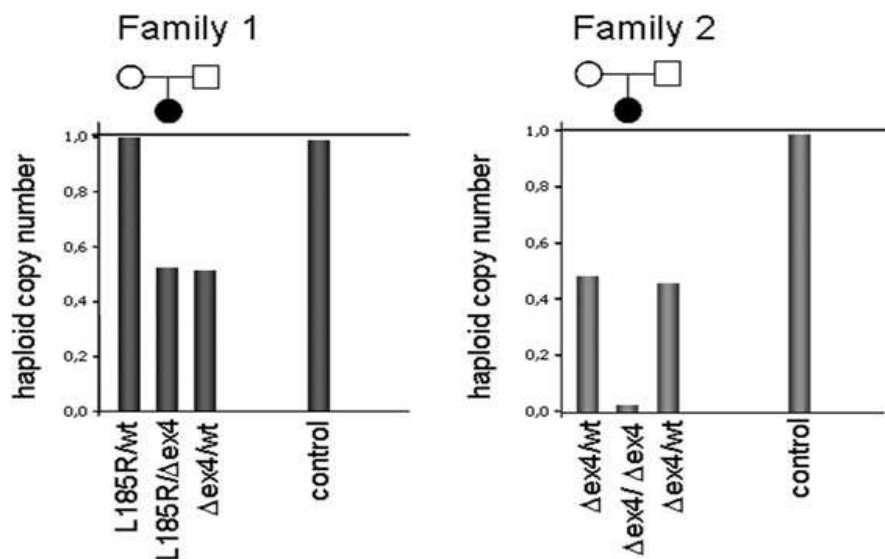


Fig. 2. Haploid copy numbers for *ETHE1* exon 4 as shown by quantitative real-time polymerase chain reaction.

Discussion

An increasing number of patients with EE are being diagnosed, especially in Mediterranean countries. Since the initial report, about 45 cases have been described worldwide. This number is probably an underestimate because this condition shares several clinical and biochemical findings with other disorders, and it can easily be misdiagnosed. In fact, one of the three Cypriot patients described in this report was at first mistaken for a case of child abuse because of the petechiae and bruises. By taking advantage of the recent identification of the role of the ETHE1 protein in sulphur metabolism

(5), a new biochemical marker can be searched in the urine of patients with EE. This metabolite is thiosulphate, which is excreted in great quantities in affected patients. We measured thiosulphate in our patients and in all of them, we consistently found elevated levels (Table 1). We propose to include the measurement of this compound in the metabolic evaluation of patients suspected of EE. We have identified two mutations in the Cypriot patients with EE. The first one is a missense mutation in exon 5 (L185R) which has previously been found in one Italian (2) and one Arab patient (4). This mutation has been classified as a structural mutation that leads to the destabilization and degradation of the *ETHE1* protein (3). The Western blot for the Cypriot patient with this mutation has confirmed this classification (Fig. 1). The second mutation found in the Cypriot patients is a deletion of exon 4. This mutation has been previously described in seven patients from the Arabian peninsula, six of whom were homozygous for the deletion (like our patient 3) and one was a compound heterozygote with the same genotype as our patient 1 (2). The exon 4 deletion is associated with the absence of the *ETHE1* protein and this has been confirmed in this study. Both patient 3 who is homozygous for the deletion and patient 1 who is heterozygous for the deletion show complete absence of *ETHE1* (Fig. 1). The exon 4 deletion is one of three *ETHE1* recurrent mutations and has been found to be associated with the same haplotype in three unrelated Arab patients examined (4). Haplotype analysis of our patients showed that they have the same haplotype as the Arab patients, possibly indicating a common origin (Table 2).

Table 2. Haplotype analysis using four intragenic single nucleotide polymorphisms (SNPs)

Marker	Patient 1 (L185R/deletion of exon 4)	Patient 3 (deletion of exon 4/deletion of exon 4)
rs.2261316	AG	GG
rs.3810381	GG	GG
rs.3810380	GG	GG
5'UTR(-41)	GG	GG

The three Cypriot carriers of the exon 4 deletion are not related, neither do they originate from the same area of Cyprus. The introduction of qRT-PCR for the evaluation of patients with monoallelic deletions is important for prenatal genetic diagnosis because we can now establish whether a subject carries a deletion in the heterozygous state. A prenatal diagnosis was performed for family 2 using qRT-PCR which showed that the foetus was homozygous for the exon 4 deletion. qRT-PCR would also be useful for prenatal diagnosis in family 1. Using this method and the direct detection of the L185R mutation by sequence analysis, we can distinguish between a compound heterozygote, a heterozygote for exon 4 deletion, a heterozygote for the L185R mutation, and a normal foetus. Our results show the usefulness of qRT-PCR in the prenatal diagnosis of EE, as well as in other genetic disorders, where exon deletions are involved.

Acknowledgement

This paper is dedicated in the memory of Dr Goula Stylianidou.

References

1. Burlina A, Zacchello F, Dionisi-Vici C et al. New clinical phenotype of branched-chain acyl-CoA oxidation defect. *Lancet* 1991; 338: 1522–1523.
2. Tiranti V, D'Adamo P, Briem E et al. Ethylmalonic encephalopathy is caused by mutations in *ETHE1*, a gene encoding a mitochondrial matrix protein. *Am J Hum Genet* 2004; 74: 239–252.
3. Tiranti V, Briem E, Lamantea E et al. *ETHE1* mutations are specific to ethylmalonic encephalopathy. *J Med Genet* 2006; 43: 340–346.
4. Mineri R, Rimoldi M, Burlina AB et al. Identification of new mutations in the *ETHE1* gene in a cohort of 14 patients presenting with ethylmalonic encephalopathy. *J Med Genet* 2008; 45: 473–478.
5. Tiranti V, Viscomi C, Hildebrandt T et al. Loss of *ETHE1*, a mitochondrial dioxygenase, causes fatal sulfide toxicity in ethylmalonic encephalopathy. *Nat Med* 2009; 15: 200–205.
6. Merinero B, Perez-Cerda C, Ruiz Sala P et al. Persistent increase of plasma butyryl/isobutyrylcarnitine concentrations as marker of SCAD defect and ethylmalonic encephalopathy. *J Inherit Metab Dis* 2006; 29: 685.
7. Zafeiriou DI, Augoustides-Savvopoulou P, Haas D et al. Ethylmalonic encephalopathy: clinical and biochemical observations. *Neuropediatrics* 2007; 38: 78–82.

8. Livak KJ, Schmittgen TD. Analysis of relative gene expression data using real-time quantitative PCR and the 2(-Delta Delta C(T)) method. *Methods* 2001; 25: 402–408.
9. Shih VE, Carney MM, Mandell R. A simple screening test for sulfite oxidase deficiency: detection of urinary thiosulfate by a modification of Sorbo's method. *Clin Chim Acta* 1979; 95: 143–145.

Chapter 4:

Morphologic evidence of diffuse vascular damage in human and in the experimental model of ethylmalonic encephalopathy.

Giordano C¹, Viscomi C², Orlandi M¹, Papoff P¹, Spalice A¹, Burlina A³, **Di Meo I**², Tiranti V², Leuzzi V¹, d'Amati G¹, Zeviani M².

¹ Department of Radiological, Oncological and Pathological Sciences, Sapienza University, Policlinico Umberto I, Viale Regina Elena 324, 00161, Rome, Italy.

²Unit of Molecular Neurogenetics, Pierfranco and Luisa Mariani Center for Research on Children's Mitochondrial Disorders, Institute of Neurology "Carlo Besta" – IRCCS Foundation, Milan, Italy.

³ Clinic of Pediatrics, University of Padua School of Medicine, Padua, Italy.

*JOURNAL OF INHERITED METABOLIC DISEASE, 2011 Oct 22.
[Epub ahead of print]*

Abstract

Ethylmalonic encephalopathy (EE) is a rare autosomal recessive disorder characterized by early onset encephalopathy, chronic diarrhea, petechiae, orthostatic acrocyanosis and defective cytochrome c oxidase (COX) in muscle and brain. High levels of lactic, ethylmalonic and methylsuccinic acids are detected in body fluids. EE is caused by mutations in *ETHE1*, a mitochondrial sulphur dioxygenase. By studying a suitable mouse model, we found that loss of *ETHE1* leads to accumulation of sulphide, which is a poison for COX and other enzymatic activities thus accounting for the main features of EE. We report here the first autopsy case of a child with a genetically confirmed diagnosis of EE, and compare the histological, histochemical and immunohistochemical findings with those of the constitutive *Ethe1*^{-/-} mice. In addition to COX depleted cells, widespread endothelial lesions of arterioles and capillaries of the brain and gastrointestinal tract were the pathologic hallmarks in both organisms. Our findings of diffuse vascular damage of target critical organs are in keeping with the hypothesis that the pathologic effects of *ETHE1* deficiency may stem from high levels of circulating hydrogen sulphide rather than the inability of specific organs to detoxify its endogenous production.

Introduction

Ethylmalonic encephalopathy (EE) is a rare autosomal recessive disorder caused by mutations in *ETHE1* (OMIM #602473), a gene

encoding a mitochondrial sulphur dioxygenase (Tiranti et al. 2004; Tiranti et al. 2009). EE is clinically characterized by the early onset of neurological degeneration, chronic diarrhea, recurrent petechiae, and orthostatic acrocyanosis, leading to death in the first years of life. Biochemical hallmarks of the disease are persistently high levels of lactate, and C4-C5 acylcarnitines in blood, markedly elevated urinary excretion of methylsuccinic and ethylmalonic (EMA) acids and defective cytochrome c oxidase (COX) in muscle and brain. The main neuroimaging features of the disease are patchy, bilateral necrotic lesions in the basal ganglia and brainstem, thinning of the brain cortical ribbon and corpus callosum, and leukodystrophic changes in the centrum semiovale (Burlina et al. 1991; Garcia-Silva et al. 1994; Garavaglia et al. 1994; Grosso et al. 2002). The pathogenic mechanisms underlying the clinical and biochemical abnormalities observed in EE have been recently elucidated. By using a constitutive *Ethe1*^{-/-} mouse model, Tiranti et al. showed that the main consequence of ETHE1 loss is the accumulation of hydrogen sulphide (H₂S) a product of intestinal anaerobes and, in trace amount, tissues (Tiranti et al. 2004). Increased concentration of sulphide in tissues (i.e. colonic mucosae, muscle and brain) causes rapid inhibition of COX activity and longterm degradation of COX subunits (Di Meo et al. 2011). In addition, H₂S blocks short-chain fatty acid oxidation by inhibiting the activity of short-chain acylCoA dehydrogenase (and possibly other beta-oxidation enzymes as well), which explains the accumulation of EMA, and has vasoactive and vasotoxic effects (Szabo 2007), which explain the vascular lesions in the skin and possibly, other organs. Recently, combined treatment with metronidazole and N-

acetylcysteine has been shown to significantly increase the lifespan in *Ethel^{-/-}* mice, and to improve the clinical outcomes in affected patients (Viscomi et al. 2010). These results were paralleled by a decrease of serum thiosulphate, a stable and readily measurable index of H₂S (Viscomi et al. 2010). An additional therapeutic approach, based on dietary restriction for branched amino acids, fatty acids and methionine, has also been proposed, but the clinical consequence of this treatment is currently undetermined (Barth et al. 2010). Clinical and experimental evidence provided so far suggests that application of treatments starting from the perinatal age could prevent or reduce irreversible brain damage. In the present study we report the first autopsy case of a child with a genetically confirmed diagnosis of EE, and compare the microscopic features found in this patient with those of the constitutive *Ethel^{-/-}* mice. In both organisms, widespread, complex vascular lesions are the pathological hallmark of the disease in the brain and gastrointestinal tract.

Case report

The patient was the only child of healthy unrelated parents. Her mother is of Sub-Saharan African ancestry, the father is European. They experienced four miscarriages before the birth of the index patient that occurred at 40 weeks of gestation by vaginal delivery. The birth weight was 3250 g. At four months, she was first admitted to hospital because of sudden bilateral and symmetrical spasms of the neck, trunk and extremities. On examination she showed: hypotonia and weakness, severe psychomotor delay, increased deep tendon

reflexes, and clonus. Hypsarrhythmia was detected by EEG and led to a diagnosis of West syndrome. Brain MRI showed multiple patchy areas of abnormal signal intensity involving the lenticular and caudate nuclei bilaterally (Fig. 1a), as well as the brainstem and cerebellar dentate nuclei. Brain proton MR spectroscopy showed a lactate peak in the areas with altered MRI signal (not shown). Blood investigation revealed increased values of lactate whereas those of pyruvate, ammonia and amino acids were normal. The levels of C4-C6 carnitines were persistently elevated: butyrylcarnitine 1.72-2.64 $\mu\text{mol/L}$ (reference values [r.v.] 0.07-0.55), iso-valerylcarnitine 0.71-1.62 $\mu\text{mol/L}$ (r.v. 0.07-0.46), hexanoyl-carnitine 0.18-0.25 (r.v. 0.00-0.14). EMA was increased in plasma (6.6, 7.9 $\mu\text{mol/L}$; normal values <2) and urine (247.4 mmol/mol creatinine; r.v. <20). Urinary organic acids also showed increased lactic, pyruvic, methylsuccinic, suberic, and adipic acids and isovaleryl glycine. Lactic acid was elevated also in the CSF (4,44 mmol/L; r.v. $\leq 1,33$). Histochemical analysis of a skeletal muscle biopsy showed diffuse COX deficiency (Fig. 1b). Biochemical analysis on muscle homogenate confirmed an isolated defect of COX activity (10% of the normal mean value). Direct sequencing of the ETHE1 gene showed the presence of a novel c.622_624delGAG leading to p.Q208del in exon 6 in the paternal allele, in compound with two nucleotide substitutions in the maternal allele: the novel c.340A>T in exon 3, leading to a p.I114F amino acid change, and the previously described c.488 G>A in exon 4, leading to p.R163Q amino acid change (Fig. 1c). Whilst the R163 residue is evolutionarily conserved and the pathogenic role of the Q163 variant has been experimentally demonstrated (Tiranti et al. 2006), the I114

residue is poorly conserved, making it possible for the I114F change to be a rare non-pathogenic variant. The ETHE1 protein failed to be immunovisualized in Western-blot analysis of proteins extracted from skeletal muscle homogenate, using a specific anti-ETHE1 antibody (Fig. 1d). On follow-up, the patient showed progressive clinical deterioration. At the age of five months bouts of petechiae on the trunk and limbs appeared, with acrocyanosis and acral edema. Platelet count was normal, as were platelet and blood coagulation tests. The frequency of her tonic spasms slowly decreased from 8 months of life, coincidental to worsening of cognitive and motor functions, with increased pyramidal signs. Mucous diarrhoea consisted of three-four bowel movements daily. At the age of 9 months she was admitted to an intensive care unit because of acute severe metabolic acidosis and coma triggered by a respiratory infection. Laboratory investigations disclosed profound lactic acidosis and rhabdomyolysis (creatin kinase: up to 11,103 U/L; normal values: 22 to 198 U/L; myoglobin, up to 412,8 nmol/L, normal values: 0 to 4,85 nmol/L). A platelet count and blood coagulation tests were within normal limits (platelets: 289.000/ml; n.v: 150.000- 350.000/ml; fibrinogen 9,4 μ mol/L; n.v: 5–12,3 μ mol/L, prothrombin time: 1.47; n.v: 1–2.) excluding a disseminated intravascular coagulation. A brain MRI showed marked anoxic ischaemic damage of the lenticular and caudate nuclei with extensive involvement of the brainstem, cortex and cerebellar dentate nuclei (Fig. 2a). The EEG showed marked, diffuse depression of cerebral activity. The baby girl died 3 days after admission due to catecholamine-refractory circulatory failure. An EEG obtained a few

hours before death showed no electric activity. After having obtained the informed parental consent a complete autopsy was performed.

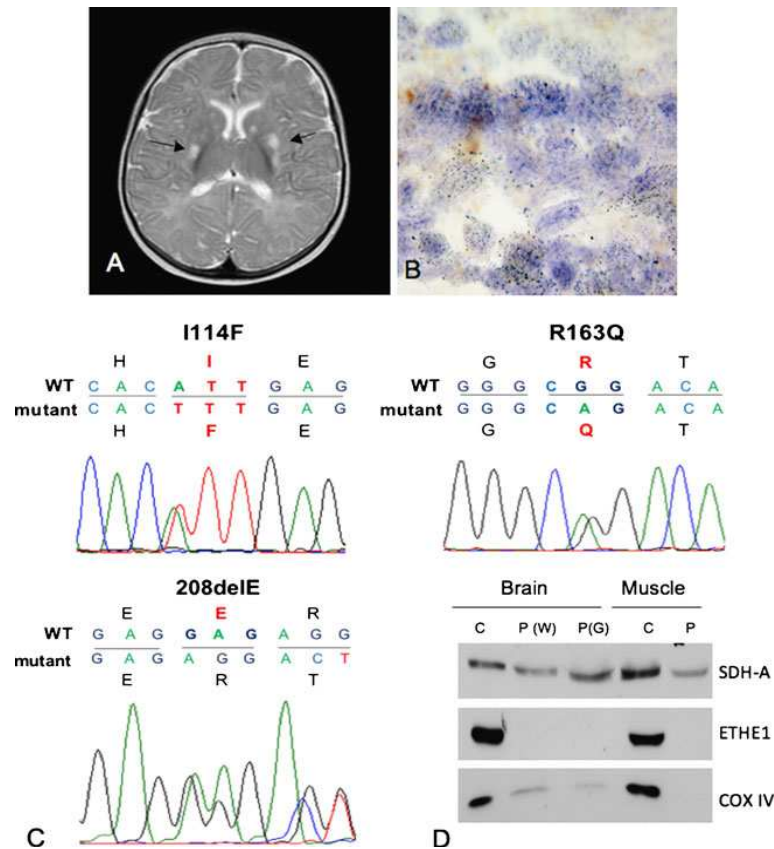


Fig. 1 Clinical and molecular features of the ETHE1 patient.

a. Brain MRI at first hospital admission (age of four months): axial T2-weighted image shows patchy area of abnormal signal intensity in the lenticular and caudate nuclei bilaterally. b. Combined COX/SDH histochemistry showing only blue-stained myocytes, consistent with profound and diffuse reduction in COX reactivity. c. Sequence electropherograms showing the novel c. 340A>T mutation, leading to a p.I114F aminoacid change, the c.488 G>A, leading to p.R163Q aminoacid change, and the novel c.622_624delGAG leading to p.Q208del. d. Western-blot analysis using an α -ETHE1 and a COXIV antibody on muscle and brain from the patient and an age matched control. An α -SDH-A antibody was used as a protein-loading standard. C=control; P=patient; W=white matter; G=gray matter

Materials and methods

Analysis of human tissues

Postmortem samples were fixed in 10% formalin or frozen in liquid nitrogen–chilled isopentane. Histological slides were stained with hematoxylin and eosin (H&E), periodic acid Schiff (PAS) and PAS plus diastase, Luxol Fast Blue and Picro Sirius Red. Combined cytochrome c oxidase/succinic dehydrogenase (COX/SDH) staining was performed on frozen sections (colon, brain, skeletal muscle, heart liver). Antibodies against CD31, smooth muscle actin, collagen IV, NeuN, glial fibrillary acidic protein (GFAP, DAKO Glostrup, Denmark), MTCOI and COXIV (Mitoscience, Eugene, OR) were used for immunohistochemical staining. For ultrastructural analysis, liver autopsy samples were fixed in 4% paraformaldehyde-phosphate buffered saline and post-fixed in osmium tetroxide. Thin sections were stained with uracyl acetate and lead citrate and examined with a CM10 Philips electron microscope. Western blot analysis was performed on protein lysates obtained from muscle biopsy and autoptic brain, using anti-ETHE1 and COXIV antibodies as reported (Di Meo et al. 2011).

Analysis of mouse tissues

The same histological analyses were performed on brain, heart, liver, kidney, spleen, gut and skeletal muscle obtained from 6 one-month old *Ethel^{-/-}* mice (Tiranti et al. 2009) and five control littermates. According to the ethical committee guidelines the animals were

sacrificed by cervical dislocation, followed by formalin fixation or rapid freezing in liquid nitrogen-chilled isopentane.

Results

Autopsy findings

The most remarkable macroscopic changes were observed in the brain, liver and gastric and colonic mucosae. The brain weighed 720 g after formalin fixation (n.v. for age 750–809) and showed diffuse edema. The leptomeninges were mildly thickened. At gross examination, both hemi- spheres showed multiple grayish areas of softening, consistent with acute ischaemic necrosis. These were particularly evident in the temporal and occipital lobes, and in the hippocampus bilaterally. The basal ganglia showed reddish-brown discolored areas, with marked vascular congestion, more prominent in the right putamen (Fig. 2b).

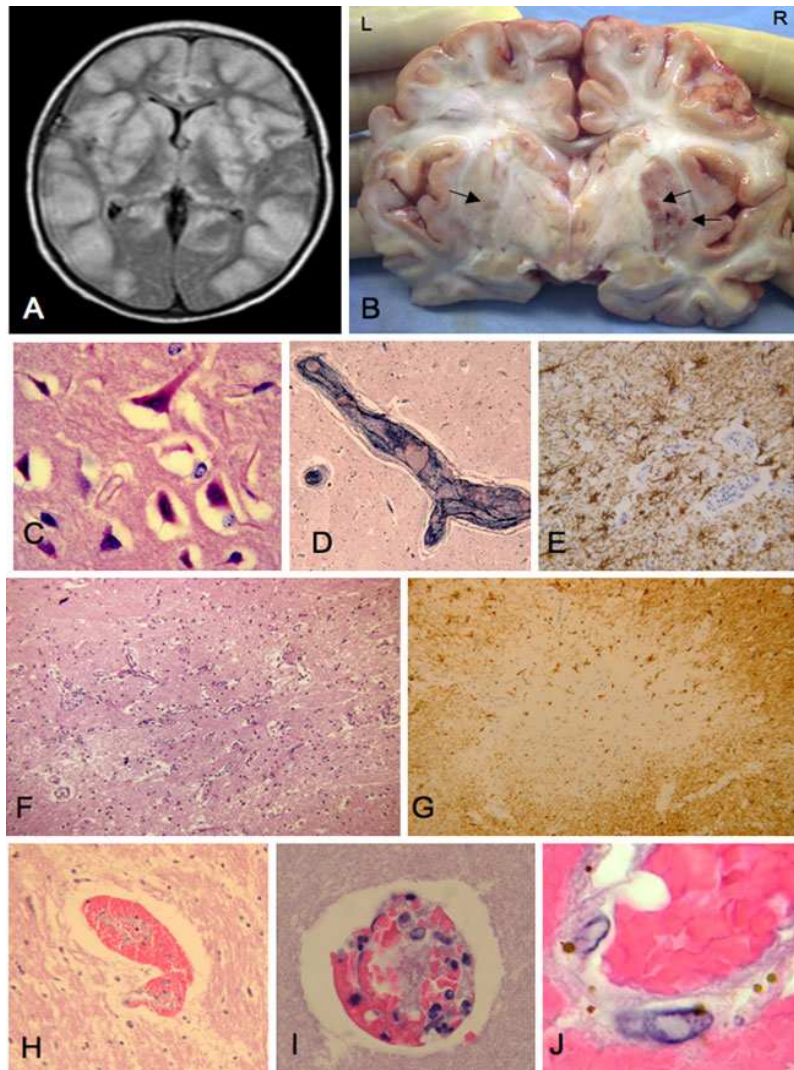


Fig. 2 Morphologic features of the brain.

a. Brain MRI on last hospital admission (age of 9 months): T2-fluid-attenuated-inversionrecovery (FLAIR) image of a transverse section of the brain shows symmetrical high intensity signals in the basal ganglia and cortex. b. Focal haemorrhagic lesions are evident in the basal ganglia, more prominent in the right putamen (L=left; R=right). c. Ischaemic cortical neurons showing nuclear pyknosis, cell body shrinkage and homogeneous eosinophilia of the cytoplasm (red neurons) (hematoxylin and eosin [H&E], original magnification 100X). d. Representative image of a medium size vessel in the white matter occluded by a fresh thrombus (phosphotungstic acid hematoxylin, original magnification 20X). e. Representative image of perivascular gliosis in the brain white matter of the patient (Immunohistochemistry [IHC] with anti-gliial fibrillary acidic protein [GFAP]

antibody, original magnification 40X). f. Left putamen: focal neuronal loss and increase vascular density consistent with previous ischaemic damage (H&E, original magnification 10X). g. Right putamen: immunohistochemistry of the same area shows reactive gliosis surrounding the lesion (IHC with GFAP, original magnification 10X). h. Representative image of acute microhemorrhage surrounding a small brain vessel (H&E, original magnification 40X). i. A recent thrombus associated with spilling of erythrocytes in a small brain vessel (H&E, original magnification 100X). j. Haemosiderin-laden macrophages surrounding a small vessel, consistent with previous episodes of bleeding (H&E, original magnification 100X).

The vessels of Willis polygon were unremarkable. Histological examination of the brain hemispheres confirmed the presence of multiple foci (<1 cm in diameter) of acute ischaemic damage, with eosinophilic, shrunken, necrotic neurons (red neurons, 2 C). Acute ischemia was secondary to occlusive thrombosis of multiple small and medium size vessels (Fig. 2d). In addition to the acute ischaemic damage, multiple foci of neuronal loss were scattered in the basal ganglia, pons and midbrain, with gliosis and focal increase of vessel density (due to collapse of the intervening neuropil). These features are consistent with previous ischaemic damage that occurred several weeks before the exitus (Fig. 2e-g). An additional finding was the presence of widespread acute perivascular micro-hemorrhages, often around vessels occluded by thrombi (Fig. 2h-i), and sparse perivascular haemosiderin-laden macrophages, consistent with chronic bleeding (Fig. 2j). These features were more frequent in the basal ganglia and frontal hemispheres, were observed also in areas not involved by ischaemic damage, and were absent in the cerebellum. Gastric and colonic mucosae were characterized by widespread petechial hemorrhages (Fig. 3a). Histological analysis revealed

multiple capillary and venular pinpoint hemorrhages (Fig. 3b), located in the mucosal and submucosal layers and, focally, in the muscularis propria as well. There were no images of thrombosis. A detailed analysis of intra-cerebral and gastrointestinal vessels revealed endothelial swelling and figures of intraluminal endothelial exfoliation, as demonstrated by CD31 immunohistochemical staining (Fig. 3c-d). The liver showed centrilobular microvacuolar steatosis. At ultrastructural examination hepatocytes revealed abundant mitochondria (Fig. 4a). Focal fibrin micro-thrombi were observed in the hepatic sinusoids. The kidneys showed diffuse micro-thrombi in the glomerular tufts and focal glomerulosclerosis. The lungs were markedly congested. Heart and skeletal muscle were morphologically unremarkable. Combined COX/SDH staining revealed diffuse, marked reduction of COX reaction in brain, paralleled by a decreased amount of the COX IV subunit immunovisualized by Western blot (Fig. 1c). In the bowel, the decrease of COX histochemical reaction was limited to luminal colonocytes (Fig. 4b), confirming previous observations on the *Eth1*^{-/-} knockout mouse model (Tiranti et al. 2009). COX activity and immunoistochemical reaction for COX subunits I and IV (Fig. 4c) were decreased in centrilobular hepatocytes.

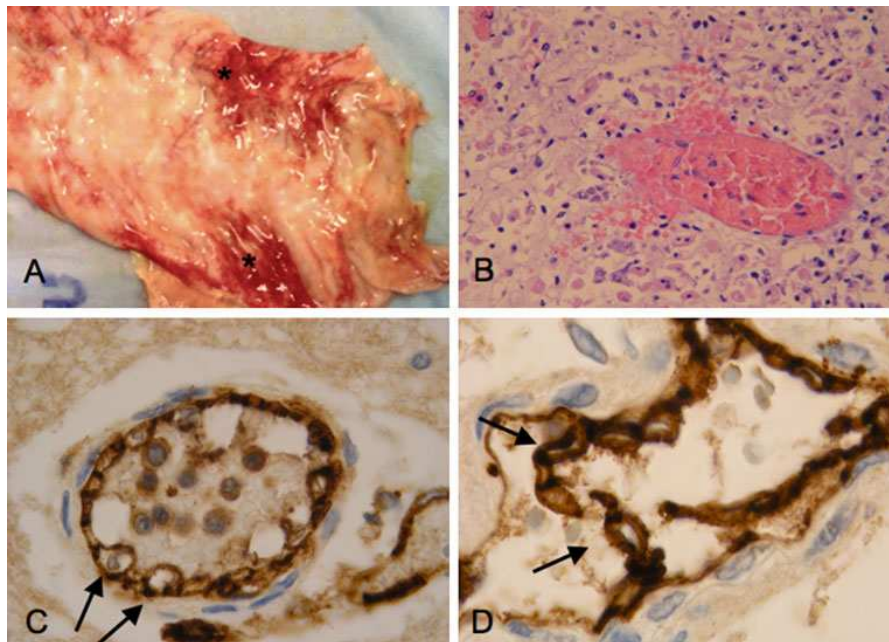


Fig. 3 Mucosal hemorrhages and immunohistochemical characterization of endothelial damage.

a. Colonic mucosa with widespread petechial hemorrhages (asterisks). b. A small vessel in the gastric mucosa. Note the vanishing of the endothelium and the dispersion of red cells in the surrounding lamina propria (hematoxylin and eosin [H&E], original magnification 100X). c. Brain: endothelial cells of a small vessel appear swollen (immunohistochemistry [IHC] with anti-CD31 antibody, original magnification 100X). d. Colon: endothelial cells of a small vessel exfoliate in the lumen (arrows) (IHC with anti-CD31 antibody, original magnification 100X)

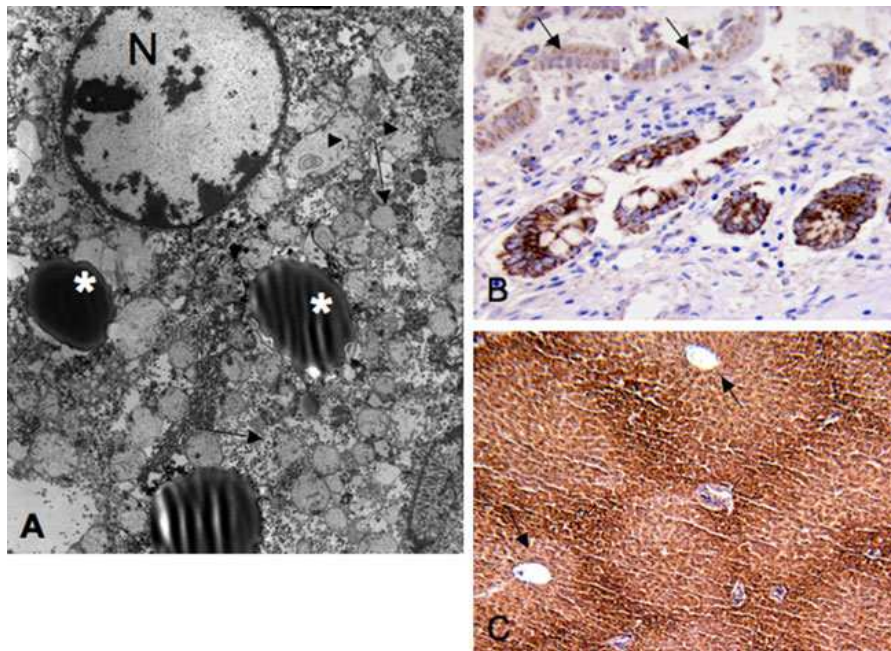


Fig. 4 Morphologic and histochemical features of liver and colonic mucosa.

a. Ultrastructural analysis of hepatocytes shows abundant mitochondria (arrows) and lipid droplets (asterisks). In some mitochondria remnants of cristae are still visible (arrowheads). Swelling of mitochondria is probably artifactual due to postmortem delay and autolysis. (Uracyl acetate lead citrate, original magnification 5000X). b. Decreased expression of cytochrome c oxidase (COX) subunit IV in the luminal colonocytes that are exfoliated in the lumen (arrows). Basal colonocytes retain COXIV expression (immunohistochemistry [IHC] with anti-COXIV antibody, original magnification 40X). c. Decreased expression of COXIV in the centrilobular hepatocytes. Arrows indicate the centrilobular vein (IHC anti-COXIV antibody, original magnification 20X)

Morphological features in $Ethel^{-/-}$ mice

We performed a detailed histological analysis on tissues obtained from six constitutive $Ethel^{-/-}$ recombinant mice and five control littermates. The brain of the $Ethel^{-/-}$ mice showed several perivascular acute microhemorrhages, and vessels surrounded by haemosiderin-laden macrophages, consistent with previous hemorrhages (Fig. 5a-b). Lesions were located in the brain hemispheres and midbrain, but not in the cerebellum, and were associated with small foci of gliosis (Fig. 5c). The haemorrhagic lesions were counted at 100x magnification on three H&E stained 5 μ M thick histological sections obtained from parallel areas 1 mm apart from each other in the same paraffin block. A mean of 11 recent or previous hemorrhages (range: 3–14) was counted in the $Ethel^{-/-}$ brains, whereas a single focus of acute hemorrhage was found in only one of the five control littermates. Acute pinpoint hemorrhages in the colonic mucosa were found exclusively in $Ethel^{-/-}$ animals, as compared to controls. Interestingly, they were limited to the luminal portion of the mucosa (Fig. 5d). The remaining organs were unremarkable.

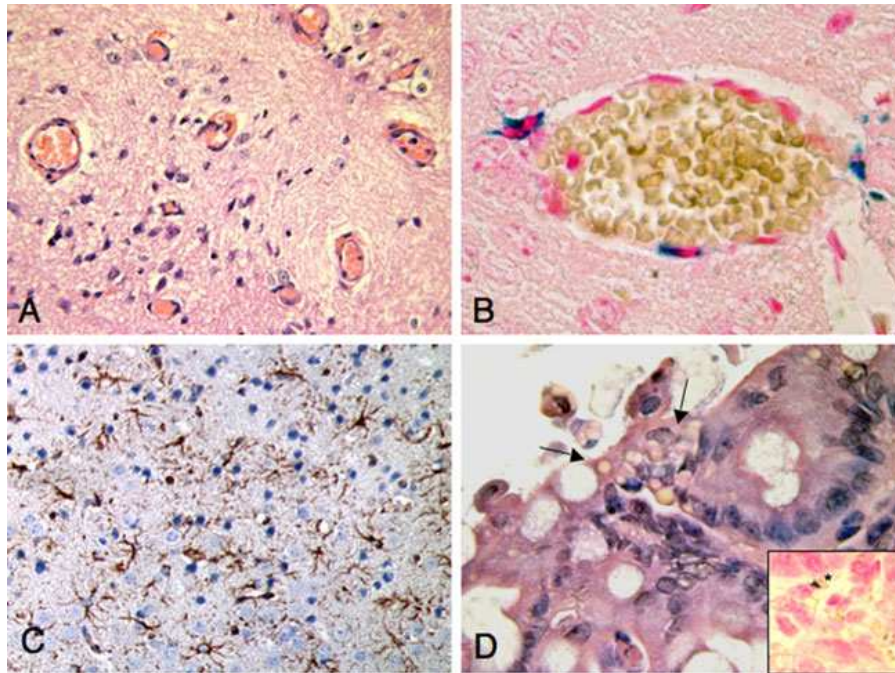


Fig. 5 Histological features of $Ethe1^{-/-}$ mice brain and colon.

a. Acute microhemorrhages surrounding small vessels in the white matter (hematoxylin and eosin [H&E], original magnification 40X). b. Haemosiderin-laden macrophages (blue), consistent with previous episodes of bleeding surround a small vessel (Perls iron stain, original magnification 100X). c. Focal gliosis in the white matter (immunohistochemistry with anti-glial fibrillary acidic protein acid [GFAP] antibody, original magnification 40X). d. Acute microhemorrhages (arrows) in the luminal portion of the colonic mucosae (H&E, 100X). The insert shows haemosiderin-laden macrophages (asterisk) in the colonic mucosae (Perls iron stain, original magnification 100X)

Discussion

Although the disease features of Ethylmalonic Encephalopathy have occasionally been investigated in a few clinical reports, this is the first systematic analysis on the pathology of this disease in a genetically confirmed ETHE1 mutant patient, carried out by histological, histochemical, and immunohistochemical investigation of autopsy specimens, and completed by detailed comparison with the morphological findings in the *Ethe1^{-/-}* mouse model. We found marked decrease of COX histochemical reaction in skeletal muscle, brain and luminal colonocytes of the patient, paralleled by decreased content of COX I and COX IV subunits, as demonstrated by immunohistochemical and Western blot analyses. The same histochemical findings were also found in the *Ethe1^{-/-}* mouse model. In addition, areas of COX deficiency were observed in the zone 2 and 3 of the hepatic acini, associated with steatosis. This is in contrast with the normal COX activity reported in the liver of both *Ethe1^{-/-}* mice and rats exposed to H₂S. Thus, the mechanisms hypothesized for alternative H₂S detoxification in rodent liver (Tiranti et al. 2004; Di Meo et al. 2011; Dorman et al. 2002) may not be effective in humans. A clinical trait characteristic of ethylmalonic encephalopathy is the presence of acrocyanosis and petechial purpura. This phenomenon has been attributed to the vasoactive and vasotoxic effects of H₂S (Tiranti et al. 2009). Hydrogen sulphide plays an important role in the regulation of vascular function. Increasing evidence supports its role as an endothelium-derived relaxing factor and a regulator of endothelial and smooth-muscle cell growth and apoptosis (Szabo

2007; Yang et al. 2004; Yang et al. 2006; Wang 2011). However, the vasotoxic effects of H₂S in vivo have not been clearly demonstrated. In this report we provide morphologic evidence of diffuse vascular damage both in an ethylmalonic encephalopathy patient and in the *Ethe1*^{-/-} mouse. Analysis of the human brain showed widespread luminal microthrombi, acute microhemorrhages and focal perivascular haemosiderinladen macrophages, the latter being consistent with previous bleedings. As a consequence, the brain showed features of both acute and chronic ischaemic damage, consistent with the features of abnormal signal intensity on repeated MRI. Brain vascular lesions seem to be a specific substrate of neurodegeneration in EE due to *ETHE1* mutations, as compared to other forms of ethylmalonic aciduria (Jamroz et al. 2011) and to disorders caused by primary respiratory chain defects such as Leigh's disease (Cavanagh and Harding 1994). Endothelial damage and loss was observed also in the gastric antrum and colonic mucosa and submucosa, associated with microhemorrhages. Interestingly, histological examination of brain and colonic mucosa of the *Ethe1*^{-/-} mouse also revealed diffuse vascular damage, with morphologic features of acute and chronic microhemorrhages that were absent in the control littermates. Nevertheless, the brain and intestinal lesions found in *Ethe1*^{-/-} mice were far less numerous and severe than those found in the patient, despite the rapidly progressive clinical downhill in these animals, leading to death by 30–35 days after birth. The discrepancy between the severity of the clinical course and the relative paucity of pathological abnormalities remains to be elucidated in this model. However, and importantly, our findings support a common pathogenic

mechanism in both humans and mice, centered on the damage of small vessels in critical organs, notably brain and colon, probably due to accumulation of hydrogen sulphide to toxic levels. Our results point to the microvasculature as the elective target in the pathogenesis of the disease, suggesting that other morphological features, for instance neurodegeneration and gliosis, are secondary to repeated ischaemic events. Other contributions to the pathogenesis must be taken into account, including the marked reduction in COX activity and the impairment of substrate utilization due to inhibition of beta-oxidation enzymes. However, it is noteworthy that conditional mice in which the *Ethel* gene was ablated in specific cell types, including nerve cells, skeletal muscle fibers or hepatocytes, do show partial COX deficiency in recombinant organs, but neither increase of specific biomarkers in body fluids (e.g. EMA, thiosulphate or lactate) nor overt clinical symptoms, and are in fact phenotypically indistinguishable from the WT littermates (Di Meo et al. 2011). Taken together, these results, and the clinical improvement determined by controlling the production of H₂S by intestinal anaerobes through metronidazole, suggest that the main pathogenic mechanism responsible for the clinical down- hill in both human patients and constitutive recombinant *Ethel*^{-/-} mice is the presence of high levels of hydrogen sulphide in circulating blood, rather than the inability of specific organs to detoxify the endogenous production of H₂S. This conclusion opens further opportunities for therapy. For instance adeno-associated virus mediated gene targeting could be exploited to express recombinant *Ethel* in the liver, the filter organ that receives blood from the gastrointestinal tract, the major source of exogenous H₂S.

Alternatively, transplantation of haemopoietic stem cells could determine the widespread diffusion of an Ethe1-proficient tissue to promoting the clearance of toxic H₂S from circulating body fluids, thus reducing the exposure of critical organs such as brain and skeletal muscle. The availability of the Ethe1^{-/-} mouse model will be an invaluable tool for testing these and other strategies in the near future and evaluate their translatability to humans.

Acknowledgements

This work was supported by Telethon Grants GGP07019 and GPP10005 to MZ; AFM grant 2010/14458 to MZ, Associazione Serena Talarico per i Giovani nel Mondo (GdA) and Fondazione Giuseppe Tomasello ONLUS (MZ and GdA).

References

Barth M, Ottolenghi C, Hubert L et al. (2010) Multiple sources of metabolic disturbance in ETHE1-related ethylmalonic encephalopathy. *J Inherit Metab Dis* Oct 27. [Epub ahead of print]

Burlina A, Zacchello F, Dionisi-Vici C et al. (1991) New clinical phenotype of branched-chain acyl-CoA oxidation defect. *Lancet* 338:1522–1523

Cavanagh JB, Harding BN (1994) Pathogenic factors underlying the lesions in Leigh's disease. Tissue responses to cellular energy deprivation and their clinico-pathological consequences. *Brain* 117:1357–1376

Di Meo I, Fagiolari G, Prella A, Viscomi C, Zeviani M, Tiranti V (2011) Chronic exposure to sulphide causes accelerated degradation of cytochrome c oxidase in ethylmalonic encephalopathy. *Antioxid Redox Signal* 5(2):353–362

Dorman DC, Moulin FJ, McManus BE, Mahle KC, James RA, Struve MF (2002) Cytochrome oxidase inhibition induced by acute hydrogen sulphide inhalation: correlation with tissue sulphide concentrations in the rat brain, liver, lung, and nasal epithelium. *Toxicol Sci* 65(1):18–25

Garavaglia B, Colamaria V, Carrara F, Tonin P, Rimoldi M, Uziel G (1994) Muscle cytochrome c oxidase deficiency in two Italian patients with ethylmalonic aciduria and peculiar clinical phenotype. *J Inherit Metab Dis* 17(3):301–303

Garcia-Silva MT, Campos Y, Ribes A et al. (1994) Encephalopathy, petechiae, and acrocyanosis with ethylmalonic aciduria associated with muscle cytochrome c oxidase deficiency. *J Pediatr* 125:843–844

Grosso S, Mostardini R, Farnetani MA et al. (2002) Ethylmalonic encephalopathy: further clinical and neuroradiological characterization. *J Neurol* 249(10):1446–1450

Jamroz E, Paprocka J, Adamek D et al. (2011) Clinical and neuropathological picture of ethylmalonic aciduria - diagnostic dilemma. *Folia Neuropathol* 49(1):71–77

Szabo C (2007) Hydrogen sulphide and its therapeutic potential. *Nat Rev Drug Discov* 6(11):917–935

Tiranti V, D'Adamo P, BriemE et al. (2004) Ethylmalonic encephalopathy is caused by mutations in *ETHE1*, a gene encoding a mitochondrial matrix protein. *Am J Hum Genet* 74(2):239–252

TirantiV, BriemE, Lamantea E et al. (2006) *ETHE1* mutations are specific to ethylmalonic encephalopathy. *J Med Genet* 43(4):340–346

Tiranti V, Viscomi C, Hildebrandt T et al. (2009) Loss of *ETHE1*, a mitochondrial dioxygenase, causes fatal sulphide toxicity in ethylmalonic encephalopathy. *Nat Med* 15(2):200–205

Viscomi C, Burlina AB, Dweikat I et al. (2010) Combined treatment with oral metronidazole and N-acetylcysteine is effective in ethylmalonic encephalopathy. *Nat Med* 16(8):869–871

Wang R (2011) Signaling pathways for the vascular effects of hydrogen sulphide. *Curr Opin Nephrol Hypert* 20(2):107–112

Yang G, Cao K, Wu L, Wang R (2004) Cystathionine γ -lyase overexpression inhibits cell proliferation via H₂S-dependent modulation of ERK1/2 phosphorylation and p21^{Cip}-WAC-1. *J Biol Chem* 279(47):49199–49205

Yang G, Wu L, Wang R (2006) Pro-apoptotic effect of endogenous H₂S on human aorta smooth muscle cells. *FASEB J* 20(3):553–555

Chapter 5

Summary, discussion and future perspectives

SUMMARY

The scope of my PhD thesis was to make progress in the pathophysiology of Ethylmalonic Encephalopathy (EE), a devastating infantile metabolic disorder affecting the brain, muscles, intestinal tract, vascular vessels, and associated with mutations in ETHE1 gene. From the biochemical standpoint EE is characterized by high levels of ethylmalonic acid (EMA) and thiosulfate in body fluids, accumulation of sulfide (H_2S) in tissues and a cytochrome c oxidase (COX) deficiency in brain, muscles and colon caused by toxic accumulation of sulfide in these tissues. Ethe1 protein possess a sulfur dioxygenase (SDO) activity that is part of a mitochondrial matrix pathway that provides the oxidation of sulfide. Our goal is to completely understand the molecular bases of the disease in order to find a winning therapeutic approach for the treatment of the human disorder. One of the most important questions that must be answered to make progress in the elucidation of the pathology of the disease is to understand the source of the accumulating toxic sulfide, the molecular mechanism by which this compound act on the complex IV of the mitochondrial respiratory chain and on other biochemical pathways, and the possible toxic effect of this compound on the normal development and physiological function of the most involved tissues .

In order to achieve these aims, I started my project generating three conditional mice models in which ETHE1 is deleted in a tissue-specific manner. It is well known that sulfide is generated in the body by two different ways: an endogenous production by the catabolism of sulphureted aminoacids, for instance cysteine and methionine, and an

exogenous production by the metabolism of the anaerobic bacterial flora in the intestinal tract. The ablation of ETHE1 gene in a single organ, for instance muscle, brain and liver, allowed to understand the contribution of endogenously-produced sulfide to the EE pathology. I found an important COX defect in the tissue in which ETHE1 was ablated, for instance muscle and brain, but not in liver, confirming the observation on the constitutive animal models that the liver is not affected from the mitochondrial respiratory chain activity standpoint. On the other hand, none of the above conditional mice models displays the other clinical and the biochemical features of the constitutive null-mouse. These data suggest that the local over-accumulation of sulfide causes the COX activity impairment, but it isn't sufficient to generate the wide clinical and biochemical spectrum of the disease.

In order to clarify how sulfide can act on the inhibition of cytochrome c oxidase activity, I decided to investigate COX from the molecular and enzymatic standpoint in the constitutive mouse and on cellular models. The study of the *Ethe*^{-/-} mouse reveals a progressive, time-dependent COX deficiency in muscle, brain and colon, The same reduction was found in the amount of mitochondrial and nuclear encoded subunits, while the levels of the mRNA of the same subunits were normal. These data suggested that the COX deficiency is caused by a progressive decrease in the amount of the holoenzyme that occurs post-transcriptionally. Treating different types of cells with increasing concentrations of NaSH, a sulfide donors, I observed the same progressive, time- and dose-dependent decrement of COX subunits, while the transcript levels were normal compared to untreated cells.

Mitochondrial *in vitro* pulse-chased translation assay in primary human fibroblasts showed that post-synthesis sulfide exposure causes COX subunit amount decrement, whereas pre-synthesis treatment showed no changes in proteins amount. These data demonstrated that chronic sulfide exposure causes a specific post-translational degradation of COX subunits.

Hydrogen sulfide is also known as a potent vasoactive and vasotoxic agent. The accumulation of this compound to higher levels could explain the vascular lesions in the skin and possibly, organs, including brain and gut, typical of the disease. We reported the first autopsy case of a child with a genetically confirmed diagnosis of EE, and compare the microscopic features found in this patient with those of the constitutive *Ethel^{-/-}* mice. In both organisms, widespread, complex vascular lesions are the pathological hallmark of the disease in the brain and gastrointestinal tract.

Another line of my work was to improve the biochemical and molecular approaches to the diagnosis of EE.

DISCUSSION

In the presence of air, most of the energy produced by eukaryotic cells is generated by mitochondrial oxidative phosphorylation. This process is driven by a respiratory chain composed of a number of complex membrane proteins that act in sequence to transfer electrons from reduced substrates through a series of oxidation–reduction reactions to oxygen (Wilson, 1982). The net result of this process is the generation of proton and ion gradients across the inner mitochondrial membrane; these gradients are used by ATP synthase to drive ATP synthesis. Several previous studies have demonstrated that the respiratory chain itself regulates the rate of oxidative phosphorylation and have identified cytochrome *c* oxidase, its terminal member, as a key enzyme in this regulation (Villani and Attardi, 1997). Most of the structural, functional, biosynthetic and genetic data on eukaryotic cytochrome *c* oxidases have come from studies with mammalian (i.e. bovine) and yeast (i.e. *Saccharomyces cerevisiae*) cytochrome *c* oxidases (Poyton, 1995). Both cytochrome *c* oxidases catalyze the concerted transfer of four electrons from ferrocycytochrome *c* to molecular oxygen, with the simultaneous pumping of protons across the inner mitochondrial membrane from the matrix to the cytoplasmic side (Babcock and Wikstrom, 1992). Both enzymes contain four redox-active metal centers (heme *a*, heme *a*₃, CuA, CuB) that participate in electron transfer. Heme *a*₃ and CuB are bridged in the resting fully oxidized form and constitute the binuclear reaction center. Electrons pass from cytochrome *c*, via CuA and heme *a*, to the binuclear reaction center, where molecular oxygen (O₂) is reduced to water. The reduction of molecular oxygen to water is coupled to the

translocation of one proton per electron across the inner mitochondrial membrane. This creates a pH and voltage gradient across the membrane. The protein matrix surrounding the metal centers in eukaryotic cytochrome *c* oxidases consists of several different polypeptide subunits. The three largest polypeptide subunits (MTCOI, MTCOII and MTCOIII) are encoded by mitochondrial genes. These polypeptides are conserved in mammalian and yeast enzymes and they have primary sequence homology to three of the subunit polypeptides of prokaryotic cytochrome oxidases (Saraste, 1990). In addition to the mitochondrially encoded subunits, these eukaryotic cytochrome *c* oxidases contain several polypeptide subunits that are encoded in the nucleus (Capaldi, 1995). The mammalian enzyme contains 10 different subunit polypeptides encoded by nuclear genes (COX4; COX5A, B; COX6A, B, C; COX7A, B, C; and COX8) (Tsukihara, 1996). The function of these subunits is currently unknown, but they plausibly regulate the activity and stability of the complex. COX deficiency is a frequent cause of disease in humans, being associated with different clinical syndromes and a spectrum of gene defects. I demonstrated that a new pathogenic mechanism is at work in Ethylmalonic Encephalopathy (EE), based on H₂S-mediated poisoning of COX. The four gasses, nitric oxide (NO), carbon monoxide (CO), hydrogen sulfide (H₂S) and hydrogen cyanide (HCN) all readily inhibit oxygen consumption by COX. This inhibition is responsible for much of their toxicity when they are applied externally to the body. However, recently these gases have all been implicated, to greater or lesser extents, in normal cellular signaling events. For instance, NO, CO and H₂S are well known to belong to the class of

gasotransmitters, regulating various biological processes in the gastrointestinal tract, smooth muscle and cardiovascular system. The inhibition of COX by NO and CO is dependent on oxygen concentration, but that of H₂S not. H₂S is both a substrate and an inhibitor for COX (Cooper CE, 2008). At high concentration (μM), H₂S binds to Fe^{II} in the reduced active site and can act as a competitive inhibitor of COX, competing with O₂ for binding to the reduced Fe^{II}-Cu^I active site. However, if the exposition to H₂S is short, this inhibition is reversible as O₂ can easily replace H₂S bound to a reduced Fe^{II} (Collman, 2009).

I found that the loss of ETHE1 protein, a mitochondrial sulfur dioxygenase (SDO), restricted to tissues as muscle and brain is associated with an isolated COX deficiency in the target tissues, but not in the others. These data demonstrated that the incapability to detoxifying the endogenous produced sulfide is sufficient to induce a COX activity impairment. However, the local over-accumulation of sulfide is not sufficient for the animal to become sick, nor for thiosulfate, an EE biomarker of H₂S levels, to increase. This data suggesting that multiorgan accumulation of sulfide and its diffusion of exogenously produced H₂S from the anaerobic bacterial flora are needed to generate the wide and fatal clinical and biochemical scenario of the ETHE1-null mouse. The exposition of cells to NaSH for short times is sufficient to induce a COX inhibition, but this phenomenon is reversible by competitive displacement by oxygen. However, I showed that, besides direct COX inhibition, chronic exposure to sulfide causes a decrease in the amount of COX holoenzyme in a time- and dose- dependent way, making the defect

permanent and irreversible. Analyzing the *Ethe1*^{-/-} tissues and NaSH treated cells transcripts for COX subunits, I found that the expression of the mitochondrial and nuclear encoded COX genes were normal. These data suggests that the decrease of COX holoenzyme must be due to either defective assembly or accelerated degradation of the enzyme. The concordant decrease of both COX holoenzyme and individual subunits, demonstrated by *in vitro* translation assay and Western blot analysis, indicates accelerated degradation of a (crippled) enzyme.

It is well known that hydrogen sulfide is a vasoactive compound, acting on myocardial cells and vascular smooth muscle. By activating K_{ATP} channels, H₂S increases the membrane potential of vascular smooth muscle cells that become hyperpolarized, causing vasorelaxation, and suggesting that it may physiologically regulate blood pressure. These evidences supports its role as an endothelium-derived relaxing factor and a regulator of endothelial and smooth-muscle cell growth and apoptosis. Based on these evidences, it is clear that accumulation of sulfide to higher levels can induce toxic effects on vascular system (Kimura, 2010). However, the vasotoxic effects of H₂S *in vivo* have not been clearly demonstrated. We performed the first systematic analysis on the pathology of this disease in a genetically confirmed *ETHE1* mutant patient, carried out by histological, histochemical and immunohistochemical investigation of autoptic specimens, and completed by detailed comparison with the morphological findings in the *Ethe1*^{-/-} mouse model. We found morphologic evidence of diffuse vascular damage with disruption of the blood brain barrier both in an ethylmalonic-encephalopathy patient

and in the *Ethe1*^{-/-} mouse. Analysis of the human brain showed diffuse loss of endothelial lining in arterioles, venules and capillaries, with swelling and nuclear discoloration of residual endothelium. Thinning of arteriolar walls was due to smooth-muscle cell loss. These changes were associated with acute microhemorrhages and perivascular hemosiderin-laden macrophages, the latter being consistent with previous bleedings. In addition, widespread luminal microthrombi were observed, often in association with the hemorrhages. Endothelial cell damage in capillaries and venules was associated with microhemorrhages in the gastric antrum and colonic mucosa and submucosa, whereas thrombosis was absent. Interestingly, histological examination of brain and colonic mucosa of the *Ethe1*^{-/-} mouse also revealed diffuse vascular damage, with morphologic features of acute and chronic microhemorrhages that were absent in the control littermates. As well as in the mouse model, a marked decrease in COX histochemical reaction and in the amount of its protein subunits were found in skeletal muscle, brain and luminal colonocytes. However, areas of COX deficiency were observed in the heart of the patient, and in the zone 2 and 3 of the hepatic lobules acini, associated with steatosis. This is in contrast with the normal COX activity reported in the liver of both *Ethe1*^{-/-} mice and rats exposed to H₂S. Thus, the mechanisms hypothesized for alternative H₂S detoxification in rodent liver may not be effective in humans. Our findings support a common pathogenic mechanism in both humans and mice, centered on the damage of small vessels in critical organs, notably brain and colon, due to accumulation of hydrogen sulfide to

toxic levels, providing the first direct morphologic evidence of the vasotoxic effect of this gasotransmitter.

A further research line concerns the improvement of biochemical and molecular approaches for the diagnosis of EE. From the biochemical standpoint, since ETHE1 protein is involved in sulphur metabolism, a new biochemical marker can be searched in the urine of patients with EE. This metabolite is thiosulphate, which is excreted in great amounts in affected patients. I measured thiosulphate in our patients and in all of them, we consistently found elevated levels. I propose to include the measurement of this compound in the metabolic evaluation of patients suspected of EE. On the other hand, using molecular diagnostic tools, we can now perform a prenatal screening to evaluate the presence of mutations in a fetus before it is born. The exon 4 deletion is one of three ETHE1 recurrent mutations and has been found in EE patients. This mutation has been previously described in seven patients from the Arabian peninsula, six of whom were homozygous for the deletion and one was a compound heterozygote with another point mutation. Using qRT-PCR in association with direct detection of point mutation by sequencing, I was able to distinguish between a compound heterozygote, a heterozygote for exon 4 deletion, a heterozygote for a point mutation, and a normal fetus. The introduction of qRT-PCR for the evaluation of patients with monoallelic deletions is important for prenatal genetic diagnosis because we can now establish whether a subject carries a deletion in the heterozygous state.

FUTURE PERSPECTIVES

The understanding of the molecular mechanism at the base of EE is needful for the development of a winning therapeutic strategy for the treatment of the disease. Since EE is caused by an accumulation to toxic levels of sulfide in the body, and because the main source of this compound seems to be the diffusion of exogenously produced H₂S from the anaerobic bacterial flora, I'm trying to develop two different strategies in order to obtain the scavenging of circulating sulfide coming from the gut.

Since the portal vein system collects virtually all the blood flow from the gastrointestinal tract to the liver, the latter is the first and main organ that detoxifies potentially harmful compounds generated during food digestion and adsorption, including those produced by the bacterial flora residing in the intestine. Restoration of the ETHE1-SDO activity in liver of constitutive Ethe1^{-/-} individuals could therefore induce a substantial clearance of colon-derived toxic H₂S, before its diffusion occurs in the systemic bloodstream and target organs, such as muscle and brain.

Adeno-Associated Virus (AAV) vectors are currently among the most frequently used viral vectors for gene therapy. Several features make AAV attractive for gene transfer: 1) it is derived from a human non-pathogenic virus and is deleted of all viral coding sequences, 2) it is able to transduce dividing and non-dividing cells, 3) it is associated with stable long-term gene transfer in animal models following a single administration, and 4) it appears to have a good safety profile in animal models. The use of tissue specific promoters for liver gene

transfer offers the advantage of long-term restricted gene expression. Since liver is the main checkpoint organ against toxic compounds from the gut, we reasoned that AAV-mediated liver-specific ETHE1 expression may be beneficial to *Ethel^{-/-}* organisms. Thereby, an AAV2/8 serotype vector expressing the ETHE1 cDNA under the liver-specific thyroxine-binding globulin (TBG) promoter is delivered in the bloodstream at a titer of 10^{10} viral particles/gm. Mice sacrificed after 2 weeks showed that both viral DNA and the ETHE1 protein was detected only in liver. Measurement in AAV-infected livers showed a total rescue of ETHE1/SDO activity. The clinical rescue of EE in treated mice is at moment under investigation.

The second strategy concerns the bone marrow transplantation (BMT) in *Ethel^{-/-}* mice. Hematopoietic stem cell or bone marrow transplantation has emerged as a major therapeutic option in the treatment of malignant diseases and has also become the treatment of choice for a number of nonmalignant disorders. The rationale of this approach in the context of EE is to evaluate if allogeneic bone marrow transplantation can ameliorate the abnormal physical characteristics typical of this disease. Although we should consider that it is difficult to ameliorate the pathogenic COX deficiency in all involved somatic cells, and particularly in muscle and brain of EE adult patients, bone marrow transplantation from normal subjects may be effective for suppressing disease phenotypes, assuming that bone marrow cells include stem cells with proliferating and multipotent capacities. Therefore, we suppose that BMT would supply functional somatic cells continuously for regenerating functional tissues by their replication and subsequent transdifferentiation. This section of my

study aims to address the issue of developing a suitable therapy for *Ethe1*^{-/-} mice by applying bone marrow transplantation and to show that this procedure causes reduction of EE phenotype. For this purpose, we will first investigate the lymphohematopoietic system in different hemopoietic compartments, such as bone marrow, peripheral blood, lymphnodes in *Ethe1*^{-/-} mice. We further plan to set up a transplant model on lethally irradiated *Ethe1*^{-/-} in order to evaluate the repopulation capacity of host lymphohematopoietic systems by normal donor cells and, in a second time, the capacity of the transplanted cells to induce the systemic clearance of H₂S and to ameliorate the typical characteristics of this disease.

References:

BABCOCK, G. T. AND WIKSTROM, M. (1992). Oxygen activation and the conservation of energy in cell respiration. *Nature* **356**, 301–309.

CAPALDI, R. A., MARUSHICH, M. F. AND TAANMAN, J.-W. (1995). Mammalian cytochrome *c* oxidase: Characterization of enzyme and immunological detection of subunits in tissue extracts and whole cells. *Meth. Enzymol.* **260**, 117–132.

COLLMAN JP, GHOSH S, DEY A, DECRE'AU RA (2009). Using a functional enzyme model to understand the chemistry behind hydrogen sulfide induced hibernation. *Proc Natl Acad Sci U S A* **106**: 22090–22095.

COOPER CE, BROWN GC (2008). The inhibition of mitochondrial cytochrome oxidase by the gases carbon monoxide, nitric oxide, hydrogen cyanide and hydrogen sulfide: chemical mechanism and physiological significance. *J Bioenerg Biomembr.* **40(5)**:533-9. *Review.*

KIMURA H (2010). Hydrogen sulfide: its production, release and functions. *Amino Acids.* **41(1)**:113-21.

POYTON, R. O., GOEHRING, B., DROSTE, M., SEVARINO, K. A., ALLEN, L. A. AND ZHAO, X.-J. (1995). Cytochrome *c* oxidase (Complex IV) from *Saccharomyces cerevisiae*. *Meth. Enzymol.* **260**, 97–116.

SARASTE, M. (1990). Structural features of cytochrome oxidase. *Q. Rev. Biophys.* **23**, 331–66.

TSUKIHARA, T., AOYAMA, H., YAMASHITA, E., TOMIZAKI, T., YAMAGUCHI, H., SHINZAWA-ITOH, K., NAKASHIMA, R., YAONO, R. AND YOSHIKAWA, S. (1996). The whole structure of the 13-subunit oxidized cytochrome c oxidase at 2Å. *Science* **272**, 1136–1144.

VILLANI, G. AND ATTARDI, G. (1997). *In vivo* control of respiration by cytochrome c oxidase in wild-type and mitochondrial DNA mutation-carrying human cells. *Proc. natn. Acad. Sci. U.S.A.* **94**, 1166–1171.

WILSON, D. F. (1982). Regulation of *in vivo* mitochondrial oxidative phosphorylation. In *Membranes and Transport*, vol. 1 (ed. A. Martinosi), pp. 349–355. New York: Plenum Press.



The research presented in this thesis was performed at the Unit of Molecular Neurogenetics, of the Foundation IRCCS Neurological Institute Carlo Besta, Milan, Italy, from January 2009 until January 2012.

I want to thank all my colleagues, my tutor Valeria Tiranti and the chief of the lab Massimo Zeviani for their experience and their important suggestions.

This work was financially supported by Telethon-Italy Foundation grant GGP07019, Fondazione Pierfranco e Luisa Mariani, grant RF-INN-2007-634163 of the Italian Ministry of Health and . AFM grant 2010/14458. The author would like to thank the Italian Association “Amici del Centro Dino Ferrari.”



All rights reserved. No part of this publication may be reproduced, stored in a retrieval system, or transmitted in any form of by any means, electronic, mechanical, photocopying, recording, or otherwise, without prior written permission of the holder of the copyright.